RD&E CENTER

Technical Report

No. 13179

DEVELOPMENT OF FIBER REINFORCED TRACK PAD MATERIALS

CONTRACT DAAE07-83-C-R013

APRIL 1986

Avco Systems Textron
201 Lowell Street
Wilmington, MA 01887

By AVST No. 0224-86-RR

U.S. ARMY TANK-AUTOMOTIVE COMMAND
RESEARCH, DEVELOPMENT & ENGINEERING CENTER
Warren, Michigan 48397-5000

NOTICES

This report is not to be construed as an official Department of the Army position.

Mention of any trade names or manufacturers in this report shall not be construed as an official endorsement or approval of such products or companies by the U.S. Government.

Destroy this report when it is no longer needed. Do not return it to the originator.

UNCLASSIFIED
SECURITY CLASSIFICATION OF THIS PAGE

REPORT DOCUMENTATION PAGE

1a. REPORT SECURITY CLASSIFICATION	1b. RESTRICTIVE MARKINGS
2a. SECURITY CLASSIFICATION AUTHORITY	3. DISTRIBUTION/AVAILABILITY OF REPORT Approved for public release; Distribution Unlimited
2b. DECLASSIFICATION/DOWNGRADING SCHEDULE	
4. PERFORMING ORGANIZATION REPORT NUMBER(S) AVST-No. 0224-86-RR	5. MONITORING ORGANIZATION REPORT NUMBER(S) 13179
6a. NAME OF PERFORMING ORGANIZATION Avco Systems Textron 6b. OFFICE SYMBOL (If applicable)	7a. NAME OF MONITORING ORGANIZATION U.S. Army Tank-Automotive Command Dept. of the Army, Warren, Michigan 48090
6c. ADDRESS (City, State, and ZIP Code) 201 Lowell Street Wilmington, MA 01887	7b. ADDRESS (City, State, and ZIP Code)
8a. NAME OF FUNDING/SPONSORING ORGANIZATION U.S. Army Tank-Automotive Command 8b. OFFICE SYMBOL (If applicable) DRSTA- RCKT	9. PROCUREMENT INSTRUMENT IDENTIFICATION NUMBER Contract DAAE07-83-C-R013
8c. ADDRESS (City, State, and ZIP Code) Department of the Army U.S. Army Tank-Automotive Command Warren, Michigan 48397-5000	10. SOURCE OF FUNDING NUMBERS PROGRAM ELEMENT NO. / PROJECT NO. / TASK NO. / WORK UNIT ACCESSION NO.

11. TITLE (Include Security Classification)

Development of Fiber Reinforced Track Pad Materials

12. PERSONAL AUTHOR(S)
Dr. Arthur L. Gurson

13a. TYPE OF REPORT	13b. TIME COVERED	14. DATE OF REPORT (Year, Month, Day)	15. PAGE COUNT
Final Report	FROM 5/83 TO 4/86	April 1986	

16. SUPPLEMENTARY NOTATION

17. COSATI CODES			18. SUBJECT TERMS (Continue on reverse if necessary and identify by block number)
FIELD	GROUP	SUB-GROUP	

19. ABSTRACT (Continue on reverse if necessary and identify by block number)

Current tank track designs use rubber pads (track pads) to enhance traction, vibration isolation, and noise reduction, and to limit damage to paved surfaces. The pads can be made integral with the track (as in the M1/T156 system), or bonded to steel plates which are then bolted to the track (as in the M60/T142 system). Typical track pad mileage is far below the mileage between major overhauls. Since replacement of the pads is expensive and time consuming, it is worthwhile to investigate ways of improving the design to increase mileage while maintaining the functions stated above.

Failure mechanisms for track pads include abrasion, cutting, chunking, and blowout. All of these are related to hysteresis heating of the rubber, which is due to the cyclic loading of the road wheels on the track. Rubber loses tensile and tear strength rapidly as temperature is increased.

20. DISTRIBUTION/AVAILABILITY OF ABSTRACT ☐ UNCLASSIFIED/UNLIMITED ☐ SAME AS RPT. ☐ DTIC USERS	21. ABSTRACT SECURITY CLASSIFICATION
22a. NAME OF RESPONSIBLE INDIVIDUAL Jack Patt	22b. TELEPHONE (Include Area Code) 313-574-8687 22c. OFFICE SYMBOL AMSTA-RTT

DD FORM 1473, 84 MAR 83 APR edition may be used until exhausted. All other editions are obsolete.

SECURITY CLASSIFICATION OF THIS PAGE

Blowout is due to severe overheating, where the inside of the pad appears to vaporize.

The properties of the pad which cause temperature related problems are low thermal conductivity, high compliance, and high internal damping. The second and third propert are important to the basic functions of the pad, so care must be taken that they are maintained to some extent in any redesign. The approach taken here is to modify the ba rubber pad design by adding reinforcement. Metal wire reinforcement was chosen because it will help directly by strengthening, and indirectly by increasing the conduction of heat to the pad surface. To maintain compliance and to add strength in the most critic direction, the mode of reinforcement chosen was uniaxial, in the direction of travel of the road wheels. The recommended baseline design was a standard T142 configuration wit brass or bronze coated steel wire of 32 mil diameter and a volume fraction of 0.013.

Analytical work included a thermal model of a track pad, which quantified the reduction in operating temperature due to reinforcement. It was also used to model the curing process. A fracture mechanics based fatigue model was constructed, to model debonding of the reinforcement as a function of cyclic loading. This showed that the baseline de should maintain a bond for a reasonable mileage, and showed what design changes would b needed to improve performance. Adhesion tests were conducted for a range of rubber compounds and wire types, and likely combinations with high adhesion were identified.

FINAL REPORT
Contract DAAE07-83-C-R013

DEVELOPMENT OF FIBER REINFORCED TRACK PAD MATERIALS

April 1986

For Management Use Of
U.S. Army Tank-Automotive Command
Warren, Michigan

Prepared by
Avco Systems Textron
201 Lowell St.
Wilmington, MA 01887

TABLE OF CONTENTS

LIST OF ILLUSTRATIONS

LIST OF ILLUSTRATIONS

LIST OF TABLES

1.0 INTRODUCTION

Current tank-track designs use rubber pads (track pads) to enhance traction, vibration isolation, and noise reduction, and to limit damage to paved surfaces. The pads can be made integral with the track (as in the M1/T156 system), or bonded to steel plates which are then bolted to the track (as in the M60/T142 system). Typical track pad mileage is far below the mileage between major overhauls. Since pad replacement is expensive and time consuming, ways of improving the design to increase mileage while maintaining the functions stated above are needed.

Failure mechanisms for track pads include abrasion, cutting, chunking, and blowout. All of these are related to hysteresis heating of the rubber, which is due to the cyclic loading of the road wheels on the track. Rubber loses tensile and tear strength rapidly as temperature is increased. Cutting and chunking occur on rough terrain, when pads are loaded unevenly by the sharp edges of rocks. Blowout is due to severe overheating, in which the inside of the pad appears to vaporize.

Pad properties that cause temperature related problems are low thermal conductivity, high compliance, and high internal damping. The second and third properties also are important to the basic functions of the pad, so care must be taken that they are maintained to some extent in any redesign. The approach taken here is to modify the basic rubber pad design by adding reinforcement. Metal wire reinforcement was chosen because it will help directly by strengthening, and indirectly by increasing the conduction of heat to the pad surface. To maintain compliance and to add strength in the most critical direction, the mode of reinforcement chosen was uniaxial, in the direction of travel of the road wheels. The recommended baseline design was a standard T142 configuration with brass or bronze coated steel wire of 32 mil (0.8 mm) diameter and a volume fraction of 0.013.

Analytical work included a thermal model of a track pad, which quantified the reduction in operating temperature due to reinforcement. It was also used to model the curing process. A fracture mechanics-based fatigue model was constructed to model debonding of the reinforcement as a function of cyclic loading. This showed that the baseline design should maintain a bond for a reasonable mileage, and showed what design changes would be needed to improve performance. Adhesion tests were conducted for a range of rubber compounds and wire types, and likely combinations with high adhesion were identified.

2.0 OBJECTIVE

The general aim of this program was to extend the service life of tank track pads. The specific goals were to 1) to develop a baseline design for a fiber reinforced T142 type track pad, 2) to present reasonable mathematical and physical bases for the design, considering thermal and adhesion behavior, 3) to carry out a series of adhesion tests, to identify promising combinations of rubber compounds and reinforcement, and 4) to model the molding process, so that ways to achieve more uniform properties by reducing over and under curing could be presented.

3.0 CONCLUSIONS

An analytical basis has been presented to support improvements in track pad life via steel wire reinforcement. It included a simple 1-D thermal analysis which gave results consistent with field data from the literature, a fracture mechanics based study of the influence of temperature and reinforcement parameters on tearing and wire debonding, a wire pullout test program, and 2-D numerical models for hysteresis heating and curing. Stress in the rubber can be reduced by orienting the wire in the direction of highest tensile stress, which is the direction of road wheel travel. One-dimensional reinforcement allows the pad to retain most of its original compliance. Temperature in the pad is reduced through stiffening, and through increased thermal conductivity in the wire direction. Additional temperature reduction can be achieved by improved surface heat transfer. By itself (i.e., ignoring reinforcement effects), the resulting temperature drop is large enough to reduce the rate of tear growth in the rubber by a factor on the order of 1/2.

The issues of wire strength and bond strength have been addressed. Wire stress at a reasonable volume fraction requires use of steel wire. (Brass, aluminum, and copper are not strong enough.) The maintenance of a bond between the wire and the rubber was recognized as a critical issue, with failure postulated as a large debond length. Bond integrity under cyclic loading has been studied using a fracture mechanics based fatigue model, which was correlated to the results of single cycle wire pullout tests. A method has been presented for estimating the improvement potential of changes in wire size and volume fraction. A test method from the literature was adapted to the nonlinear behavior exhibited by the rubber. Wire pullout tests were conducted as part of this program, using several rubber types, and several types of adhesive and metallic coatings on the wires. The strongest bond by far was achieved with a high sulfur, natural rubber compound and brass coated steel wire. Good bonds were achieved with an EV cure rubber, using adhesive on a copper coated steel wire and on a brass coated steel wire. The process of applying the adhesive required on etch for the copper surface, but not for the brass surface. In any case, use of an adhesive proved to be very cumbersome. A good bond was also achieved using a TACOM standard compound (14A) with bronze coated steel wire, and no adhesive. Because adhesive was not needed, and because the rubber compound had already been shown to perform well in track pads, this combination is recommended for testing.

Numerical studies were carried out with a two-dimensional finite difference thermal analysis code written specifically for this project. The code models hysteresis heating and the curing process for track pad sized rectangular blocks. The results for hysteresis heating showed that the increase in thermal conductivity due to steel wire reinforcement can lead to moderate decreases in pad temperature. Stiffening effects can be important because they directly reduce the heat input from cyclic loading. Improvements in surface heat transfer can lead to temperature reductions on the same order as those due to increased thermal conductivity. For a baseline case with steel wire reinforcement, a numerical model of cyclic loading showed the following reductions in temperature rise from the following phenomena:

stiffening	25%
enhanced thermal conductivity	15%
enhanced surface heat transfer	15%

The combined effect is a 46% reduction in temperature rise, which could have a significant effect in reducing tearing and blowout failures. Reduced temperature also helps maintain bond strength.

Curing models showed that the improved thermal conductivity due to wire reinforcement can improve the uniformity of the cure in a thick rubber track pad. Other means of improving cure uniformity were investigated. Preheating and post-heating at temperatures below the mold temperature (by 30 to 40°C) were shown to hold promise, and work by inducing higher temperature for longer time at the pad center.

4.0 RECOMMENDATIONS

4.1 Wire Reinforced Track Pads

Fabricate wire reinforced track pads as per Figure 4-1. Bronze coated wire (hose wire) and TACOM baseline triblend (compound 14A MIL-T-11491C AT) are recommended. Consider slotted sides for improved surface heat transfer. Baseline wire size is 32 mil (0.8mm) diameter, and baseline volume fraction is 0.013. Wire spacing is 0.25 inch (6.4mm).

4.2 Cure Cycles

If nonuniformity of cure is a problem, consider revising the cure cycle by subjecting the rubber to an appropriate preheat and/or post-heat, or a longer mold time at a lower temperature. Explore the cost saving possibilities of reducing the required mold time by adding a post-heat, out of the mold, at a lower temperature.

5.0 DISCUSSION

5.1 Background Data

Typical mileage for M60/T142 track pads, as reported by TACOM, is:

2,000 miles on pavement
900 miles on gravel
250 miles on rocky cross-country terrain.

In contrast, the distance run between major overhauls in 6,000 miles. Costs as reported several years ago were $5 per mile for fuel, and $27 per mile for track. Clearly, if the time and material involved in replacing worn track pads could be reduced, significant savings could be achieved. A goal for the long term would be to increase pad mileage to the mileage between major overhauls.

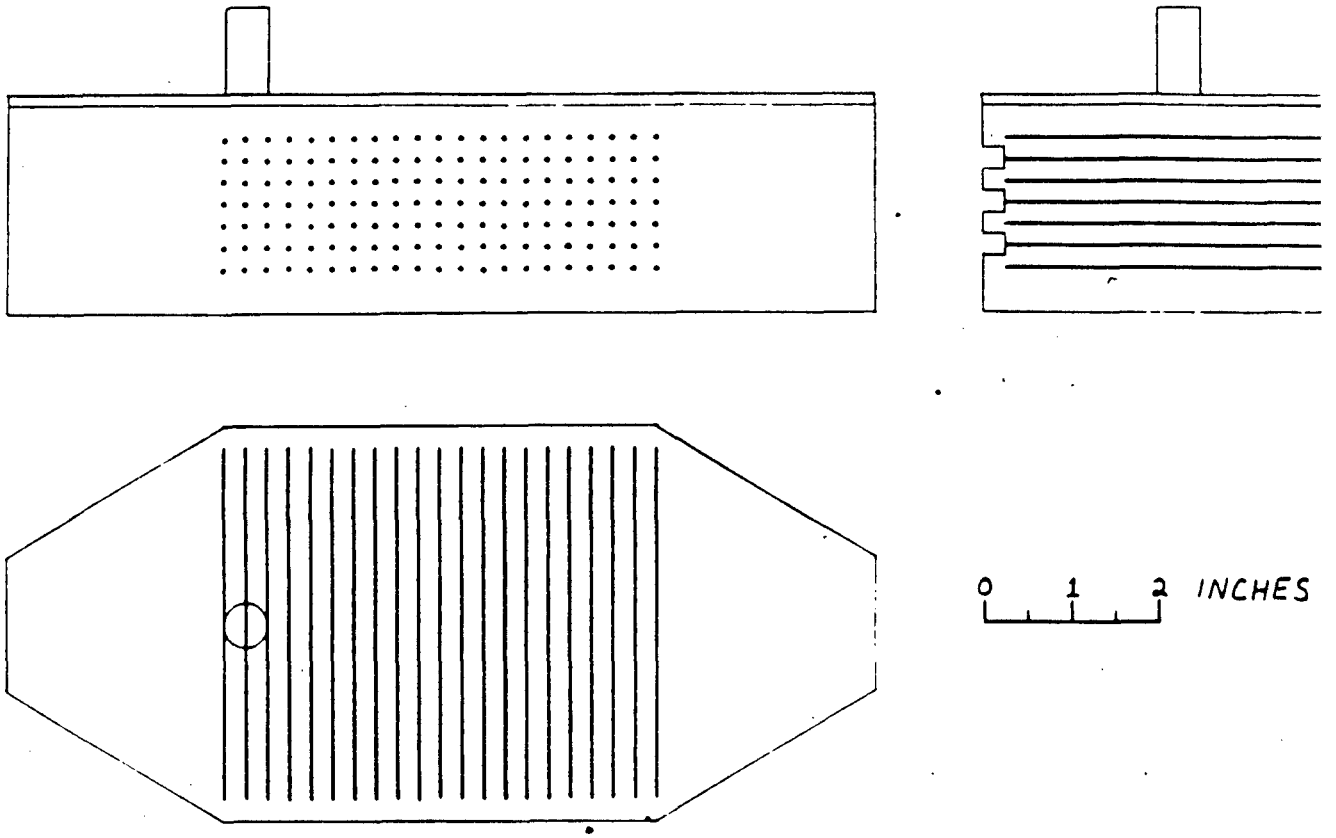

Figure 4-1 Suggested Baseline Reinforcement Configuration

Measurements of temperature rise as a function of time in M60/T142 track pads for various surfaces have been reported[1]. Approximate values, extrapolated to steady state (more than two hours running time), are given below:

Surface	Avg Speed (MPH)	ΔT(interior),°C	ΔT(Surface),°C
Paved	20	70	50
Gravel	20	90	-
Cross Country	16.7	105	-

Under desert conditions, the initial temperature of the pads can be as high as 50°C, due to the high ground temperature. Thus, the pad internal temperature can be as high as 155°C (310°F). For changes in vehicle velocity, the rate of hysteresis heating, and thus the temperature rise, will be in direct proportion to the velocity.

The effect of temperature on tensile strength of rubber is shown in Figure 5-1[2]. Tear strength and tensile strength are generally closely related. In Figure 5-1, the material that most closely resembles track pad material is the Styrene-Butadiene Rubber (SBR) compound. Strength is still falling rapidly as temperature rises at 140°C.

The rate of tear growth as a function of temperature under given loading conditions may be a good way to judge the effect of temperature on track pad mileage. Standard extrapolation techniques show a highly nonlinear positive relationship between rate of tear growth and temperature. Moderate reductions in temperature could therefore result in large increases in pad mileage.

In a test described to us by TACOM, a tank was run over a glass block on which a metal bar was placed (to model a rock). As the road wheels rolled over the pad, the event was photographed through the glass plate. This record clearly showed high tensile strains on the surface of the pad, in the direction of travel of the road wheel. The deformations imply a large tensile stress in the indicated strain direction. This helped in the choice of a direction for the reinforcement. See Figure 5-2.

5.2 Analysis

5.2.1 Influence of Temperature on Rate of Tearing

Figure 5-1 shows tensile strength as a function of temperature. Tensile strength is equivalent to the fatigue strength with one cycle to failure. The failure mode of track pads is closer to a many cycle fatigue mode, with tears growing a small increment with each cycle of loading. A way of evaluating the effect of temperature on this process is a Williams-Landel-Ferry (WLF) relation[3], fit to data for rates of tear growth at temperatures of 20°C and 70°C. The relation can be expressed as:

R = rate of tear

T = temperature

T_g = glass transition temperature (-63°C for SBR)

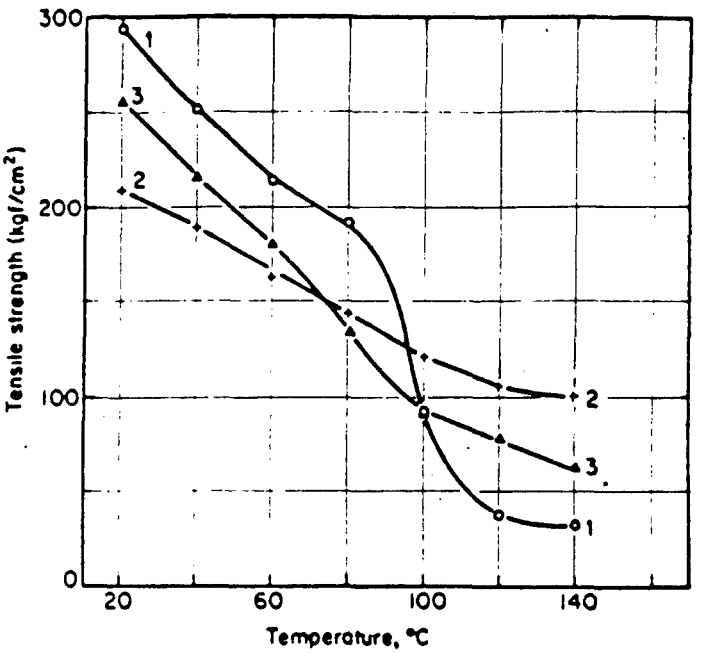

FIG. 3.3 Tensile strength *v.* temperature
Curve 1 Natural rubber gum compound
Curve 2 Natural rubber containing 50 parts lampblack per 100 of rubber
Curve 3 SBR containing 50 parts HAF black per 100 of rubber

Figure 5-1. Strength Vs Temperature (Ref. 2)

$$\frac{R(T)}{R(T_o)} = \frac{a(T_o)}{a(T)}$$

$$\log_{10}[a(T)] = \frac{-8.86(T-T_s)}{101.6+T-T_s}$$

$$T_s = T_g + 20°C \qquad (1)$$

Using this formulation, the effect of a change in temperature on the rate of tear growth for a given loading can be estimated. Figure 5-3 was generated using T_o = 160°C. Reducing the temperature from 160°C to 120°C results in the rate of tear growth dropping by 64%. These temperatures are outside the range of the data. Nevertheless, the trend offers some useful insights.

5.2.2 1-D Thermal Analysis of Track Pad

Much can be learned from reducing the problem to its simplest analytical form, and examining a closed form solution. The simplest model of the track pad is one-dimensional, through the thickness, with uniform heat generation due to hysteresis, convective boundary conditions, and steady state[4]. A summary is as follows:

W = heat input rate per unit volume from hysteresis

T = temperature, T_s = T(surface), T_f = T(free stream)

k = thermal conductivity

h = surface heat transfer coefficient

Y = direction of heat flux, boundaries at Y = 0, L

ρ = density

c = specific heat

t = time

$$\rho c\frac{\partial T}{\partial t} = 0 = k\frac{d^2T}{dY^2} + W$$

$$-k\frac{dT}{dY} = h(T_s-T_f) \text{ at } Y = 0,L \qquad (2)$$

0118n

Choose Fiber Orientation Based on Tensile Stress, Heat Flow

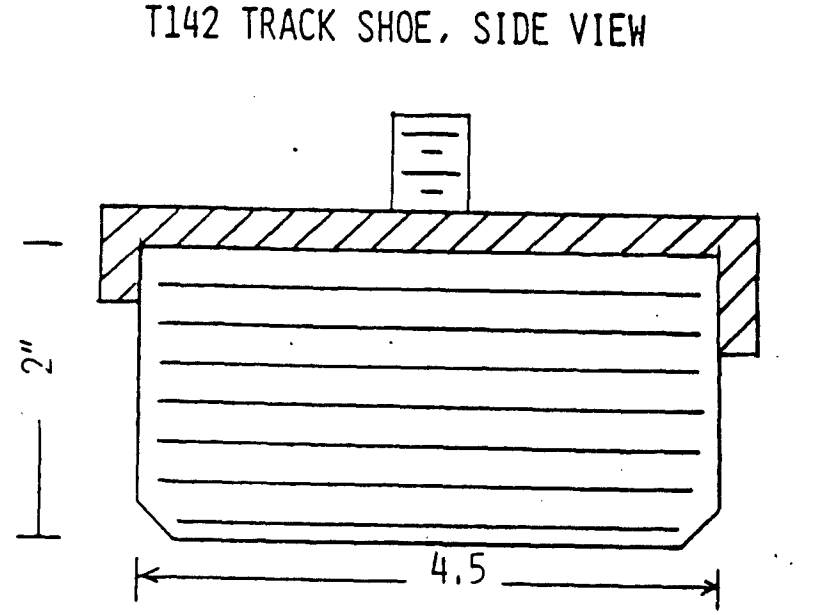

Figure 5-2. Orientation of fiber reinforcement. Fibers are continuous and unidirectional

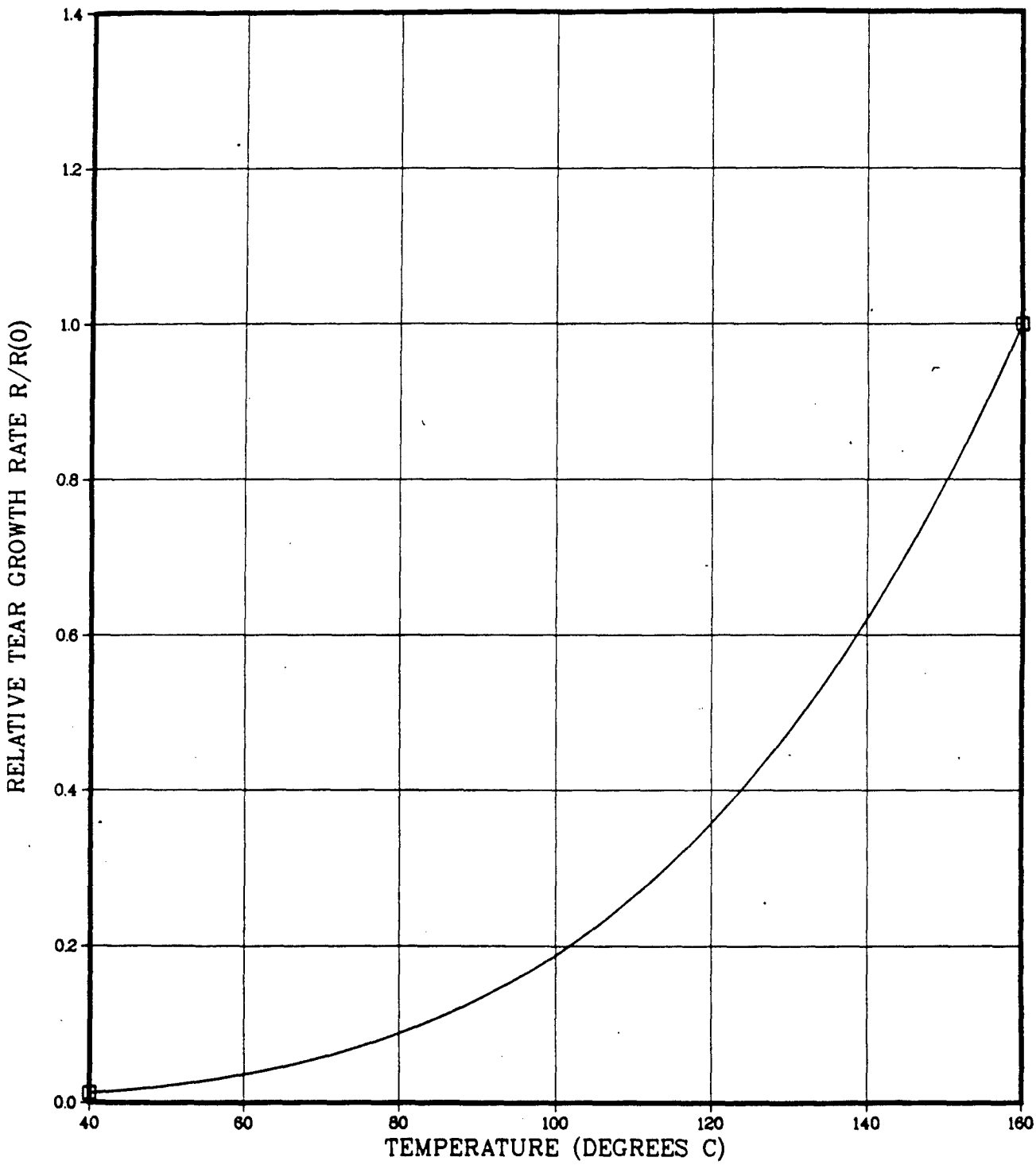

Figure 5-3. Relative tear growth rate in SBR as a function of temperature (WLF formulation)

Integration yields

$$T = W\left[\frac{Y(L-Y)}{2k} + \frac{L}{2h}\right] + T_f$$

$$\Delta T = T - T_f, \quad \Delta T_{max} = \Delta T(L/2) = (WL/2)[(L/4k) + (1/h)]$$

$$\Delta T(Y=0,L) = \frac{WL}{2h} \tag{3}$$

Clearly, internal temperature will be reduced if W is reduced, or if k or h are increased.

Temperatures calculated from the baseline formulation are compared below to actual measurements[1,5]. Field track pad temperature measurements were extrapolated approximately to steady state for comparison purposes. (The references also reported numerical predictions made using a detailed finite element model.) The relevant inputs for the 1-D model are as follows:

$W = 3.*10^{5}$ erg cm^{-3} s^{-1}

$k = 3.17*10^{4}$ erg cm^{-1} s^{-1} $°C^{-1}$

$h = 1.7*10^{4}$ erg cm^{-2} s^{-1} $°C^{-1}$

L = 2.125 inches = 5.4 cm,

measurements at Y = 0, 1.6 cm

Using the 1-D equations,

$\Delta T(Y=0) = 48°C$

$\Delta T(Y=1.6\text{ cm}) = 76°C$ (4)

$\Delta T(Y=2.7\text{ cm}) = 82°C$

Extrapolating from time-temperature data presented in Ref. 1 gives the following steady state estimates:

$\Delta T(\text{surface}) = 50°C$

$\Delta T(\text{interior, } Y = 1.6\text{ cm}) = 70°C$ (5)

The closeness of the results indicates that the basic 1-D model is sound. Now, the terms W, k, and h will be examined to see how pad temperatures might be reduced.

Here, the loading of the pad by the road wheel is modeled as simple one-dimensional compression, and the pad rubber as a simple linear visco-elastic material (small strain). The heat input per unit volume per load cycle can be expressed as[6]:

$$(W/cps) = \frac{\pi}{2}\tan(\delta)*(\text{Elastic Strain Energy})$$

$$= \frac{\pi}{4}\tan(\delta)\frac{\sigma^2}{E}, = 1.1486 \text{ psi, for} \qquad (6)$$

$\tan(\delta)$ = damping factor ($\simeq$ .09 for SBR)

E = elastic dynamic modulus (1040 psi for Interational Rubber Hardness Degrees (IHRD) = 70)

σ = average compressive stress ($\simeq$ 130 psi for an M60 tank)

cps = loading cycles per second

The average number of compressive load cycles for a given time can be expressed as

$$N_C = \text{Number of load cycles} = \frac{V*t*N_{RW}}{L_T} \qquad (7)$$

V = velocity of vehicle (20 mph = 29.3 ft/s)

t = time

N_{RW} = number of road wheels (6)

L_T = length of track ($\simeq$ 40 ft)

then,

$$cps = \frac{N_C}{t} = \frac{V*N_{RW}}{L} = 4.4 \qquad (8)$$

$$W = (W/cps)*cps = 5.05 \text{ psi}\cdot s^{-1}$$

$$= 3.49*10^5 \text{ erg}\cdot cm^{-3}\cdot s^{-1}$$

This is close to the value given in the literature[5].

Equation 6 shows that the means available to lower W are to lower the damping factor and to raise the elastic modulus. The mode of reinforcement shown in Figure 5-2 will enforce a zero strain condition in the wire (X) direction. For simple vertical (Y) loading, and zero lateral (Z) stress, simple elasticity gives the following:

E = elastic modulus

ν = Poisson ratio ($\simeq 0.5$ for rubber)

ϵ_x, ϵ_y = normal strains in the X and Y directions

σ_x, σ_y, σ_z = normal stresses in the X, Y and Z directions

$$\epsilon_x = 0 = \frac{1}{E}(\sigma_x - \nu\sigma_y),\ \sigma_x = \nu\sigma_y$$

$$\epsilon_y = \frac{1}{E}(\sigma_y - \nu\sigma_x) = \frac{1}{E}\sigma_y(1 - \nu^2)$$

$$\sigma_y = \frac{E}{1-\nu^2}\epsilon_y \simeq \frac{4}{3}E\epsilon_y \qquad (10)$$

The effective modulus in the Y direction is raised by 1/3 due to the constraint of the reinforcement. Because $\epsilon_x = \sigma_z = 0$, all of the work is still done by σ_y. Equation 6 (for uniaxial loading) thus still applies, but with the effective modulus as shown above. Thus, W is reduced by 25%. Reinforcement in a second direction would raise the pad stiffness to the order of the bulk modulus of the rubber (~ 100,000 psi), which would probably impair the suspension functions of the pad. 1-D reinforcement should be acceptable, since the stiffness remains of the same order as when no reinforcement is present.

The damping factor can be changed by changing the material. While tan(δ) is taken as 0.09 for SBR, a value of 0.06 is usually reported for natural rubber (NR) compounds. Compounding changes, such as adding different amounts or types of carbon black, will directly change the elastic modulus.

Metallic wire reinforcement will directly affect the thermal conductivity in the pad. For small wire volume fractions, the effect transverse to the wire direction can be ignored. In the wire direction, thermal conductivity at steady state will be a simple volume average of the values for the wire and the rubber.

A specific example is as follows: The wire is carbon steel, 0.032 inch (0.8 mm) diameter, spaced 0.25 inch (6.4 mm) apart in a square array, oriented uniaxially.

$$k_{wire} = 28\ Btu*ft/(ft^2*hr*°F) = 4.85*10^6\ erg*cm/(cm^2*s*°C)$$

$$k_{rubber} = 3.2*10^4\ erg*cm/(cm^2*s*°C)$$

0118n

wire volume fraction $V_f = 0.0129$

$$k = V_f * k_{wire} + (1 - V_f) * k_{rubber}$$

$$k = 9.4*10^4 \text{ erg*cm/(cm}^2\text{*s*°C)} \quad (11)$$

This is a significant increase over the value for the rubber. It cannot, however, be used directly in the 1-D formulation (equation 3), because the wire direction is not the direction of the minimum pad dimension (the Y direction). Later, 2-D numerical results will be presented which use this increased thermal conductivity in the wire direction.

Surface heat transfer can be influenced by the free stream temperature T_f, and by the heat transfer coefficient h. T_f is effectively the temperature of the heat sink into which energy is transferred from the body in question. h is a property of the free stream material, velocity, manner of flow (laminar vs turbulent), the size of the body, and other factors. For instance, h for a free stream liquid is usually higher than for a free stream gas, all other factors (ie, free stream velocity) being equal. The form presented for a six inch body length and 100°F free stream air with laminar flow over the pad is[7]

$$h = 0.0157 \text{ Btu°F}^{-1}\text{hr}^{-\frac{1}{2}}\text{ft}^{-\frac{5}{2}} * (V_\infty)^{\frac{1}{2}}$$

$$h(20 \text{ mph}) = 5.11 \text{ Btu/(ft}^2\text{hr°F)}$$

$$= 2.90*10^4 \text{ erg/(cm}^2\text{s°C)} \quad (12)$$

The functional form shows the influence of the free stream velocity V_∞. The computed value at 20 mph is somewhat higher than that used in the 1-D model. For the 2-D numerical studies, a compromise value is used for 20 mph travel:

$$h = 2.35*10^4 \text{ erg/(cm}^2\text{s°C)} \quad (13)$$

Equation 12 shows that increasing free stream velocity can increase surface heat transfer; this suggests that a blower system might be useful. Another way to increase h is to increase the effective surface area. For instance, short slots on the X surface (normal to the wire direction) could double the effective area on that surface, thus doubling h in the X direction.

5.2.3 Mechanical Loads From Sharp Asperities

The type of loading which results from running over sharp asperities (ie, rocks, debris) can be seen deduced from a calculation[8], which is

summarized in Figures 5-4 and 5-5. (The calculation is for a unit thickness, plane stress.) The angle γ arises from the action of the road wheel, and causes tensile stresses in parts of the pad. The orientation of this tensile stress helped motivate the choice of the direction of reinforcement.

5.2.4 Stress In Reinforcement

For the reinforcement to work properly, the wires must not break, and must maintain adhesion with the rubber. Simple estimates of the tensile stress in the wires and the shear stress at the wire-rubber interface are given in Figures 5-6 and 5-7. A high value of compressive stress is used to model the effect of very uneven terrain. The results show that a high strength wire is preferable. Steel tire cord is more than adequate, while aluminum, copper, or brass wire would require higher volume fractions.

5.2.5 Fracture Mechanics Approach To Debonding

In the above discussion, debonding is approached by estimating the shear stress at the bond interface. A better approach is to use a fracture mechanics formulation[9,10]. The basis of the formulation is a Griffith-type energy model in which energy for debonding comes from the net loss in the sum of the potential energy of the load and the strain energy in the rubber. (The reinforcement is assumed rigid, hence storing no strain energy.) Energy conservation can be written as:

$$\delta(\text{Surface energy} + \text{Potential energy} + \text{Strain energy}) = 0 \qquad (14)$$

(δ indicates a differential)

One development assumes a constant displacement of the loading device; hence, the potential energy does not change, and strain energy falls as the debonded or torn area grows due to unloading of material near the new free surface[9]. The other development assumes a constant load[10]. In that formulation, potential energy drops and strain energy rises as debonding progresses.

An alternate failure mechanism of tearing through rubber rather than debonding reinforcement is also explored[9,10]. This is an unlikely failure mechanism for reinforced track pads. Analysis will concentrate on the debonding problem.

A test method has been developed for measuring the adhesive fracture energy per unit area (G_a) needed to debond a wire-rubber interface[10]. The load is fixed and G_a is independent of crack length, so when debonding starts, it is total, and the test piece (Figure 5-8) fails completely. This value of G_a represents one cycle to failure, but as discussed before, track pads must withstand many cycles to failure. Existing data[9] can be used to relate lower values of G_a to debond growth per cycle. Hence, some estimate of fatigue life can be made.

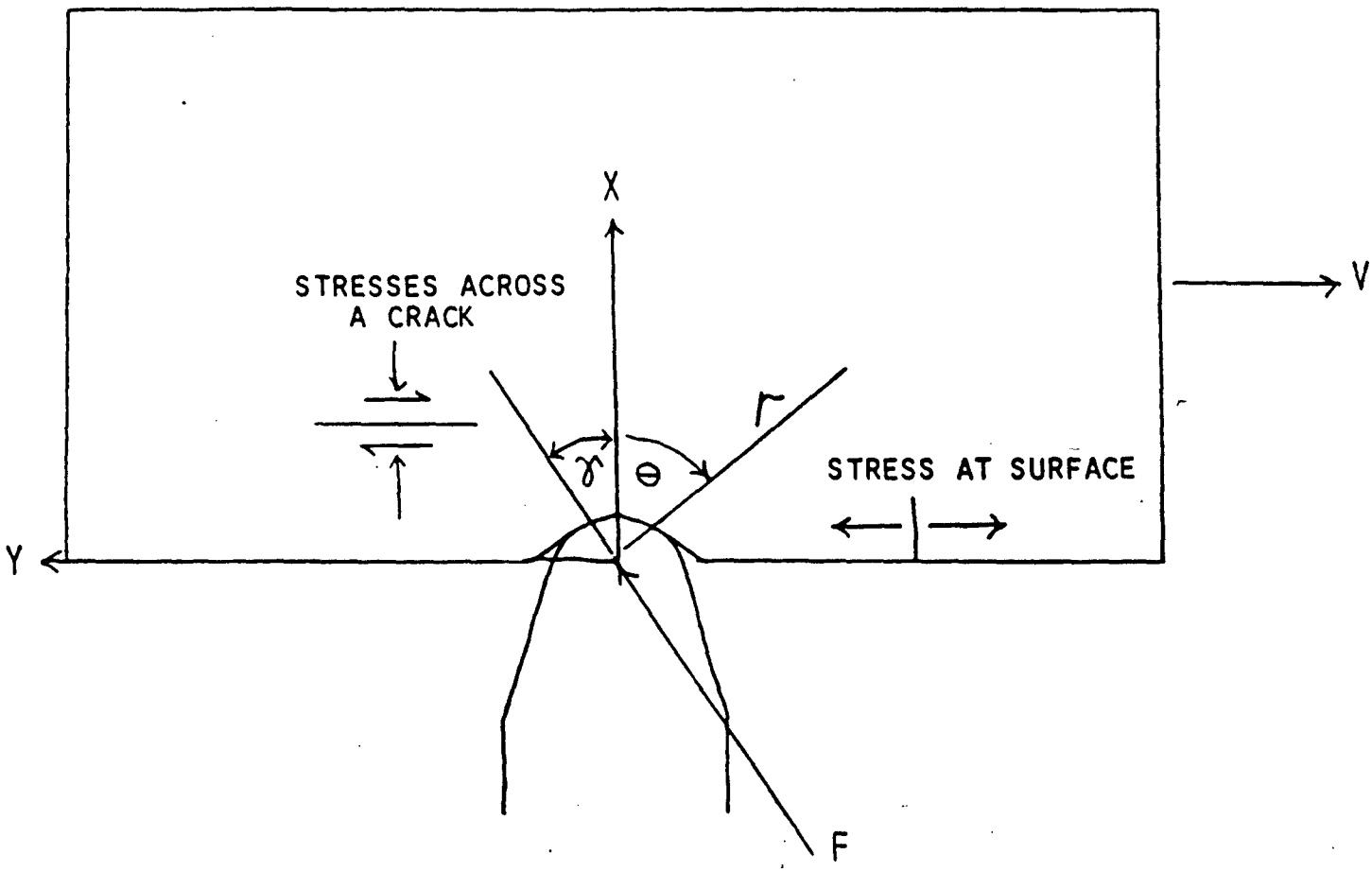

Figure 5-4. Track shoe moving over surface asperity

$$\sigma_r = \frac{-2E}{\pi r} \cdot \cos(\gamma + \theta)$$

$$\sigma_x = \sigma_r \cos^2(\theta), \quad \sigma_y = \sigma_r \sin^2(\theta), \quad \tau_{xy} = \sigma_r \sin(\theta)\cos(\theta)$$

ON SURFACE, AT $\theta = +\frac{\pi}{2}$, $\sigma_y = \frac{+2E}{\pi r} \sin(\gamma)$

(TENSILE STRESS AT SURFACE)

INSIDE, τ_{xy} CAN CAUSE CRACK GROWTH (INHIBITED BY COMPRESSIVE σ_x)

Figure 5-5. Mathematical form of the stresses

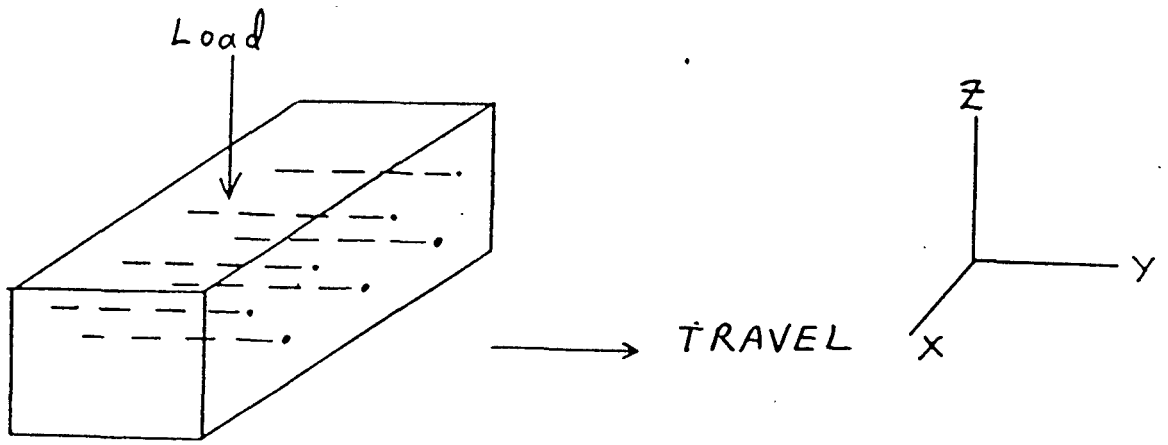

Fibers impose plane strain; $\sigma_y = \nu \sigma_z$

Fiber stress by force equilibrium; $\sigma_f = -\nu \sigma_z \frac{(1-VF_f)}{VF_f}$

$\nu = 0.5$, $VF = 0.01$, $\rightarrow$ $\sigma_f = -49.5 \times \sigma_z$

$\sigma_z \sim -1500$ psi $\rightarrow$ $\sigma_f = 74250$ psi (Need high fiber strength)

Figure 5-6. Uniaxial fiber loading in pad under compression

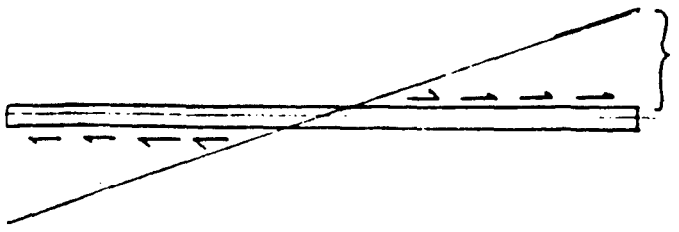

$$\tau = \tau_m \cdot \frac{2x}{l}, \quad d\sigma_f \cdot \pi r^2 = \tau \cdot 2\pi r\, dx$$

integrate, $\sigma_f \sim \tau_m \frac{l}{r}$

$$\tau_m = \sigma_f \frac{r}{l} \sim 74250_{psi} \times \frac{.005}{4} = 93\ psi$$

Need good bonding

Figure 5-7. Shear stress at fiber-rubber interface

Referring to the wire pullout specimen shown in Figure 5-8, the energy balance (Equation 14) can be written

$$\delta[G_a * 2\pi ac - F_p\beta + \int_0^{\beta} F d\beta] = 0, \quad \beta = c * \frac{\Delta L}{L_o} \tag{15}$$

β is the displacement of the wire which occurs when the newly debonded length c stretches by the strain $\Delta L/L_o$. The first term in brackets is the new surface energy created when the debond grows by length c. The second term is the drop in potential energy of the applied load due to the displacment β. The third term is the gain in strain energy due to stretching of the rubber adjacent to the debonded length c by the strain $\Delta L/L_o$. Applying the differential to equation 15 gives

$$G_a = \frac{1}{2\pi a L_o}[F_p \Delta L - \int_0^{\Delta L} F d(\Delta L)] \tag{16}$$

The term in brackets is a nonlinear complementary energy function, as shown in Figure 5-9. For linear stress-strain behavior, Equation 16 can be simplified as follows:

$$\bar{A} \equiv A - \pi a^2, \quad \sigma_p = \frac{F_p}{\bar{A}}, \quad \varepsilon = \frac{\Delta L}{L_o} = \frac{\sigma_p}{E}$$

$$\int_0^{\Delta L} F d(\Delta L) = \frac{F_p \Delta L}{2} \tag{17}$$

$$G_a = \frac{F_p^2}{4\pi \bar{A} a E}$$

This is the form derived in the literature[10].

As discussed before, G_a from Equation 16 or 17 is a surface energy term for failure in one loading cycle. When the applied load is less than the failure load (F_p), the test piece can withstand more than one cycle to failure. The following example shows how the number of cycles to failure for a less than critical load could be estimated.

Consider a wire pullout specimen with linear elastic behavior (Equation 17) and with the following conditions at failure:

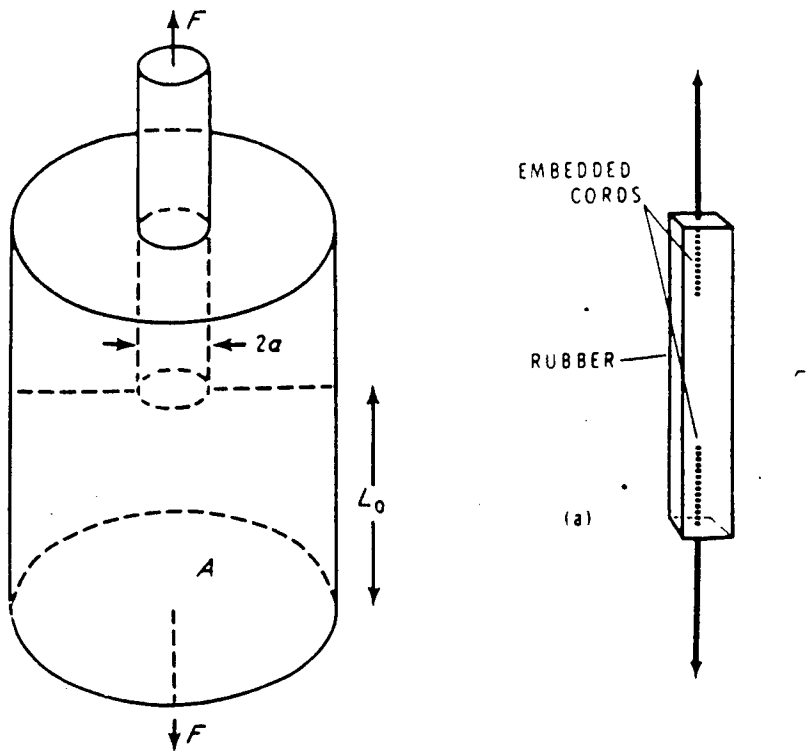

Figure 5-8. Wire pullout test piece (Ref. 10)

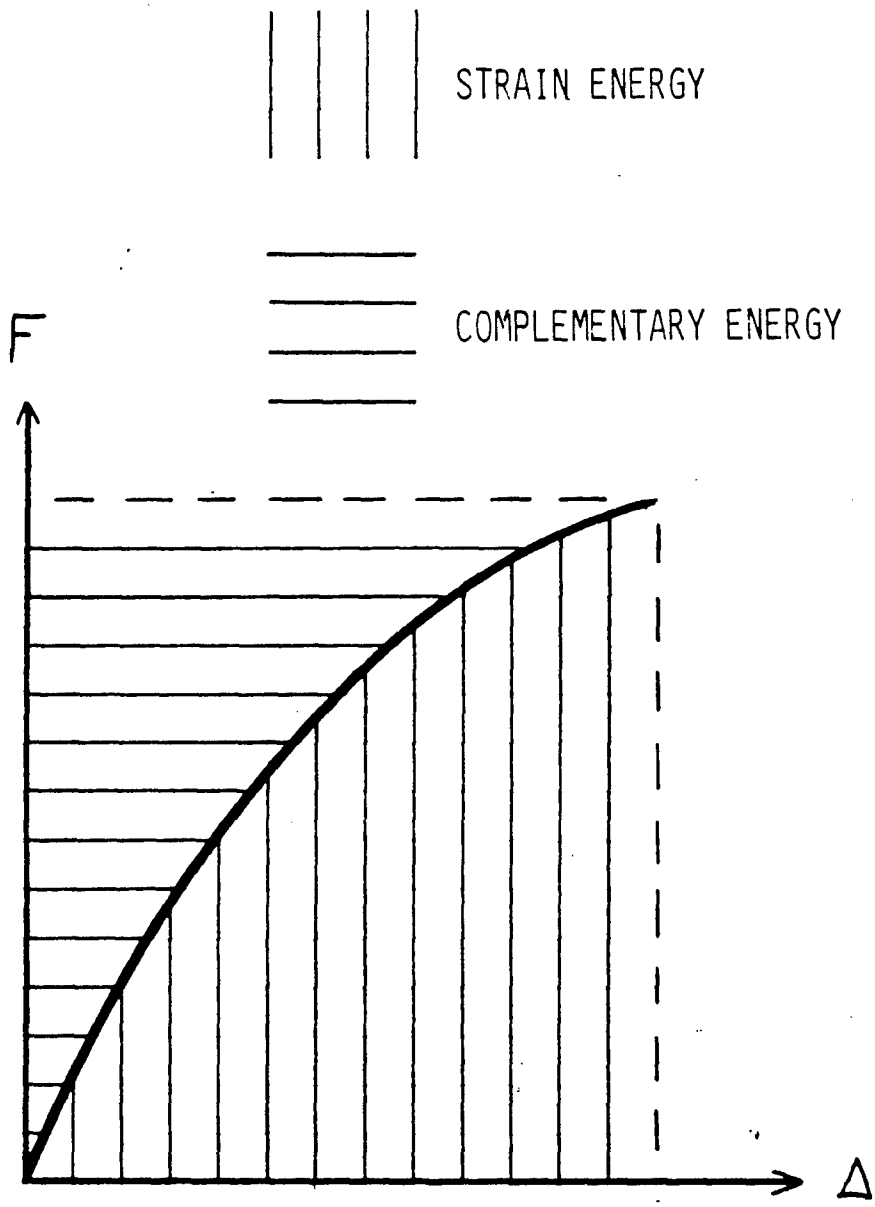

Figure 5-9. Nonlinear elastic behavior

$F_p = 32$ lbf

$A = 0.25$ in^2

$L = 1$ inch, $\Delta L = 0.7$ inch

$E = 183$ psi

$a = 0.016$ inch (18)

$G_a = 111.3$ lb/in $= 19.5$ kJ/m^2 (Equation 17)

This is typical of the values of G_a reported in Reference 10 for brass coated steel wire in rubber. It represents one cycle to failure. Now,consider the case of cyclic loading with a maximum force of 8 lb. Using Equation 17, this gives an available debonding energy per unit area G = 1.2 kJ/m^2. The data from Reference 9 is presented in Figures 5-10 and 5-11, which give the debond growth per cycle as a function of the available debonding energy. The data for reinforced rubber is slightly to the left of that for rubber alone, indicating that the bond energy is somewhat less than the tear energy in the rubber itself. Using the dashed line in Figure 5-11, the debond growth per cycle is roughly 40 nm (nano-meters), or 4×10^{-6} cm. Thus, for the debond to grow by 1 cm, 250,000 load cycles would be required.

A calculation similar to the one above can be carried out for the reinforced track pad configuration, shown in Figure 5-12 with the pad idealized as a rectangular block. Since the loading is through a steel plate, both bonded and debonded sections of the pad see the same strain. The rubber is idealized as linear elastic, and a small strain elastic modulus is used. As derived in Equation 10, the effective modulus in the bonded region is taken as 4/3 the modulus of the rubber alone. Bonded and debonded regions thus see the same vertical strain, but different stresses. Recognizing that the debonded length c is the variable, Equation 14 can be written as

$$\frac{d(\text{Surface Energy})}{dc} = \frac{-d(\text{Potential Energy} + \text{Strain Energy})}{dc} \qquad (19)$$

For linear elastic behavior, the gain in strain energy equals half of the loss in potential energy, as is the case in Equation 17. The terms in Equation 19 are computed as follows:

$$F = (L_x - c)L_z\frac{4}{3}E_R\epsilon_y + c^*L_zE_R\epsilon_y$$

$$= L_zE_R\left(\frac{4}{3}L_x - \frac{c}{3}\right)$$

$$\text{Potential Energy (P.E.)} = -F^*\delta Y = -F\epsilon_yL_y$$

$$\text{P.E.} = \frac{-F^2L_y}{L_zE_R\left(\frac{4}{3}L_x - \frac{c}{3}\right)^2} \qquad (20)$$

0118n

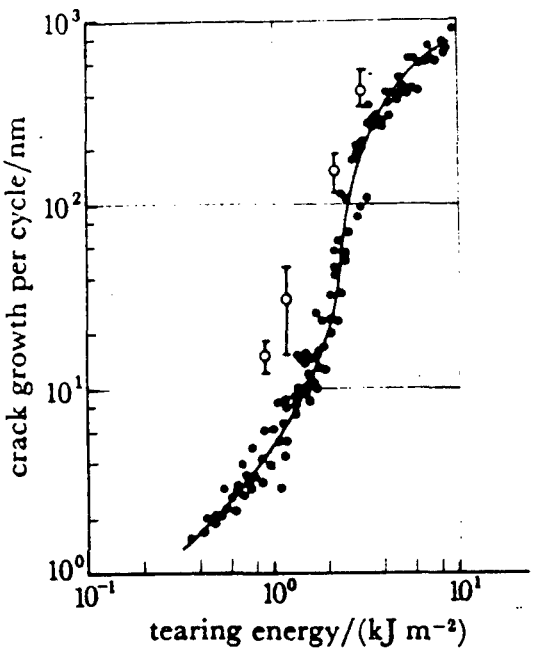

FIGURE 10. Comparison of averaged crack growth rates in laminates of standard construction (o) with resul from independent measurements on tensile strip test-pieces of the ply rubber (•). The bars indicate th range of the results for the laminates.

Figure 5-10. Comparison of Averaged Crack Growth Rates (Ref. 9)

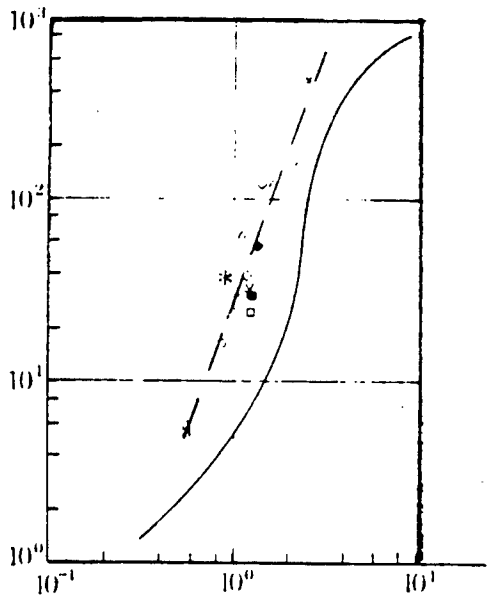

symbol						■	◆		*
ply separation/mm	1.1	2.0	2.3	2.0	3.9	1.3	1.3	1.3	1.3
laminate thickness/mm	6.9	3.4	7.0	9.7	6.9	3.5	3.5	6.2	6.5
cord angle, ψ/deg	22	22	22	22	22	30	15	22	22
number of cords per inch	10	10	10	10	10	10	10	5	3½

Averaged crack growth rates for laminates of various constructions. The line is the same as that drawn through the independently measured crack growth characteristics shown in figure 10.

Figure 5-11. Debond Growth Per Load Cycle (Ref. 9) Scales as in Figure 5-10, Dashed Line Added Here.

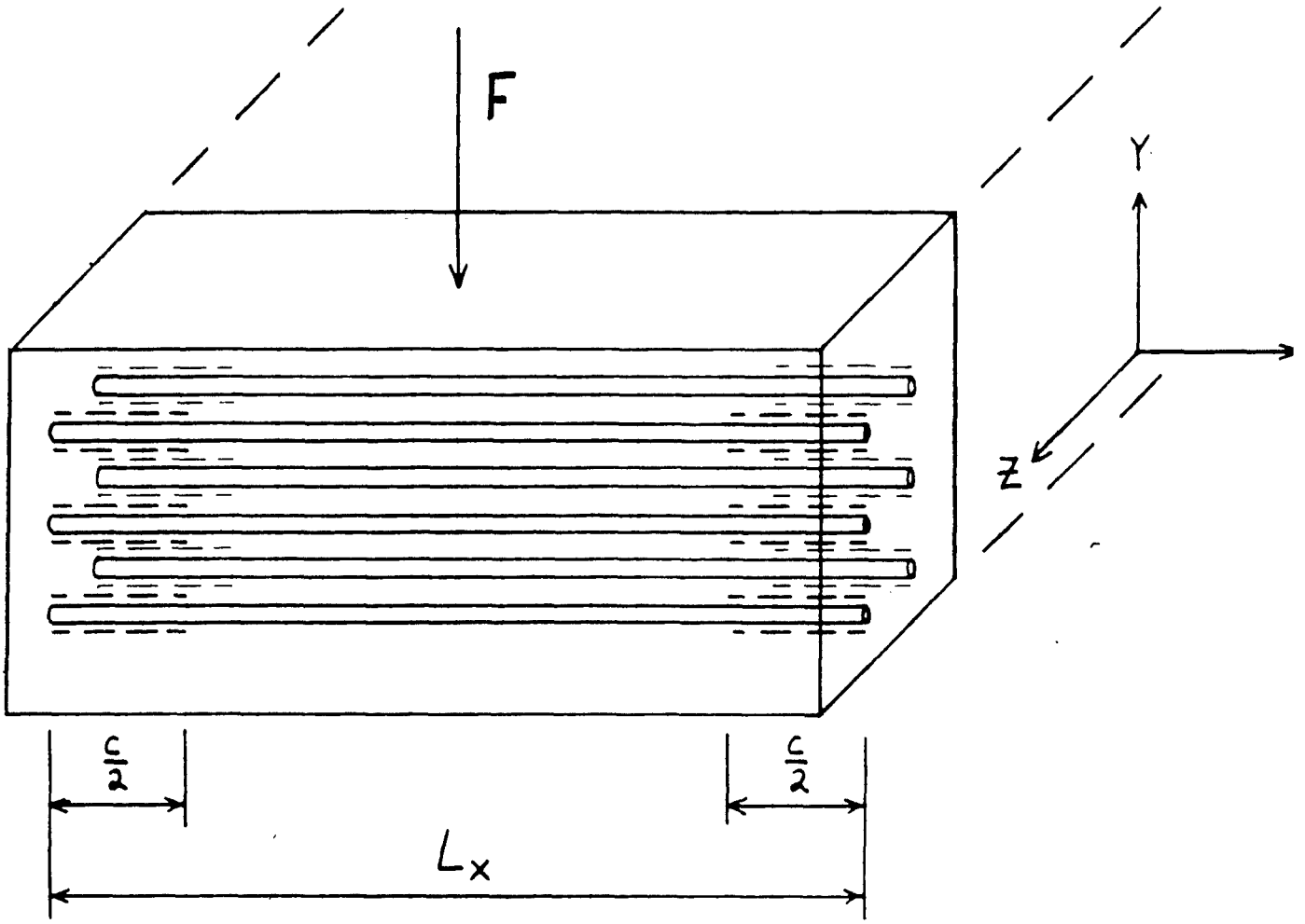

Figure 5-12. Debonding Under Compressive Loading

Surface Energy (Su.E.) = $G\pi DcN_w$

N_w = number of wires in the block, D = wire diameter

wire volume fraction = $V_f = \frac{\pi}{4}\frac{D^2 N_w}{L_y L_z}$

$$Su.E. = G\pi Dc * \frac{4V_f L_y L_z}{\pi D^2} \qquad (21)$$

As discussed before,

$$\frac{d}{dc}(\text{Strain Energy}) = -\frac{1}{2}\frac{d}{dc}(\text{P.E.})$$

Equation 19 then becomes

$$G\pi D * \frac{4V_f L_y L_z}{\pi D^2} = \frac{F^2 L_y}{6L_z E_R (\frac{4}{3}L_x - \frac{c}{3})^2}$$

$$G = \frac{DF^2}{24 . V_f L_z^2 E_R (\frac{4}{3}L_x - \frac{c}{3})^2} \qquad (22)$$

Typical numbers are

Wire diameter D = 0.032 inch

Load F = 5000 lbf

Wire Volume fraction V_f = 0.013

L_z = 8 inches

rubber elastic modulus E_R = 1000 psi (small strain)

L_x = 4.5 inches

debonded length c = 1 inch

$G = 7.07$ lb/in = 1.24 kJ/m^2 (23)

Using Figure 5-11 (dashed line), this corresponds to $6*10^{-6}$ cm of debond length per load cycle.

This can be translated into a relation between mileage and debonded length as follows:

0118n

track length L_T = 40 ft

number of road wheels N_{RW} = 6

distance travelled X = 1000 miles

$$\text{number of load cycles } N_c = \frac{X * N_{RW}}{L_T} = 7.92 * 10^5$$

$$c = 6 * 10^{-6} \text{ cm/cycle} * N_c, = 4.75 \text{ cm}, = 1.87 \text{ inches} \quad (24)$$

This indicates that some significant debonding will take place over that distance. Equation 22 indicates how improvements could be made. Wire diameter could be made smaller, and wire volume fraction could be increased. Going to a finer wire size (.016 inch diameter) or a higher V_f (.026) would cut G by a factor of 2 (to 0.62 kJ/m^2). The debond length per cycle (dc/dN_c) from Figure 5-11 would then be 6 x 10^{-7} cm; one tenth of the previous value. Debonded length would then be 0.187 inch.

Several approximations were made so that this analysis could proceed; it is useful to discuss their impact on the results. First, the effect of friction on the debonding process was not considered. Since the pad, and the bonds, are loaded in compression, this might significantly decrease dc/dN_c. Second, temperature effects may increase dc/dN_c as the pad temperature increases. (See section on material development, and Appendix B). Third, the use of the data from Figure 5-11 in this manner involves approximations due to both the scatter in that data and the extrapolation to a different test geometry. The results still retain validity, but the trends may be more accurate than the absolute numerical results. For instance, the example in the previous paragraph shows that fatigue life is very sensitive to the bonded area, as reflected in the wire size and wire volume fraction. If a given choice of wire diameter and volume fraction gives marginal results in testing, modest changes in these parameters could result in large improvements in performance.

5.2.6 2-D Time Dependent Thermal Solution Method via Finite Differences

The track pad size is roughly 2 inches x 4.5 inches x 10 inches. The more important temperature variations will be seen in the short dimensions, so, for the 2-D model, the long dimension is omitted. The grid model is shown in Figure 5-13. X and Y were used as the horizontal and vertical directions. A 6 x 6 grid was found sufficient to accurately model typical test cases, as were found in References 4 and 11. (These were 1-D and 2-D problems, typically solved by expansion techniques).

The governing equation, analagous to the first of Equations 2, but with time dependence and two spacial dimensions retained, is

$$\rho c \frac{\partial T}{\partial t} = k_x \frac{\partial^2 T}{\partial X^2} + k_y \frac{\partial^2 T}{\partial Y^2} + W \quad (25)$$

k_x = k in X direction, increased by presence of wire

k_y = k in Y direction, ≈k of rubber

0118n

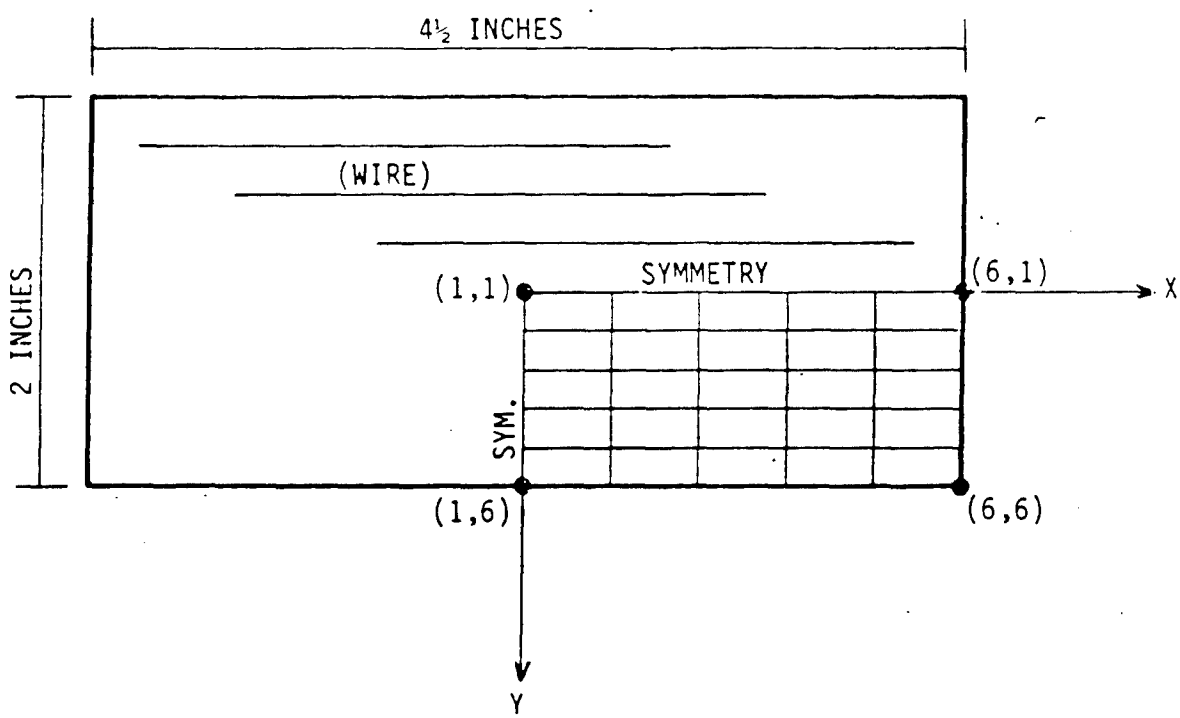

Figure 5-13. Two-dimensional pad geometry. Computational grid (NI = NJ = 6), lines of symmetry shown, wire orientation shown

Two types of boundary conditions will be considered. The first, a convective boundary condition, is analagous to the second of equations 2:

$$\frac{\partial T}{\partial n} = \frac{-h}{k_n}(T_s - T_f) \tag{26}$$

n = outward normal direction.

This would typically apply to a body sitting in an air stream. The second type of boundary condition is a specified surface temperature, and would apply to a body held in a heated mold:

$$T_s = T_m \tag{27}$$

The finite difference time step requires a finite difference form of Equation 25. Where (I,J) represent node points (I varies in the X direction, J in the Y direction) in Figure 5-13, and ΔX, ΔY are the distances between node points, the typical finite difference form of the second derivative is

$$\frac{\partial^2 T}{\partial X^2} = \frac{T(I+1,J) - 2T(I,J) + T(I-1,J)}{(\Delta X)^2} \tag{28}$$

This is modified at the line of symmetry (I = 1) and at the boundary (I = NI). At the line of symmetry, I = 1, and T(I-1,J) will be equal (by symmetry) to T(I+1,J). Therefore

$$\left.\frac{\partial^2 T}{\partial X^2}\right|_{I=1} = \frac{2[T(2,J) - T(1,J)]}{(\Delta X)^2} \tag{29}$$

At the boundary, first consider the condition given by Equation 26. The first derivative at the surface can be put into difference form:

$$\left.\frac{\partial T}{\partial X}\right|_{I=NI} = \frac{T(NI+1,J) - T(NI-1,J)}{2(\Delta X)}, = \frac{-h_x}{k_x}[T(NI,J) - T_f] \tag{30}$$

T(NI+1,J) is a fictitious value, lying outside of the body. It is useful because it can be computed from Equation 30, and then used to compute the second derivative:

$$T(NI+1,J) = T_{out} = T(NI-1,J) - 2(\Delta X)\frac{h_x}{k_x}[T(NI,J) - T_f] \tag{31}$$

0118n

A similar development applies for $\partial^2 T/\partial Y^2$.

When integrating forward in time, the time step must be chosen small enough to maintain accuracy. Some guidance can be found in Reference 11. Consider the 1-D difference form of Equation 25:

$$\frac{\rho c \Delta T}{\Delta t} \simeq \frac{k[T(I+1) - 2T(I) + T(I-1)]}{(\Delta X)^2} \tag{32}$$

From dimensional considerations, one can write

$$\Delta t \text{ is order of } \frac{[(\Delta X)^2 \rho c]}{k}$$

$$= \text{constant} * \frac{(\Delta X)^2}{\bar{D}}, \quad \bar{D} \equiv \frac{k}{\rho c} \tag{33}$$

The constant is sometimes taken as 0.5 for a special solution method[11]. Here, it is taken initially as 0.2, Δt is calculated for the X and Y directions, the smaller value chosen, and further reduced to some convenient integral value. (In calculations presented later, Δt is 25 seconds, reduced from the 33.39 seconds calculated for the Y direction).

5.2.7 Curing Model

So far, the formulation has concentrated on modeling the hysteresis heating of fully cured rubber track pads. Because the formulation calculates temperature throughout the pad as a function of time, and because a fixed temperature boundary condition can be used, the curing process itself can be modeled. This is important because thick rubber parts are difficult to cure evenly, due to the low thermal diffusivity of rubber, but good performance requires a fairly even cure. The difficulty arises because the outside of the block, being close to the mold walls, usually sees a more severe temperature-time history than the inside of the block.

A common approximation used to model the dependence of rate of cure on temperature is the temperature coefficient of vulcanization (TC), and is the factor by which the rate of cure increases for a 10°C increase in temperature over some reference temperature (T_{REF})[11]. A standard value from the literature is TC = 2. The equation used here to describe this process is

$$\frac{d(SC)}{dt} = (TC)^{[0.1(T-T_{REF})]} \tag{34}$$

0118n

where SC is state of cure. As a simple example, consider an ideal cure which is 27.5 minutes at 290°F (143.3°C). Taking 143.3°C as the reference temperature, Equation 34 gives rates of curing for differing temperatures. The actual state of cure, in equivalent time at $T = T_{REF}$, can be expressed as

$$SC = \int_0^t \frac{d(SC)}{dt} dt = \int_0^t (TC)^{[0.1(T(t)-T_{REF})]} dt \qquad (35)$$

This is easily added to the finite difference formulation, which updates the temperature at each node as time progresses. A different curing relation, such as a different equation or tabular data, could also be used.

5.3 Material Development

5.3.1 Material Selections

A range of rubber compounds was considered, based on physical properties and adhesive bonding to reinforcement. A series of test compounds were devised based on Bergstrom's baseline SBR[12], and included both elemental sulfur (conventional) and EV (sulfur donor, efficient vulcanization) cure systems. Compounds with conventional cures can bond to bare brass or bronze coatings, with no adhesive needed. EV cure systems sometimes give better physical properties, and can also be less sensitive to overcuring. (The inside of the pad can be more fully cured without causing reversion (property degradation) near the surface). However, EV cure systems do not give bonding to brass or bronze coatings, so an adhesive must be used. If the decision is made to use an adhesive. then brass or bronze coatings are no longer a constraint with regard to bonding. (They are still useful for corrosion protection, as was found when test specimens were prepared.) Other rubber compounds tested were an all NR compound with conventional cure, a compound from a companion program, and a TACOM standard triblend (14A, MIL-T-11891C(AT)) conventional cure compound.

Some rubber compounds used in this study are given in Tables 5-1 and 5-2. Table 5-1 shows compounds made expressly for this program (Avon Custom Mixing, Holbrook, Mass). Table 5-2 shows a compound made for the companion program[13], which was tested in this program. The 14A compound is detailed in the MIL spec. Samples were supplied by Avon Custom Mixing, and Goodyear (custom compounded by Avon, from stock by Goodyear). A conventional cure compound of unknown composition was also supplied by Avon for experimentation. Some important features of the compounds are summarized below.

Designation	Rubber Type	Cure Type
20A	SBR	conv.(high sulfur)
20B	SBR	EV (low sulfur)
20C	SBR	conv. (high sulfur)

0118n

20D	SBR	conv. (med. sulfur)
20E	NR	conv. (high sulfur)
A54	SBR/BR/NR	conv. (med. sulfur)
14A	SBR/BR/NR	conv. (med. sulfur)

Here, high sulfur means 3.5 phr, which is a standard recommendation for adhesion to brass.

Four types of wire were considered: solid brass wire, brass coated steel wire (tire wire) bronze coated steel wire (hose wire), and a steel wire with a thick copper coating. The latter, whose trade name is Copperply^R, has 30% of the thermal conductivity of solid copper, yet retains the strength of steel, since it is roughly 80% steel by volume. (Samples of tire wire, hose wire, and Copperply^R were obtained from National-Standard Company, Niles Mich.).

Samples of several types of metal-rubber adhesives were obtained from Lord Chemical Corporation, Erie, Pa. These can be applied to the wire, which is then inserted into the uncured rubber. The adhesive then co-cures with the rubber. Before curing, the adhesive is not bonded to the wire, so the surface coat is fragile. The adhesive of choice was Chemlok^R 252, a solvent based adhesive. It was chosen because it appeared to be the easiest to apply, and gave a relatively durable, flexible coat in the uncured state. (Water based adhesive coats were brittle when dry). To clean a copper surface in preparation for this adhesive, the following was used, based on the manufacturer's recommendation; a one minute etch in a 25% by weight solution of ammonium persulfate, followed by a water rinse. Initial cleaning was an acetone wash and an air or towel dry. Note that an etch was not required for the wires with brass or bronze surfaces because these were resistant to oxidation. The adhesive was applied by dipping, then dried in an oven at low heat. When necessary, the adhesive was diluted with solvent to give a thin coat, as per instructions from the supplier. Coated wires were sometimes stored for several days before the specimens were molded and cured.

5.3.2 Adhesion Tests

A series of adhesion tests were conducted as described in Equations 14 through 18. The test specimens were rubber blocks, 0.5 inch x 0.5 inch x 3 inches long, with wires inserted 1 inch into the block, along the centerline, from each end (see Figure 5-8). Samples were prepared by laying up the uncured rubber and the wires in a special mold, and curing in a heated press. Typical cures were 30 to 60 minutes at 290°F in the press, then cooling under tap water and room temperature. Samples were tested using an Instron testing machine, with a load rate of 50 pounds per minute. As discussed before, the proper loading method for the test is prescribed force (dead load), rather than prescribed displacement.

The adhesion test results are summarized in Table 5-3. G_a is calculated using the nonlinear formulation (Equation 17), and a linear small strain approximation using Equation 18 with an engineering stress-strain secant modulus. This gives the following:

0118n

Table 5-1 Rubber Formulations (PHR)

	20A	20B	20C	20D	20E
SBR 1500	100	100	100	100	-
N300 HAF	45	45	45	45	45
ZnO	5	5	5	5	5
Stearic Acid	2	2	2	2	-
UOP 88	3	3	3	3	-
Neozone D	1	1	1	1	-
Heliozone Wax	1	1	1	1	-
Process Oil	3	3	3	3	3
Sulfur	3.5	0.25	3.5	1.8	3.5
Amax	0.8	-	1.2	-	
Sulfsan R	0.5	-	0.75	-	0.5
Methyl Tuads	-	0.5	-	-	-
Morphax	-	2.5	-	-	-
Santocure NS	-	-	-	0.9	
NR					100
Zinc Stearate					1.5
Santocure MOR					0.8

Table 5-2 Long-Life Tank Tread (REF. 13) Formulation A54

	A54
Philiprene 1609	40.6
Cis-4 1350[1] O- Cis-4 135[2]	25.8
Pale Crepe	60
Saf Black	42
Zinc Oxide	3
Stearic Acid	2
Sulfur	2
Santocure	1.5
Thermoflex A	1
Piccopale 100	3.5
Santoflex AW	1.5
UOP 88	5
Heliozone Wax	1

[1]Cis-4 Polybutadiene master batch (100 parts Cis-4 1203, 80 parts Philblack I and 35 parts Philrich 5).
[2]Cis-4 Polybutadiene master batch (100 parts Cis-4 1203, 90 parts Philblack I and 50 parts Philrich 5).

Table 5-3: Wire Adhesion Tests (all wire diameters 0.032 inch except as noted)

TEST #	SPECIMEN #	RUBBER TYPE	WIRE TYPE	SURFACE PREP.	PULLOUT FORCE (LB)	PULLOUT ΔL (INCHES)	NONLINEAR G_a(kJ/m²)	LINEAR G_a(kJ/m²)
1	1332-85	20B	BRASS	CLEANING	25.4	0.68	10.1	15.0
2	1332-86	20B	BRASS	CLEANING	21.5	0.55	6.5	10.3
3	1332-87	20B	BRASS	CLEANING	17.5	0.35	3.8	5.3
4	1332-88	20B	BRASS	CLEANING	21.0	0.50	6.0	9.1
5	1332-89	20B	BRASS	CLEANING	21.9	0.51	6.7	9.7
6	1332-93	20B	STEEL (BRASS COAT)	CLEANING	7.0	0.1	0.3	0.6
7	1332-117-1	CONV. CURE	COPPERPLY®	ETCH, RINSE, ADHESIVE	30.0	0.4	8.5	10.5
8	1332-117-2	CONV. CURE	STEEL (BRASS COAT)	CLEANING	33.5	0.6	10.8	17.5
9	1400-1	20A	BRASS	CLEANING	25.5	0.35	5.5	7.8
10	1400-2	20A	BRASS	CLEANING	27.0	0.35	5.9	8.2
11	1400-3	A54	BRASS	CLEANING	31.3	0.60	9.6	16.4
12	1400-4	A54	BRASS	CLEANING	27.7	0.50	8.2	12.1

Table 5-3: Wire Adhesion Tests (Cont'd)

TEST #	SPECIMEN #	RUBBER TYPE	WIRE TYPE	SURFACE PREP.	PULLOUT FORCE (LB)	PULLOUT ΔL (INCHES)	NONLINEAR G_a(kJ/m²)	LINEAR G_a(kJ/m²)
13	1400-8	20B	BRASS	CLEAN, NO ETCH, ADHESIVE	32.0	1.2	23.0	33.4
14	1400-9	20B	COPPERPLY®	CLEAN, NO ETCH, ADHESIVE	18.0	0.35	4.2	5.5
15	1400-13	20E	BRASS	CLEANING	36.5	0.9	18.8	28.6
16	1400-15	20E	BRASS	CLEANING	30.0	1.0	19.9	26.1
17	1400-16	20D	BRASS	CLEANING	7	0.09	0.42	0.5
18	1400-17	20B	BRASS	ETCH, RINSE, ADHESIVE	28.2	0.52	9.6	12.8
19	1400-18	20B	COPPERPLY®	ETCH, RINSE, ADHESIVE	41	1.1	27.0	39.3
20	1400-24	20E	STEEL (BRASS COAT)	CLEANING	40	1.6	40.0	55.7
21	1400-25	20E	BRASS	CLEANING	33.5	0.7	16.2	20.4
22	1400-43	14A(AVON)	STEEL (BRASS COAT)	CLEANING	46.0	0.4	10.5	16.0
23	1400-47-1	14A (GOODYEAR)	STEEL (BRASS COAT)	CLEANING	41.6	0.4	9.3	14.5
24	1400-48-2	14A (GOODYEAR)	STEEL (BRONZE COAT, 0.037 INCH DIAM)	CLEANING	54.0	0.75	23.2	30.5

$$E = \frac{\sigma}{\varepsilon} = \frac{F_p L_o}{\bar{A}\Delta L}, \qquad G_a(\text{linear}) = \frac{F_p \Delta L}{4\pi \bar{A} L_o} \tag{36}$$

The force-displacement test records are shown in Figures 5-14 through 5-22. They include relatively poor results and very strong results. The curves show a distinct nonlinearity, especially at the higher displacements (ΔL). In all cases, L_o = 1 inch, so the engineering strain equals ΔL in inches.

Several conclusions were drawn from the test results, some of which were supported by consultation with suppliers. These were:

1) Brass coated steel wire can give a higher adhesion than solid brass wire (Tests 15, 16 and 21 vs. test 20). The supplier of the wire attributed this to diffusion in the solid brass wire, which changes the surface composition. This cannot occur in the coated wire, since the brass components cannot diffuse into the steel.

2) The adhesive worked well for the EV cure rubber, increasing G_a for a given rubber-wire combination by a large margin (tests 1-5 vs. test 13). A surface etch is not needed with brass, and may even reduce adhesion, but is needed to clean the oxide layer from copper (tests 13, 14, 18, 19).

3) The best adhesion was obtained for a high sulfur, conventional cure, natural rubber compound, with brass coated steel wire (test 20).

4) For the TACOM standard (compound 14A), adhesion to the bronze coated wire was roughly twice that obtained for the brass coated wire (tests 22-24). The supplier commented that this difference in adhesion is a function of the rubber compound, and is not unusual. Better results might have been obtained with an adhesive. If this compound were to be used to make steel wire reinforced pads, a bronze coat with or without adhesive, or a brass or copper coat with adhesive, would be recommended for trial.

5) The wrong choices can lead to very low adhesion, so design choices should be tested.

According to the supplier, brass coating withstands storage better, because it is less sensitive to moisture. Bronze coated steel wire must therefore be stored carefully, in a low moisture environment, before use as reinforcement in rubber.

Some descriptions of other adhesion tests refer to a tearing of rubber rather than a debonding of the interface, indicating that the bond was stronger than the rubber itself. In all of our tests, the wires pulled out with clean surfaces, indicating a failure of the bond rather than the rubber.

0118n

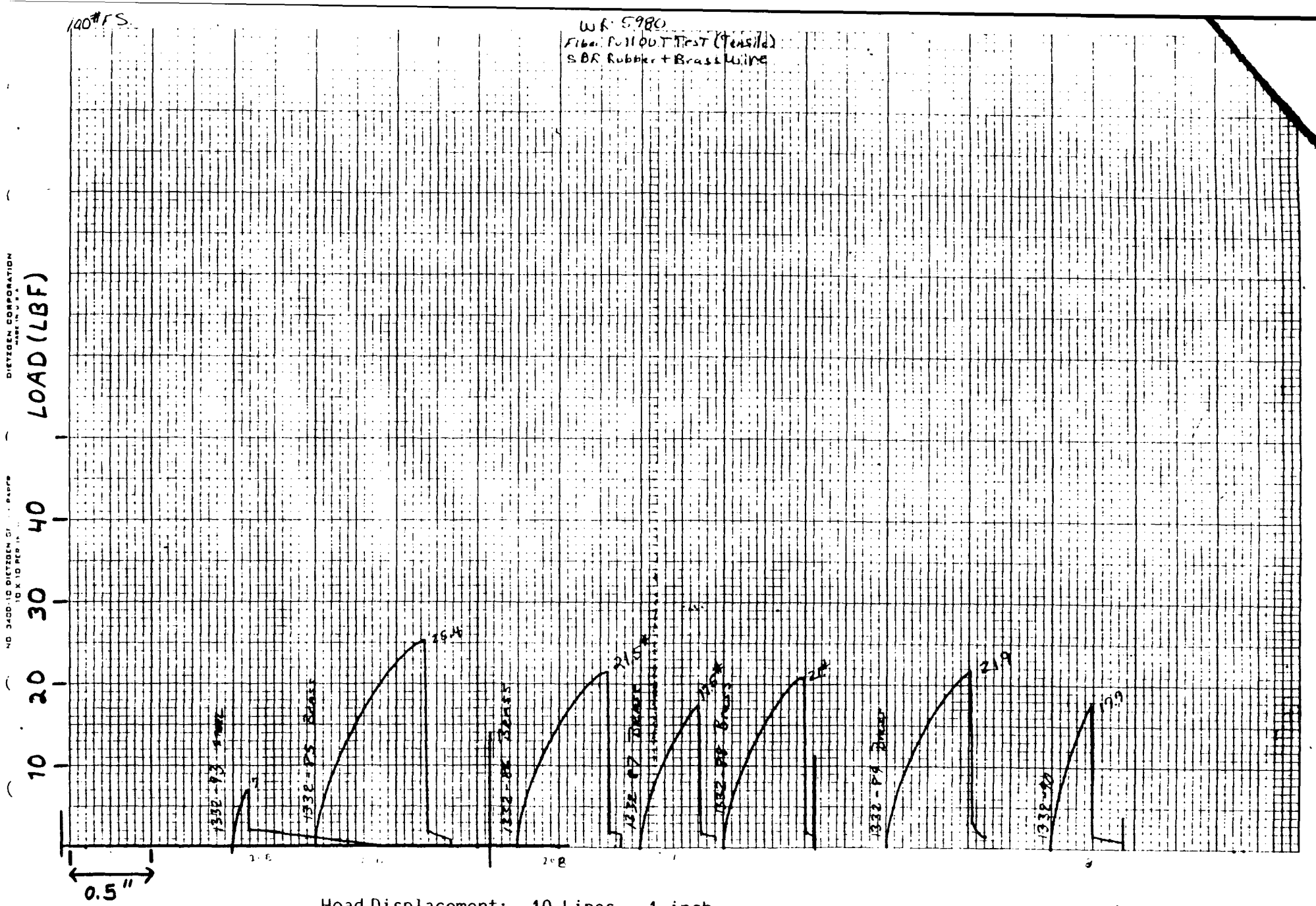

Head Displacement: 10 Lines = 1 inch

Figure 5-14 Wire pullout adhesion tests

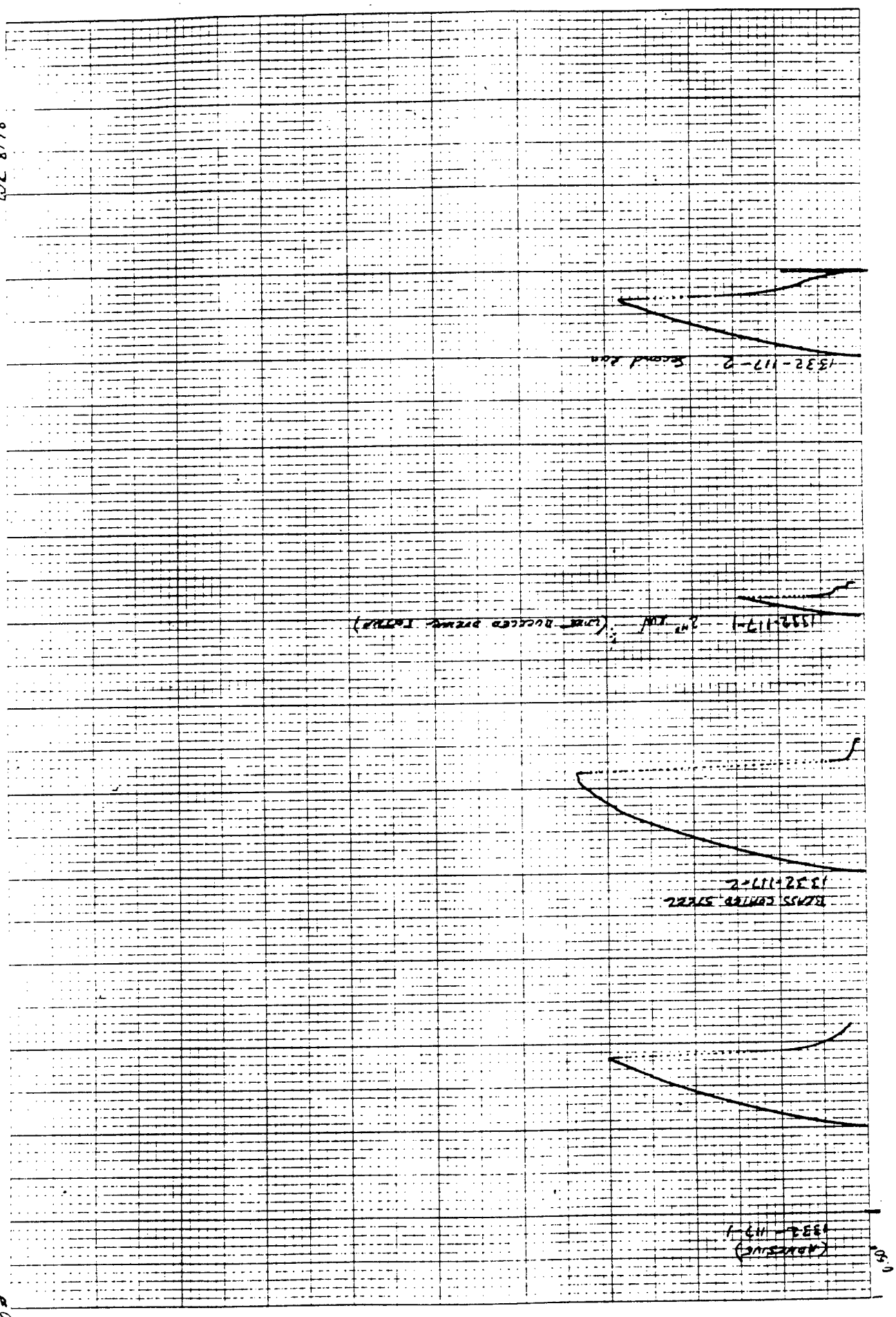

Figure 5-15. Wire pullout adhesion tests

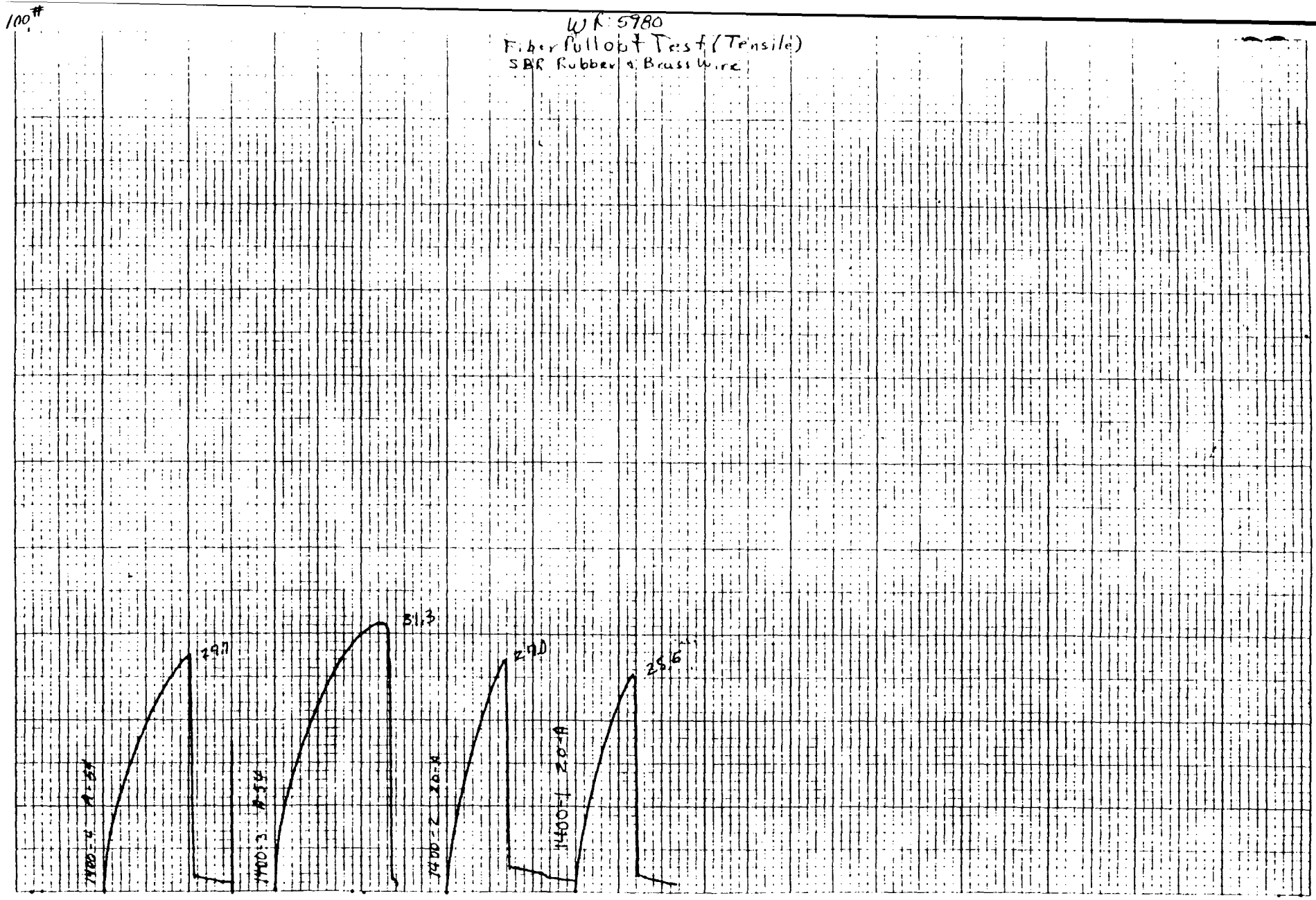

Figure 5-16. Wire pullout adhesion tests

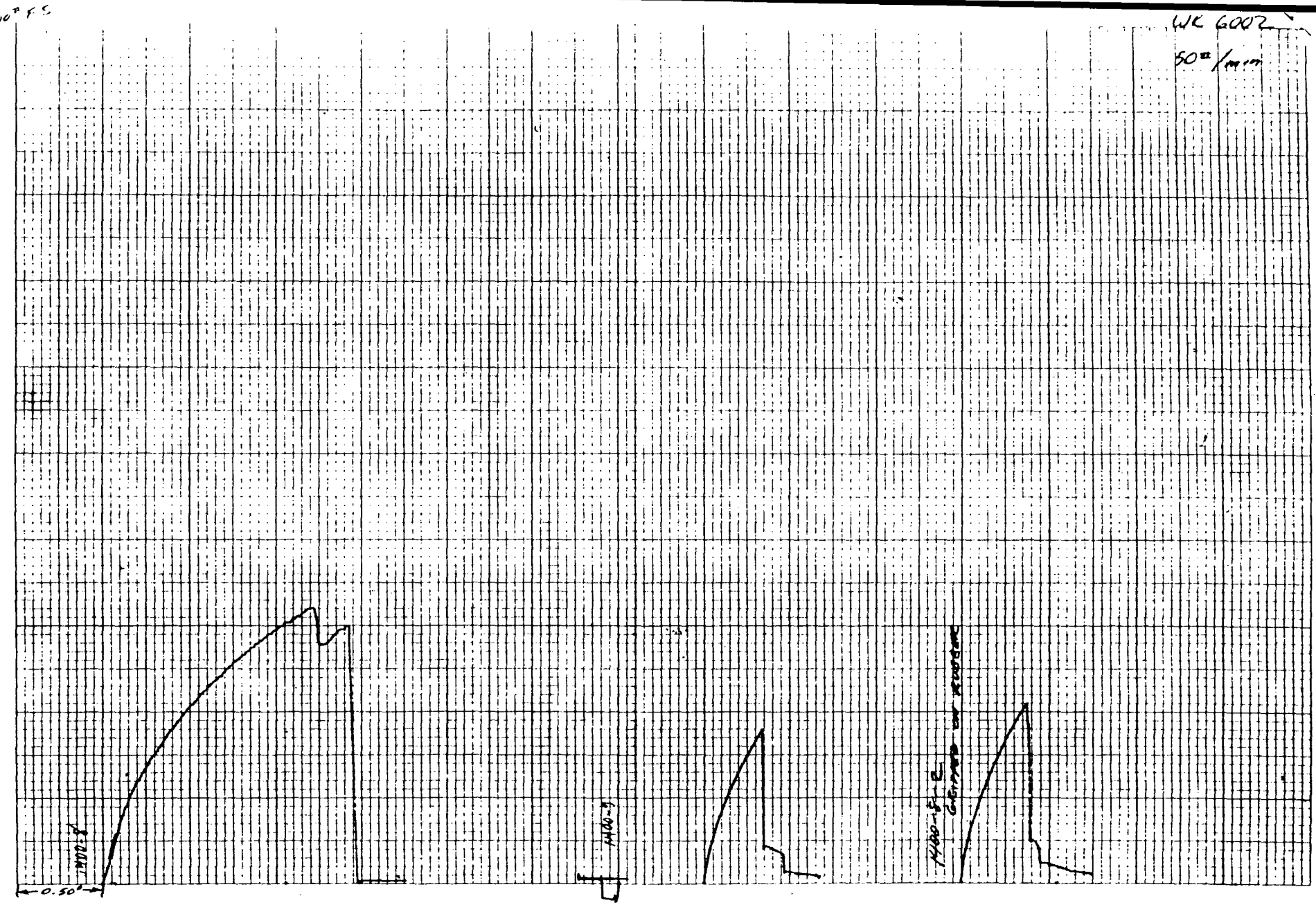

Figure 5-17. Wire pullout adhesion tests

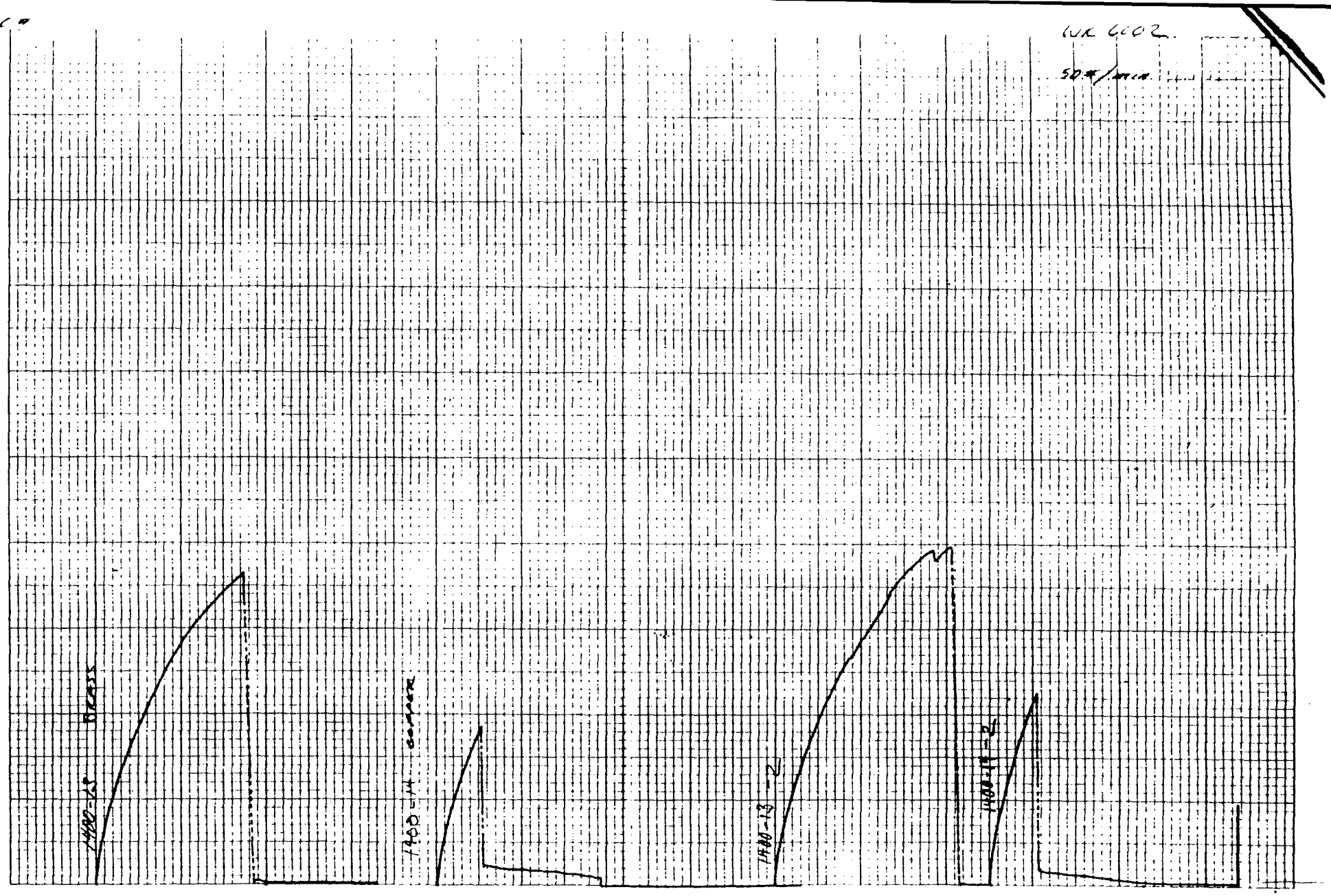

Figure 5-18. Wire pullout adhesion tests

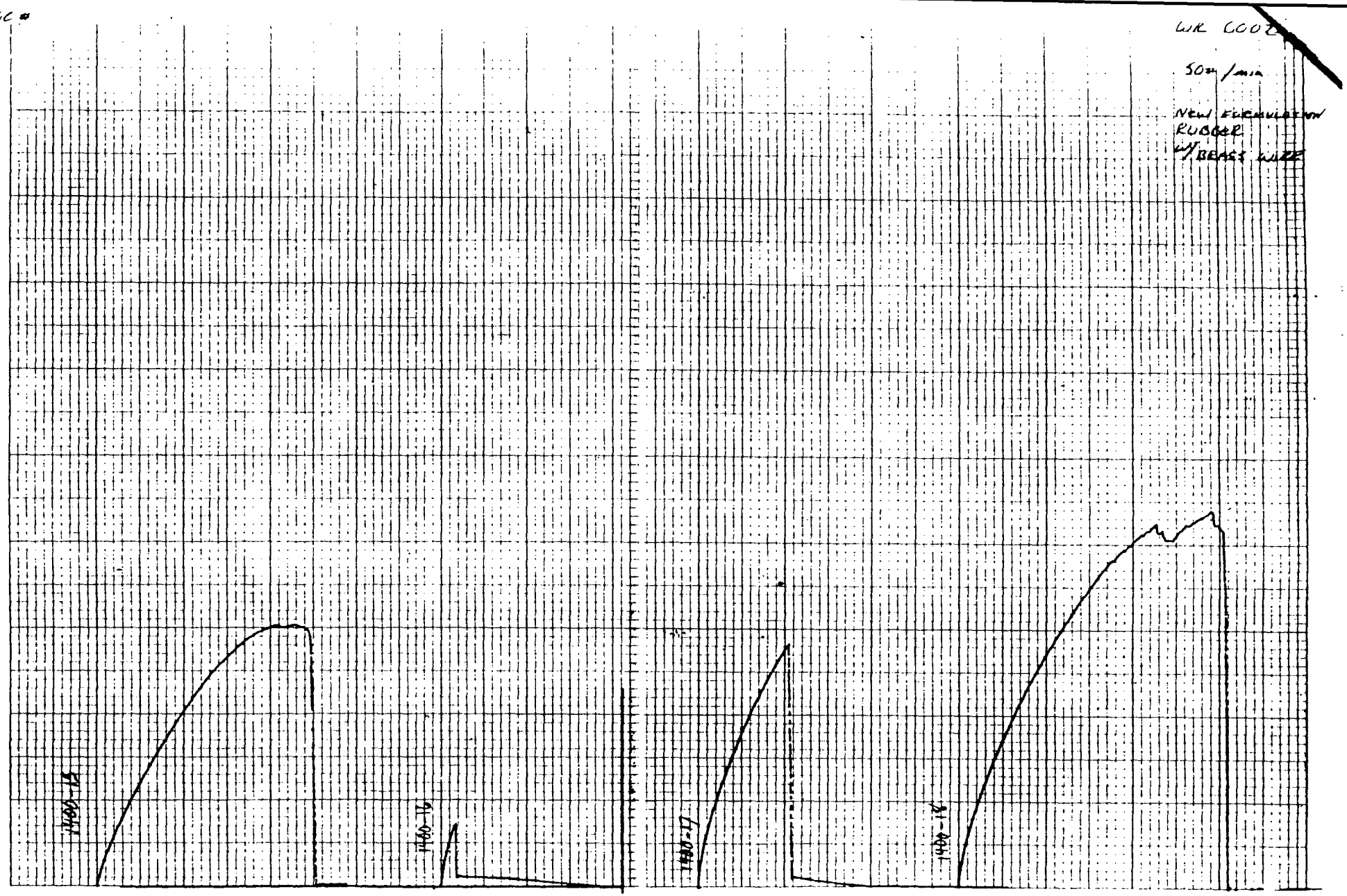

Figure 5-19. Wire pullout adhesion tests

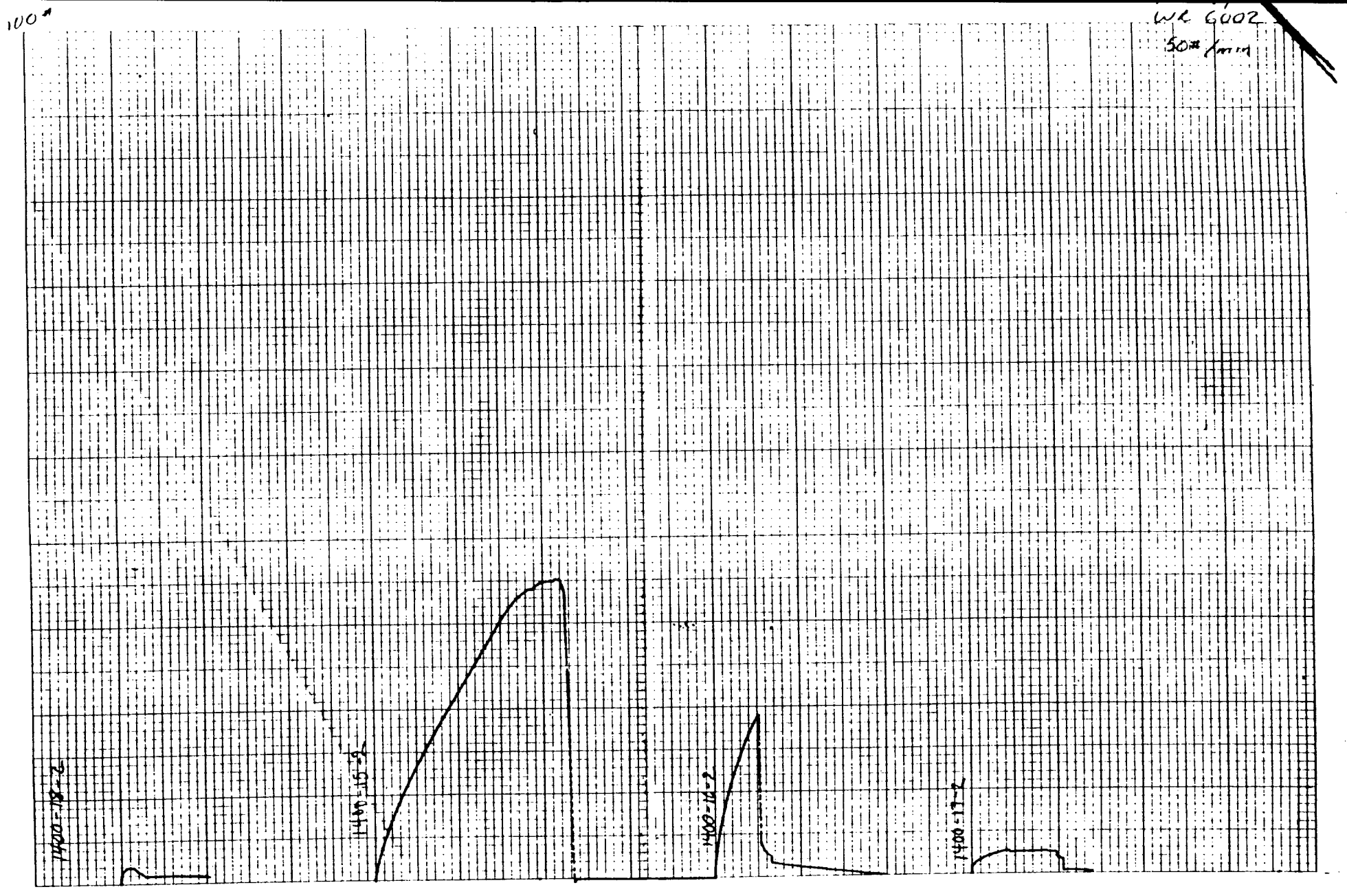

Figure 5-20. Wire pullout adhesion tests

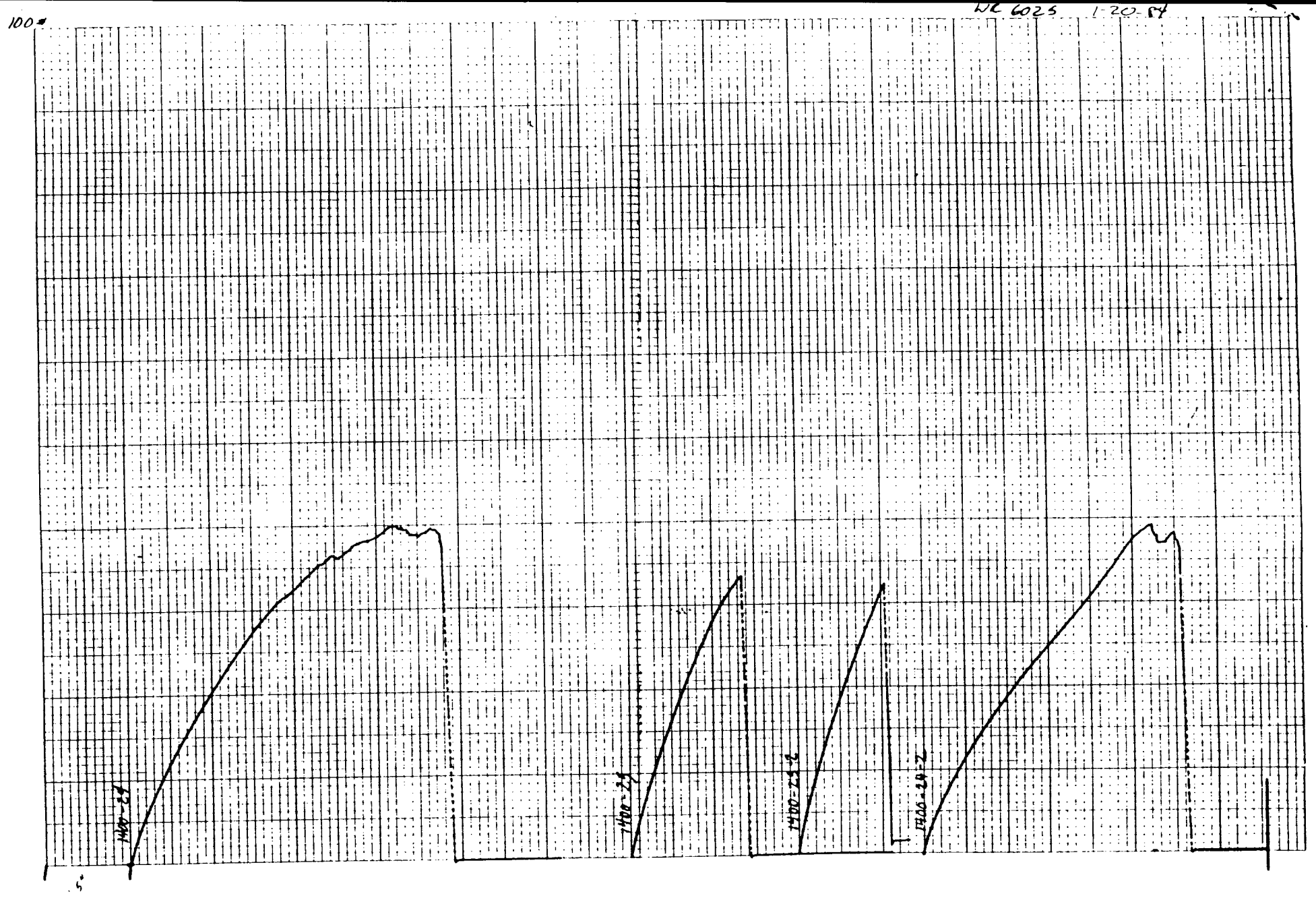

Figure 5-21. Wire pullout adhesion tests

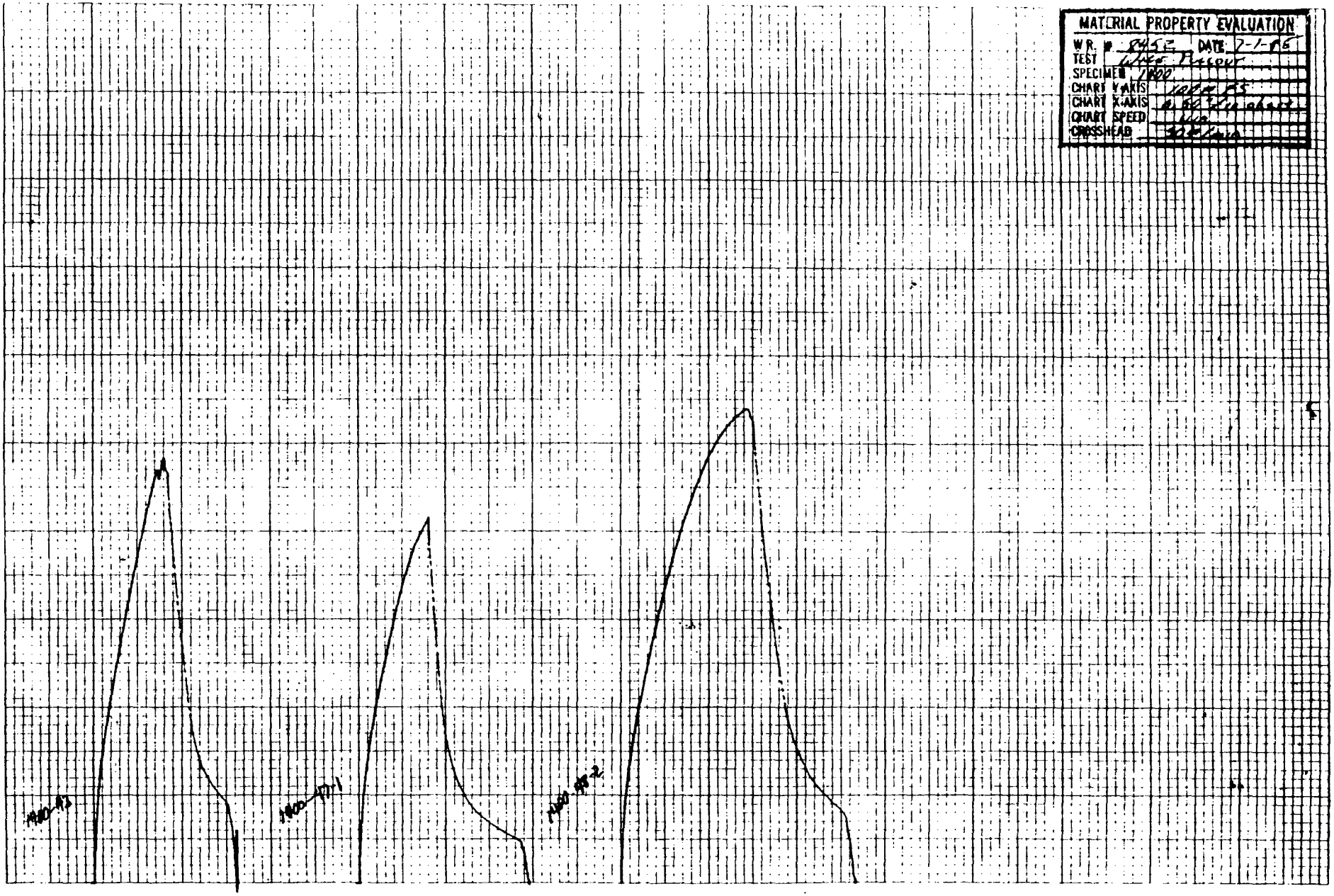

Figure 5-22. Wire pullout adhesion tests

Equation 17 shows that for equal values of G_a, the rubber with the higher modulus will have the higher pullout force. This could be an important consideration when comparing adhesive performance, when specimens have different geometries, or different rubber properties. In other words, G_a is a property of the adhesive interface, and is independent of rubber stiffness or specimen geometry.[10]

A brief comment is indicated on how to handle different measured values of G_a in terms of computing number of cycles to failure at an available surface energy G. One possible method is to scale G by the ratio of some reference value of G_a to the actual test value. A typical value[10] of G_a is 20 kJ/m², so set $G_a(ref) = 20$ kJ/m². Then,

$$G^* = G \cdot \frac{G_a(ref.)}{G_a(meas.)} \tag{37}$$

A higher measured value of G_a results in a lower value of G*, which then gives more cycles to failure.

5.3.3 Effect of Temperature on Tire Cord Adhesion

A recent telephone inquiry to the Malaysian Rubber Bureau on this subject resulted in the following unpublished data for adhesion of brass plated steel tire cord to rubber.[14]

Temperature °C	Steel Cord Adhesion (Newtons)
23	1,207
50	1,059
60	1,078
70	1,020
80	1,015
100	929
120	891
140	793

The NR compound used in this study consisted of: NR 100, ZnO 5, Zinc ethyl hexanoate 2, Flectol H 0.5, HAF black 40, oil 4, Silica 10, Resorcinol 2, Hexamine 2, Santocure MOR 0.7 and Sulfur 3. The cure condition used for molding the steel tire cords into the rubber is 27 minutes at 140°C. The test piece was similar to that used in ASTM D2229, with 12.5 mm cord embedment[15]. The data shows that there is some loss of adhesion with temperature. Temperature also affects rubber stiffness, with stiffness roughly proportional to absolute temperature for temperatures between -20°C and +70°C.[16] Using this, plus Equation 17, the change in G_a can be written

0118n

$$\frac{G_a(2)}{G_a(1)} = \frac{[F_p(2)]^2\bar{T}(1)}{[F_p(1)]^2\bar{T}(2)}, \quad \bar{T} = \text{absolute temperature} \tag{38}$$

If the linear dependence of stiffness on absolute temperature holds to 140°C, the reduction in G_a from the value at room temperature is roughly 70%. At 70°C, the reduction is roughly 40%. This level of change is significant, and shows that room temperature data may not be adequate in some applications. On the helpful side, stiffening due to increased temperature will decrease the energy available for debonding, in a load controlled configuration.

5.4 Summary

Design ideas are presented for reinforced tank track pads. The ideas are based on observations of TACOM test results for loading of a track pad by an asperity, the desirability of maintaining rubber-like compliance in a reinforced pad, the advantage of reducing pad heat build-up from cyclic loading, and the need to maintain a strong bond between the reinforcement and the rubber. An outgrowth of the analysis were some observations on methods of achieving greater uniformity in curing.

The main features of the suggested baseline design are steel-based wire, with brass, bronze, or copper coating, aligned in the direction of travel, with a volume fraction of 0.013 and a diameter of 0.032 inch. See Figure 5-28. Methods are presented for estimating the effects on performance of changes in wire volume fraction and diameter.

The program included thermal and mechanical analyses, plus a series of adhesion tests. The thermal analysis included a simple 1-D closed form model, and a numerical, 2-D, time dependent model. The 2-D model was used to simulate both heating due to cyclic loading, and the curing process. Part of the mechanical analysis was a fracture mechanics based treatment of debonding of wire reinforcement as a function of load magnitude, configuration, and number of loading cycles. A test method was chosen which yielded adhesive surface energy per unit area. In the testing program, good results were achieved with both conventional and EV cure rubber compounds. Bonding to EV cure rubber required an adhesive. It was very sensitive to proper surface preparation and adhesive application. Conventional cure compounds could bond well to brass and bronze coated steel wire, but bond strength was a strong function of rubber type and sulfur content. The best performance was measured for a conventional cure, natural rubber compound with high sulfur content. Tests were run for a TACOM baseline triblend (compound 14A), with brass and bronze coated steel wire. The bronze coat gave the better performance.

LIST OF REFERENCES

1 D. R. Lesuer, "Investigation into the Failure of Tank Track Pads," Lawrence Livermore Laboratory, presented to Tank and Automotive Components and Materials Symposium, June 24 and 25, 1981.

2 Allen, Lindley, and Payne, eds., Use of Rubber in Engineering, Proc. of Conf. at Imperial College of Science and Technology, London, 1966, Maclaren and Sons, Ltd.

3 Hepburn and Reynolds, Elastomers: Criteria for Engineering Design, Applied Science Ltd., 1979, Ch. 5.

4 Carslaw and Jaeger, Conduction of Heat in Solids, Clarendon Press, 2nd Edition, 1959.

5 D. R. Lesuer et. al., "Investigation into the Failure of Tank Track Pads, Technical Report for FY-79 and FY-80," TACOM R and D Lab. Tech. Report #12583, Lawrence Livermore National Laboratory UCID 19035, Oct. 1980.

6 Freakly and Payne, Theory and Practice of Engineering With Rubber, Applied Science Ltd., 1977.

7 Roshenow and Choi, Heat, Mass, and Momentum Transfer, Prentice-Hall, 1961.

8 S. Timoshenko and J.N. Goodier, Theory of Elasticity, 2nd ed, McGraw-Hill, 1951, Art. 33.

9 Breidenback and Lake, "Application of Fracture Mechanics to Rubber Articles, Including Tyres," Phil. Trans. R. Soc. Lond. A299, 189-202 (1981).

10 Gent, Fielding-Russell, Livingston, and Nicholson, "Failure of Cord-Rubber Composites by Pullout or Transverse Fracture," Journal of Materials Science 16 (1981), pp. 949-956.

11 D. A. Hills, Heat Transfer and Vulcanization of Rubber, I.R.I. Monograph, Elsevier, 1971.

12 Bergstrom, E.W., "Wear Resistant Rubber Tank Track Pads," Rock Island Arsenal, October 1975.

13 Hamilton, J., "Development of Long Life Track Pad Materials," Final Report, TACOM Contract DAAE07-83-C-R054, August, 1984.

14 private communication, Malaysian Rubber Producers Research Association, Washington, D.C., April 16, 1986.

15 Barker, L.R., and Bristow, G.M., "A Curing System for Rubber Bonded to Brass-Plated Steel Tyre Cord," NR Technology, vol 11, Part 2, 1980, pp 21-27.

16 Lindley, P.B., Engineering Design with Natural Rubber, NR Technical Bulletin, Malaysian Rubber Producers' Research Association, 1974.

0118n

APPENDIX A

FINITE DIFFERENCE CALCULATIONS

APPENDIX A .. FINITE DIFFERENCE CALCULATIONS

A computer program was written to carry out calculations using the analysis presented in the previous section. Cases were run for heating by cyclic loading, and for various cure cycles. A list of the material properties, and graphs of temperature and cure state vs time for cases of cyclic loading and curing, are contained in this appendix. For the cyclic loading cases, steady state values of temperature were calculated using a series solution from Reference 4 for a rectangular block with convective boundary conditions.

Figures A1 and A2 show temperature at the pad center as a function of time for various loading, reinforcement, and surface conditions. The heating rate is reduced in Figure A2 to account for the stiffening effect of the wires. As stated before, the copper coated steel wire is a commercially available product, which is roughly 20% copper by volume. (Because of the added complication of etching, rinsing, and applying an adhesive to promote bonding to the rubber, this product was not as attractive as the brass coated steel wire). In all of the calculations, the initial temperature was 20°C. When wires were present, the wire volume fraction was 0.013. The relative effect of each aspect of the reinforcement on the center temperature can be seen by tabulating the steady state values:

Baseline	T = 85°C
Stiffening Alone	68
Stiffening + enhanced k_x (steel)	61
Stiffening + enhanced k_x(steel) + double h_x	56
Stiffening + enhanced k_x (copper coated) + double h_x	51

The largest single effect is the stiffening, since this directly reduces the rate of energy input by 25%. The effect of the wires on thermal conductivity plus the effect of a slotted surface on surface heat transfer are somewhat smaller, but of the same order. A reasonable case could be made for softening the rubber compound so that a reinforced pad would have the same compliance as the original unreinforced pad. Then, the enhancement of k_x and h_x would dominate. Temperature effects alone could cut the tear growth rate in half (see Figure 5-3). Note that the effect on k_x of the copper coated wire could be achieved with the steel wire by roughly doubling the volume fraction.

The next set of graphs represent temperature and cure state vs time for several cure cycles imposed on steel wire reinforced pads (X direction, V_f = 0.013). The target value of cure was in most cases 27.5 minutes at 290°F (143.3°C), which is typical of what is used for track pad rubber compounds. Both fixed temperature and convection boundary conditions are used; the former represents conditions in the mold, while the latter represents conditions outside the mold.

Figures A3 and A4 represent a simple two stage cure, in which a block initially at room temperature (20°C) is held in a mold at 270°F (132.2°C) for 65 minutes, then taken out to cool at room temperature. The temperature plot (A3) shows that the center of the pad is at deficit in the mold, but retains temperature longer outside the mold. The cure state plot (A4) shows that while the outside of the pad is reasonably close to the target value, the center in this case is very much undercured.

Figures A5 through A8 show two different three stage cure cycles, in which the block is heated in an oven (convection b.c., 100°C) before being put into the mold (temperature b.c., 132.2°C). When removed from the mold, the block is cooled at room conditions (convection b.c., 20°C). The first three stage cycle proved to have too little time in the mold; not even the outside was fully cured. Time in the mold was increased in the second three stage cycle, resulting in a cure which was fairly close to optimum both at the center and the surface of the pad.

Figures A9 and A10 represent a four stage cure cycle, in which an oven post-heat at 100°C is added. The state of cure is slightly more even than that of the previous, three stage cure cycle. Time in the mold was 45 minutes, vs. 65 minutes for the three stage cycle (a significant reduction).

In the previous cases, the mold temperature was 270°F. Figures A11 and A12 show a two stage cure with the mold set at 300°F (148.9°C), then cooling at room temperature. The pad is held in the mold long enough to achieve optimum cure at the center. Figure A12 shows that this results in severe overcure near the outside of the pad.

So far, all of the curing cycles have been for the case of steel wire reinforcement (X direction, V_f = 0.013). For comparison, the cycle depicted in Figures A7 and A8 was rerun without the wire reinforcement. The results were that the cure state on the outside did not charge noticeably, but the cure state at the center was lower by roughly 20%. See Figures A13 and A14. In a last example, the same cycle was applied to a pad reinforced with the higher conductivity Copperply^R wire. This brings the cure state at the center substantially closer to optimal. See Figures A15 and A16.

Figures A-17 through A20 depict the following case: The rubber is injection molded, and enters the mold at a uniform temperature (100°C). There is no reinforcement. The case of 30 minutes in the mold at 290°F (143.3°C), followed by 60 minutes of post-heat out of the mold at 100°C, is shown in Figures A-17 and A-18. In Figures A-19 and A-20, the mold condition is 60 minutes at 133.3°C, 10°C less than the previous case. Mold time was doubled because a 10°C drop in mold temperature cuts the cure rate in half (see equation 34). The results clearly show the gain in cure uniformity resulting from a longer, cooler cure. Figures A-21 and A-22 show a variation of the second case, with the 100°C post-heat dropped. As shown before for the reinforced rubber, a post-heat at a temperature lower than the mold temperature can add significantly to the cure.

The conclusions that can be drawn from these models of curing are as follows: 1) Simple two stage cures can result in severe undercure and/or overcure. 2) Preheating prior to molding can greatly improve the uniformity of cure. 3) Post-heating appears to be less important than preheating, for uniformity of cure. It can, however, allow significantly less time in the mold. 4) Curing at a lower temperature for a longer time can significantly improve the uniformity of the cure. 5) The effect of metallic reinforcement on curing can be important.

Listings of the computer codes used in these calculations, plus abbreviated output, are included in Appendix B. The output includes tables of values used to generate the figures.

TABLE A-1

THERMAL PROPERTIES

ρ (RHO) = 1.15 $\frac{\text{grams}}{\text{cm}^3}$ density

$C = 1.8*10^7 \frac{\text{erg}}{\text{gram}^{\circ}\text{C}}$ heat capacity

$K_y = 3.2*10^4 \frac{\text{erg}}{\text{cm}^2\text{sec}\left(\frac{^{\circ}\text{C}}{\text{cm}}\right)}$ rubber thermal conductivity

$K_x = K_y$ no metal reinforcement

$K_x = 9.4*10^4$ steel wire reinforcement

$K_x = 1.87*10^5$ copper coated wire reinforcement

$H = 1.7*10^4 \frac{\text{erg}}{\text{cm}^2\text{sec}^{\circ}\text{C}}$ heat transfer coefficient (smooth surface, no movement)

$H = 2.35*10^4$ smooth surface, ~20mph

H is doubled for grooved surface

CURE MODEL

Ideal: 27.5 min at 290F

$T_c = 2$

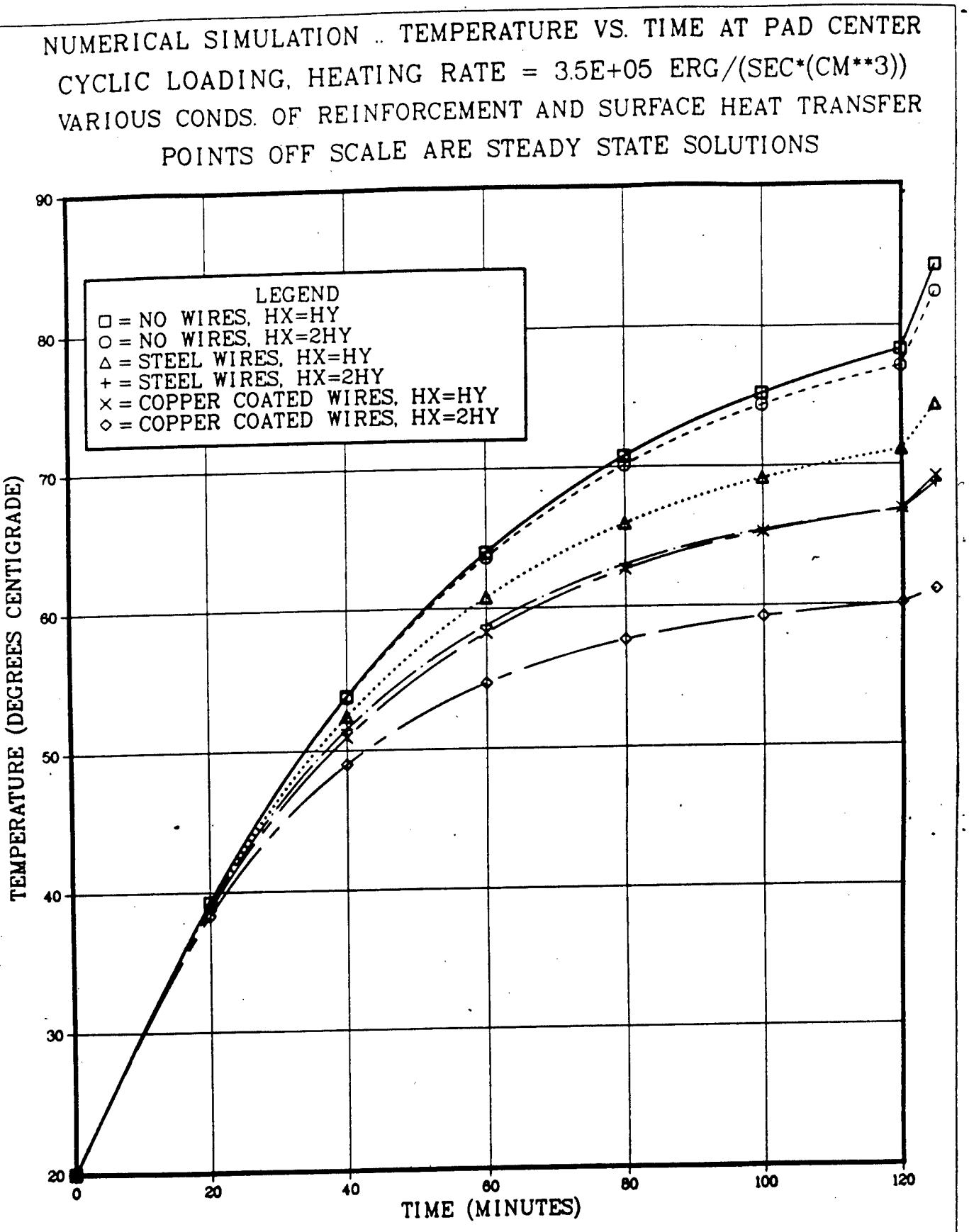

Figure A-1 Hysteresis Heating

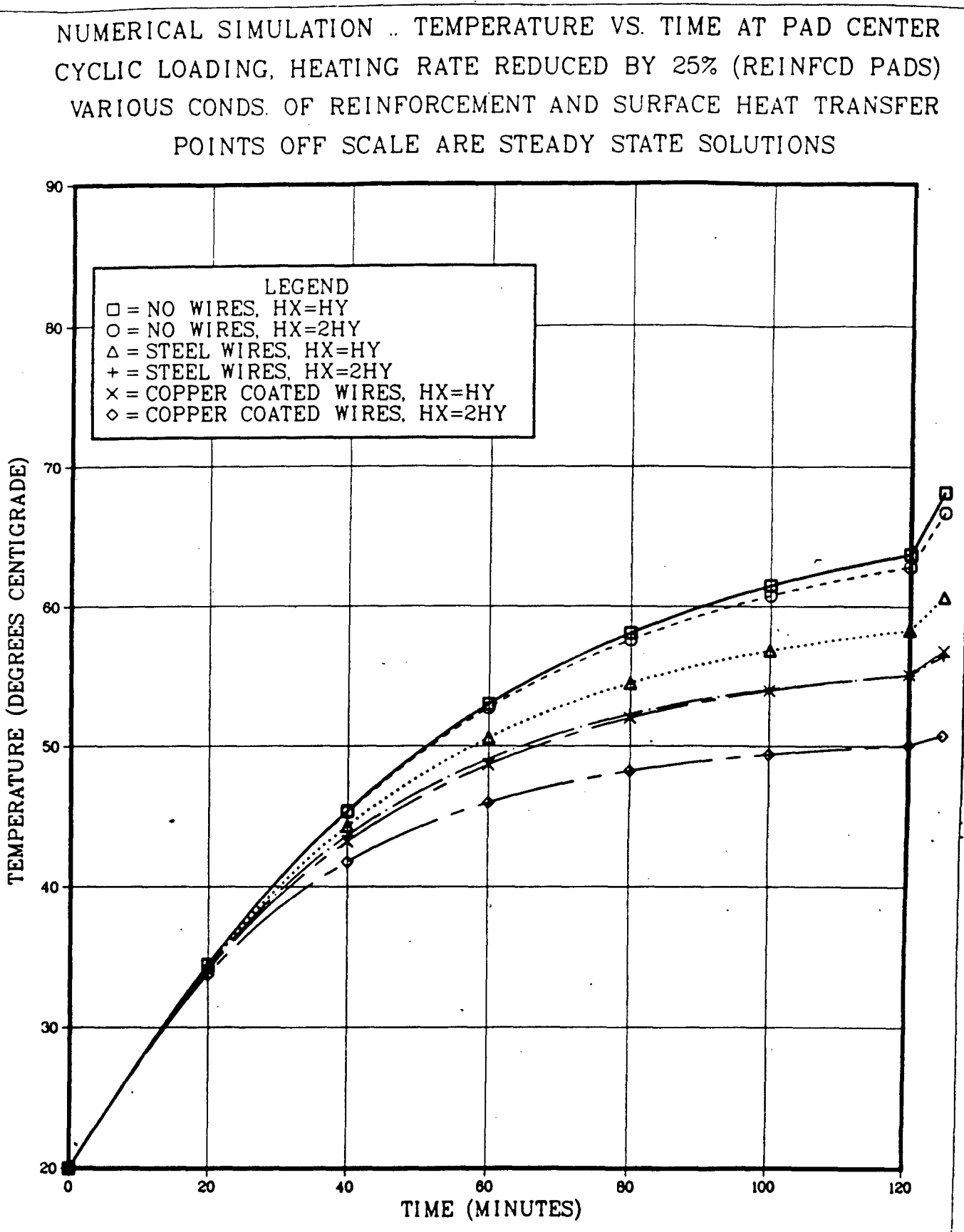

Figure A-2 Hysteresis Heating

THIS PAGE LEFT BLANK INTENTIONALLY

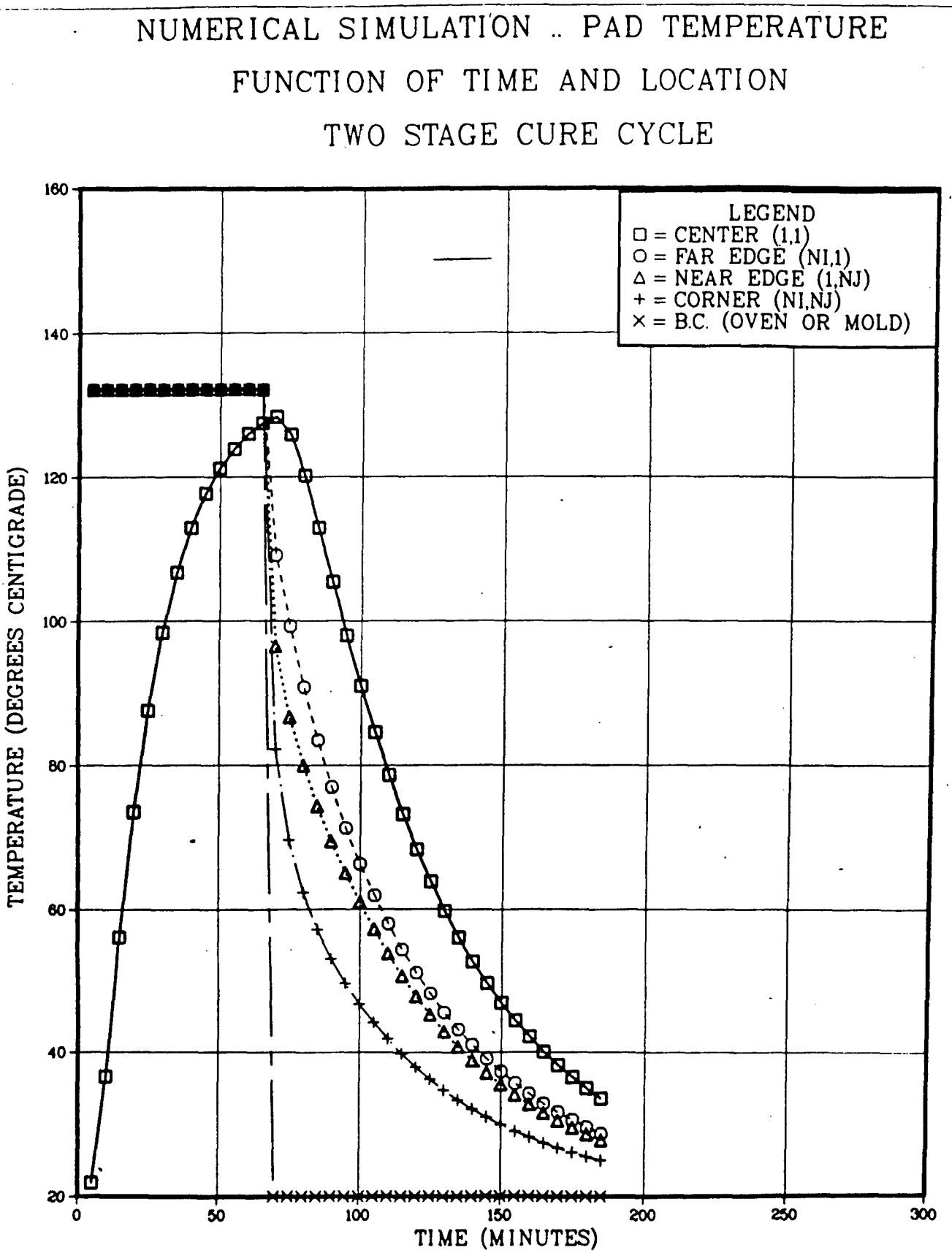

Figure A-3 Two Stage Cure Cycle, Temperature Vs Time

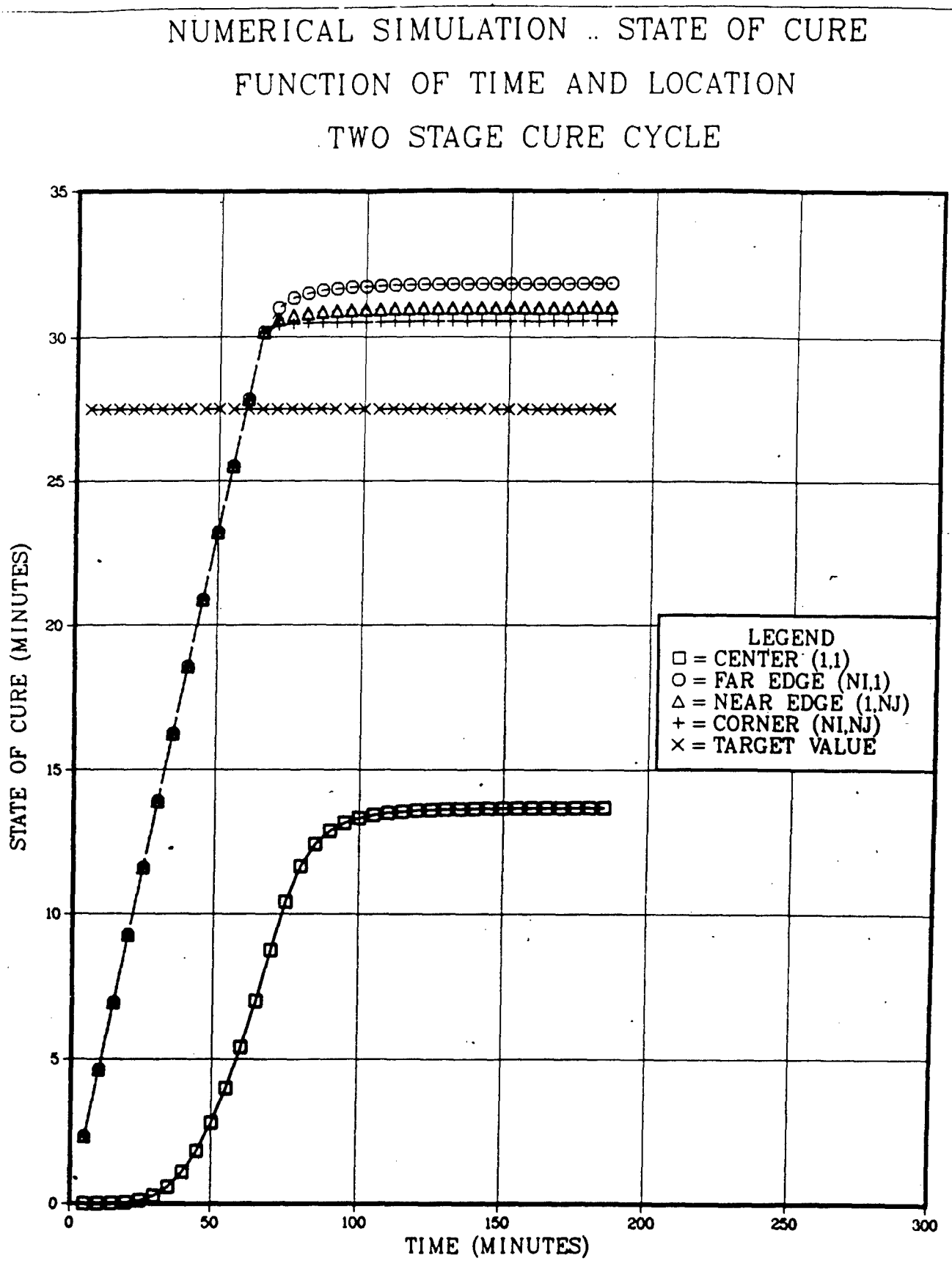

Figure A-4 Two Stage Cure Cycle, Cure State vs Time

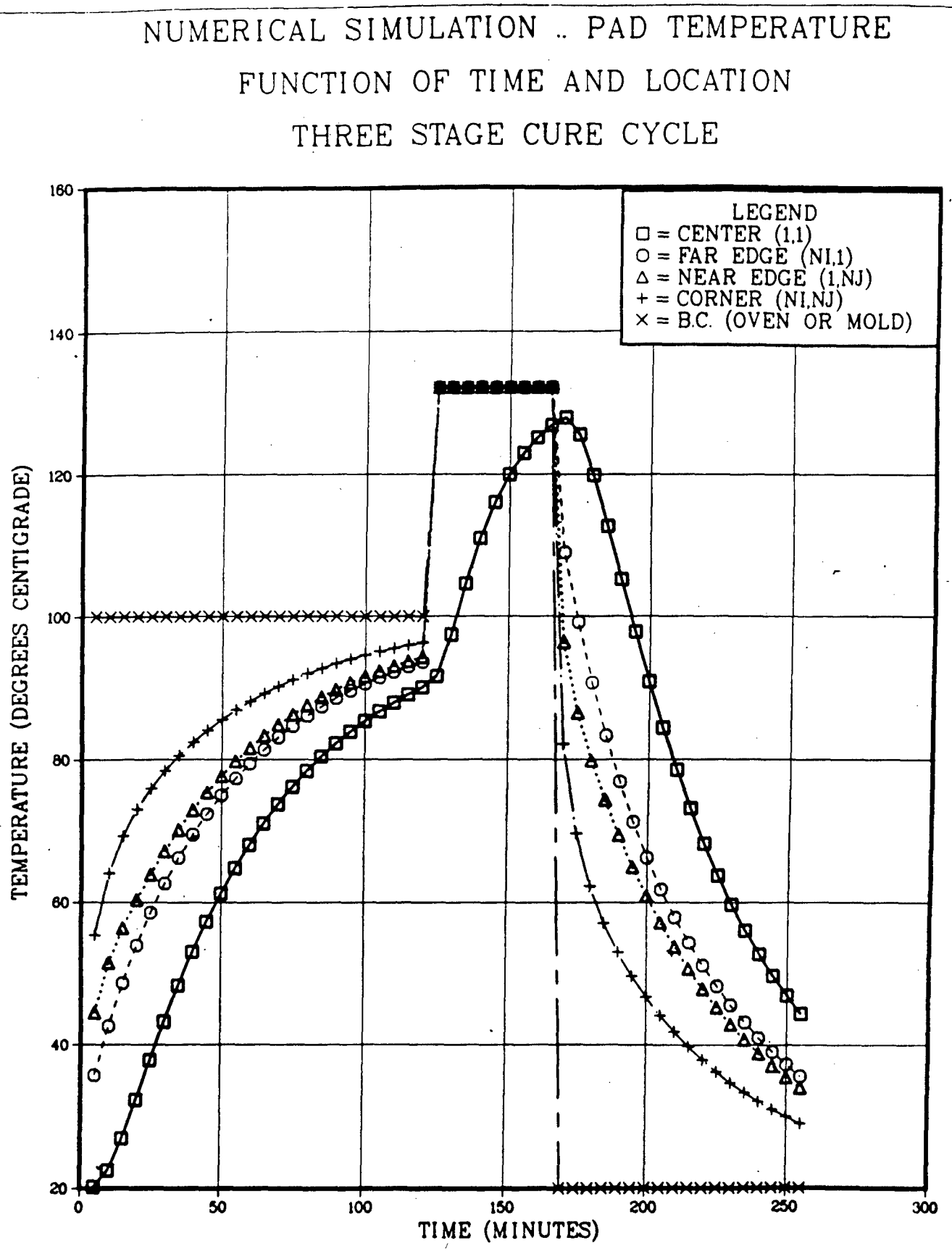

Figure A-5 Three Stage Cure Cycle, Temperature vs Time

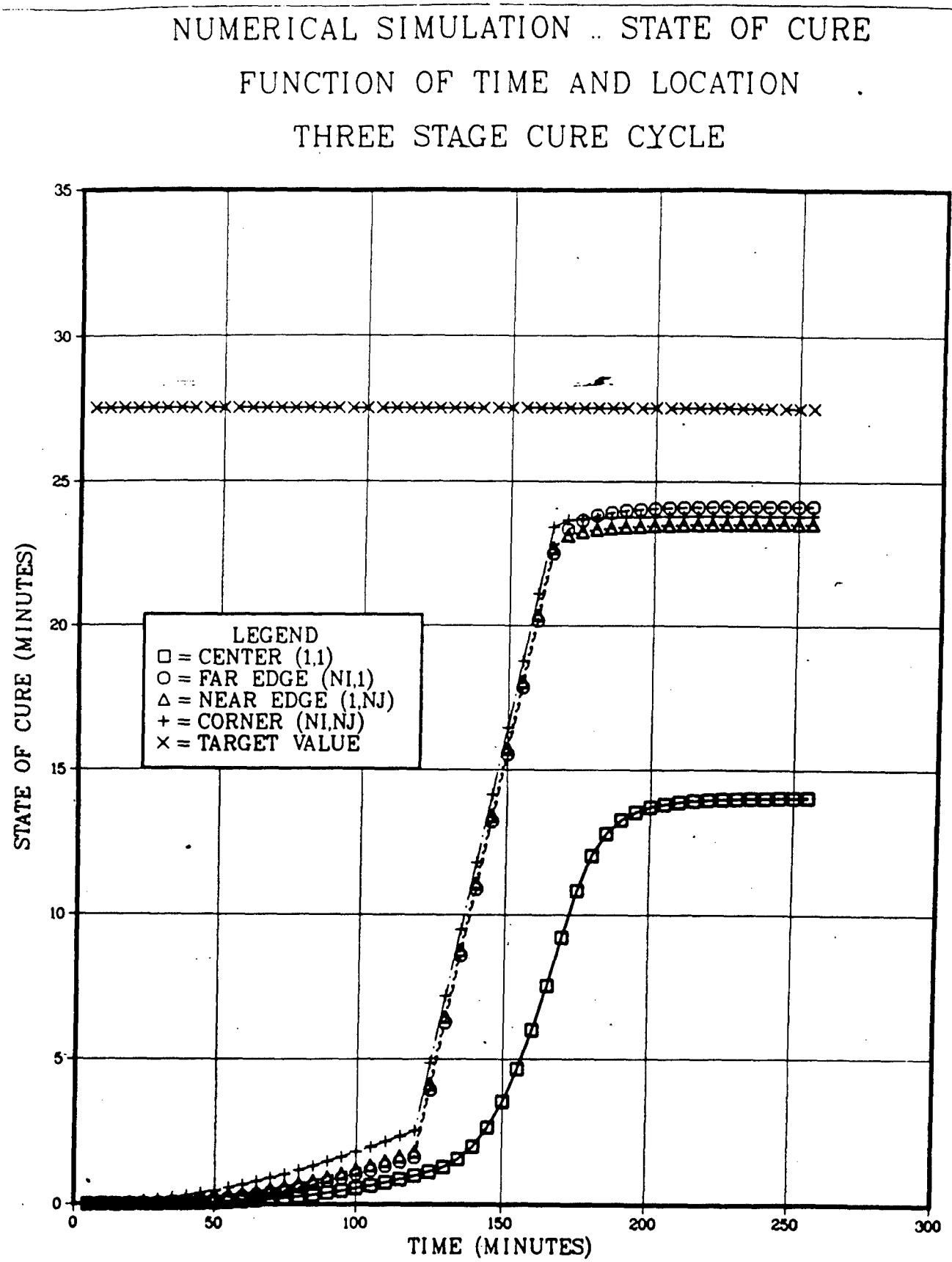

Figure A-6 Three Stage Cure Cycle, Cure State vs Time

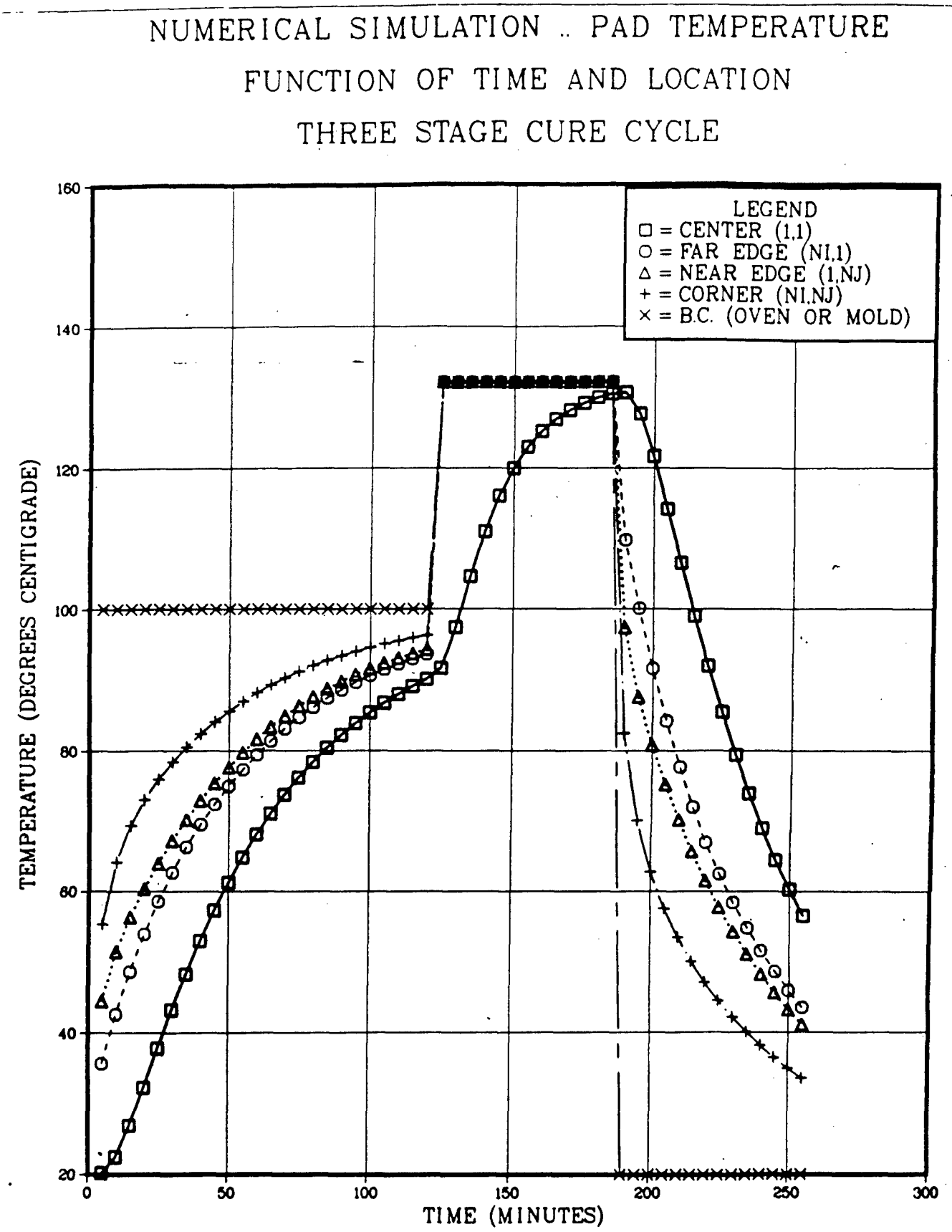

Figure A-7 Three Stage Cure Cycle, Temperature vs Time

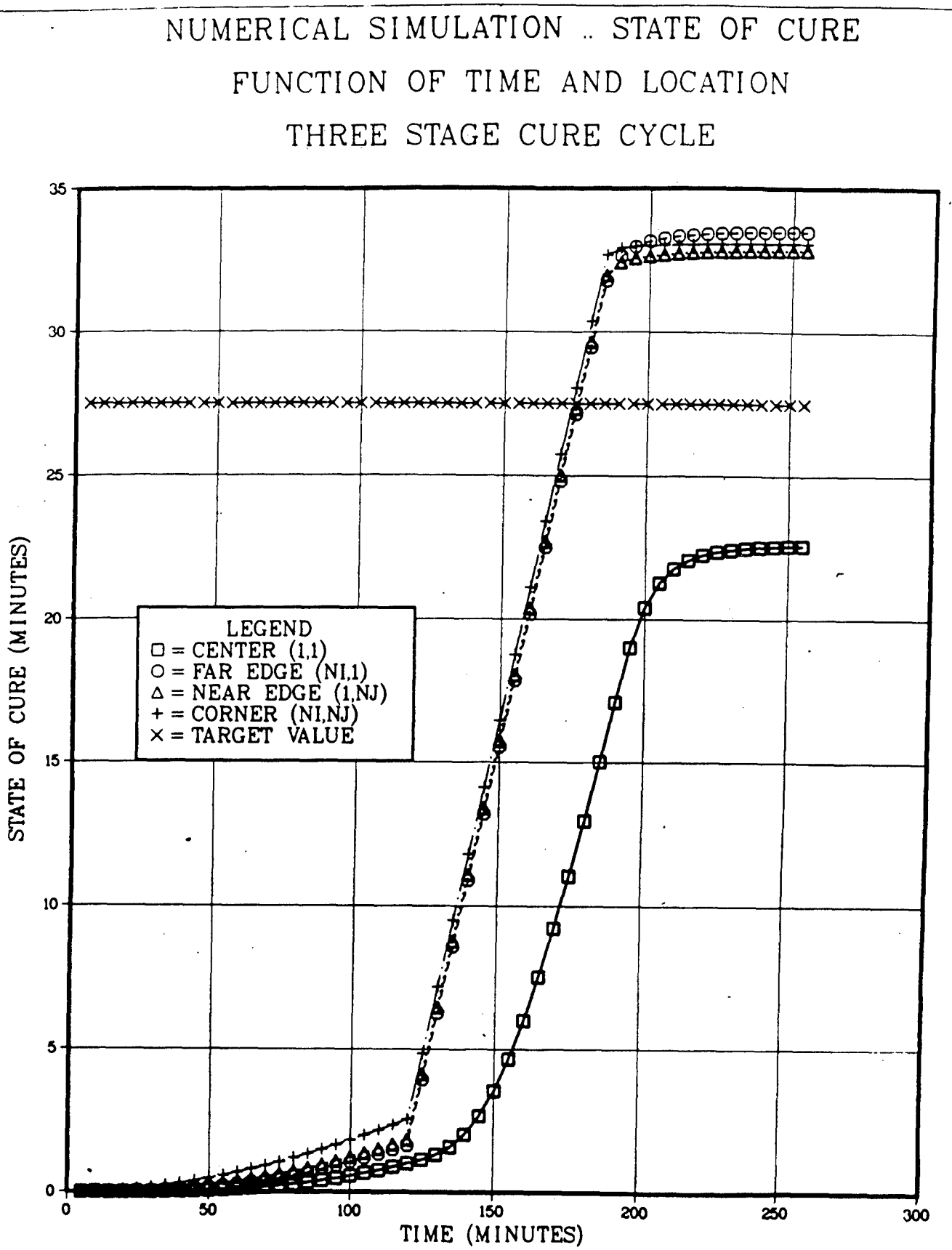

Figure A-8 Three Stage Cure Cycle, Cure State vs Time

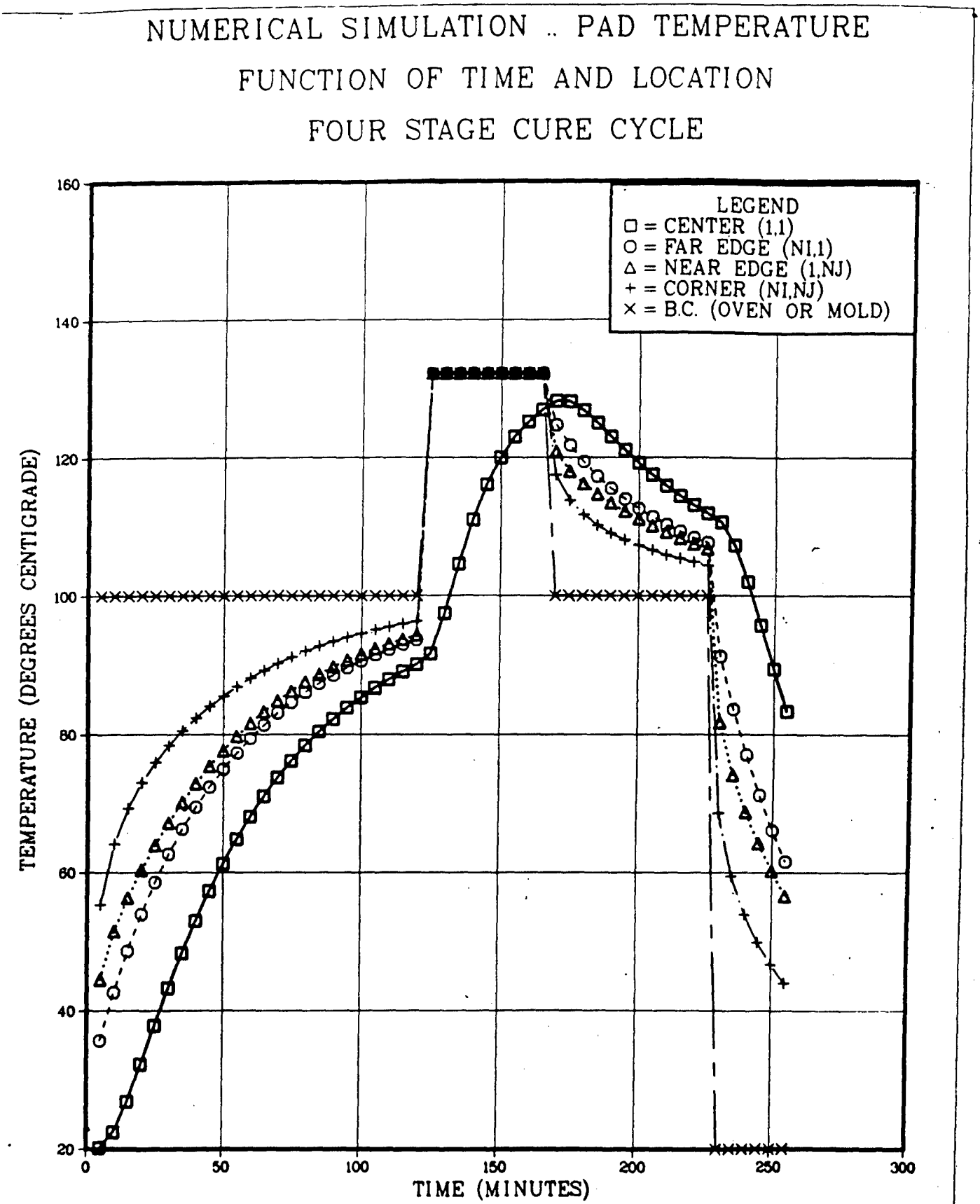

Figure A-9 Four Stage Cure Cycle, Temperature vs Time

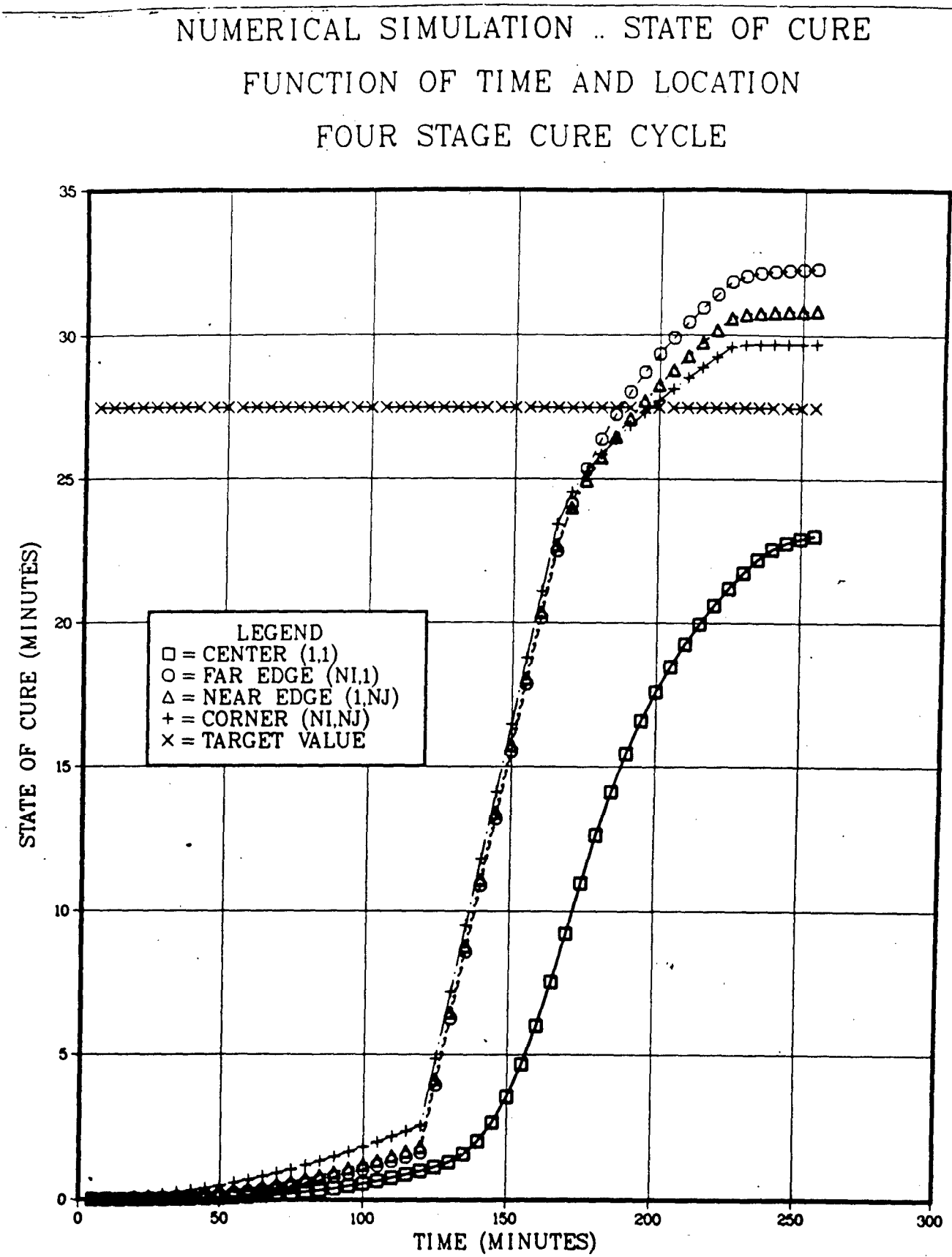

Figure A-10 Four Stage Cure Cycle, Cure State vs Time

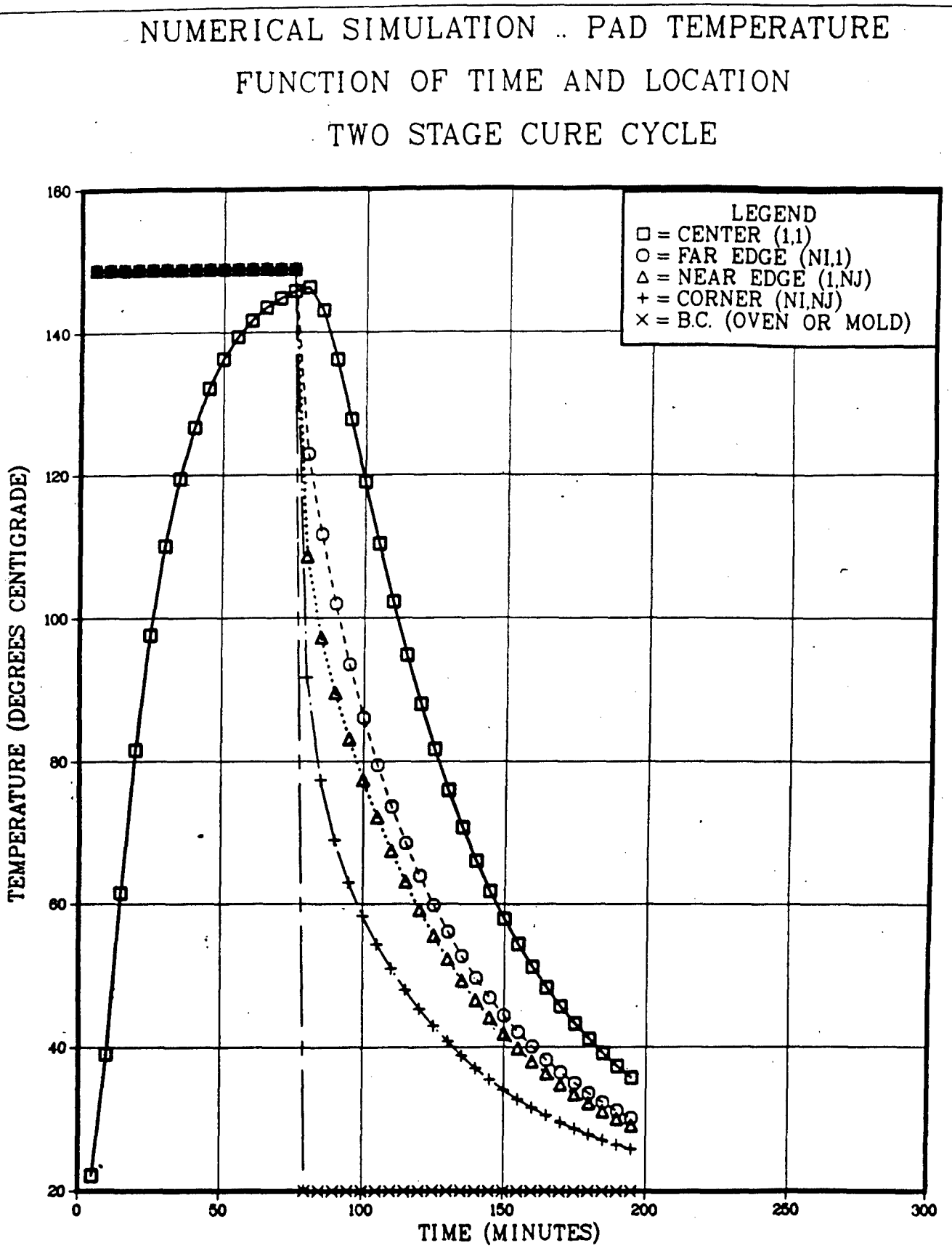

Figure A-11 Two Stage Cure Cycle, Temperature vs Time

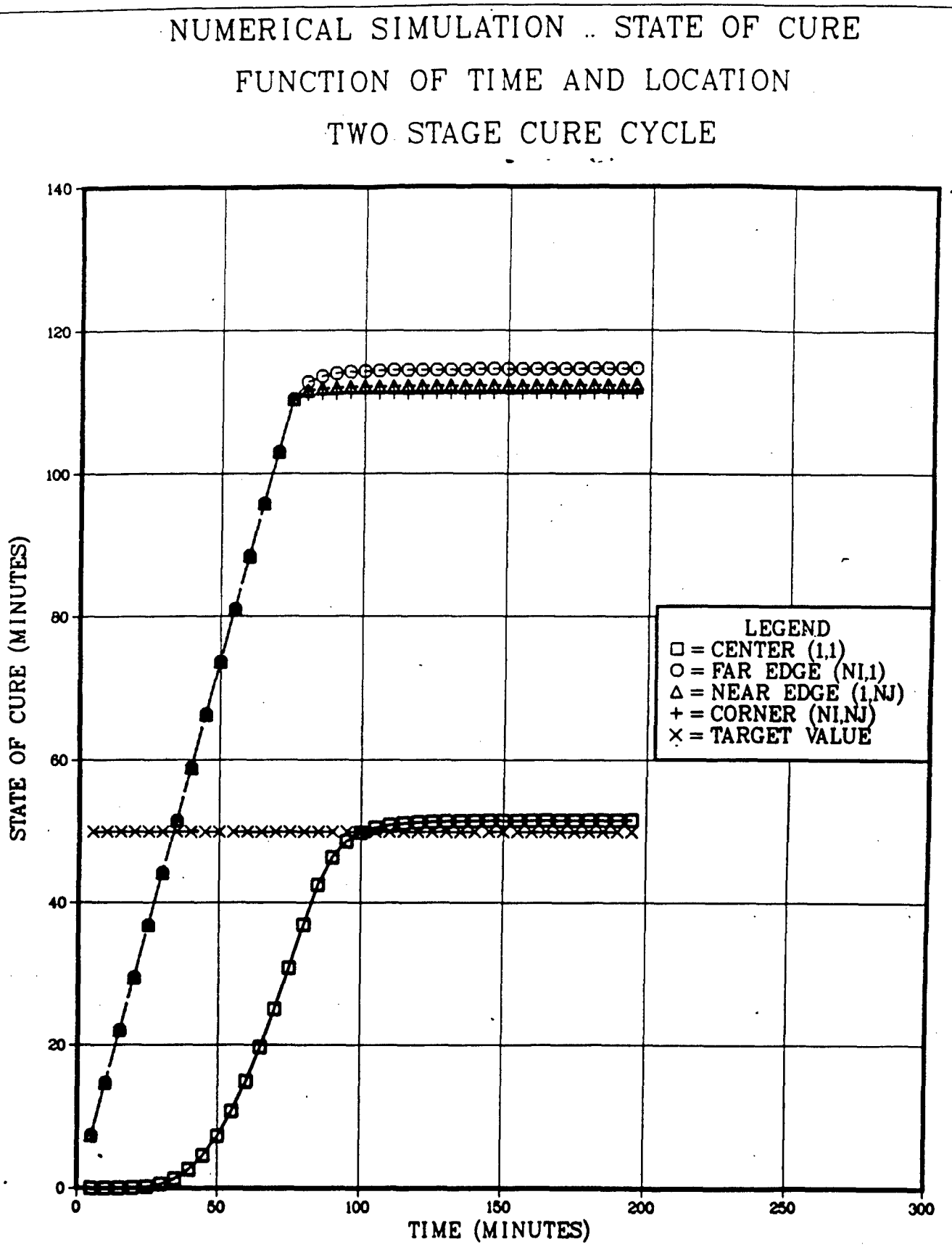

Figure A-12 Two Stage Cure Cycle, Cure State vs Time

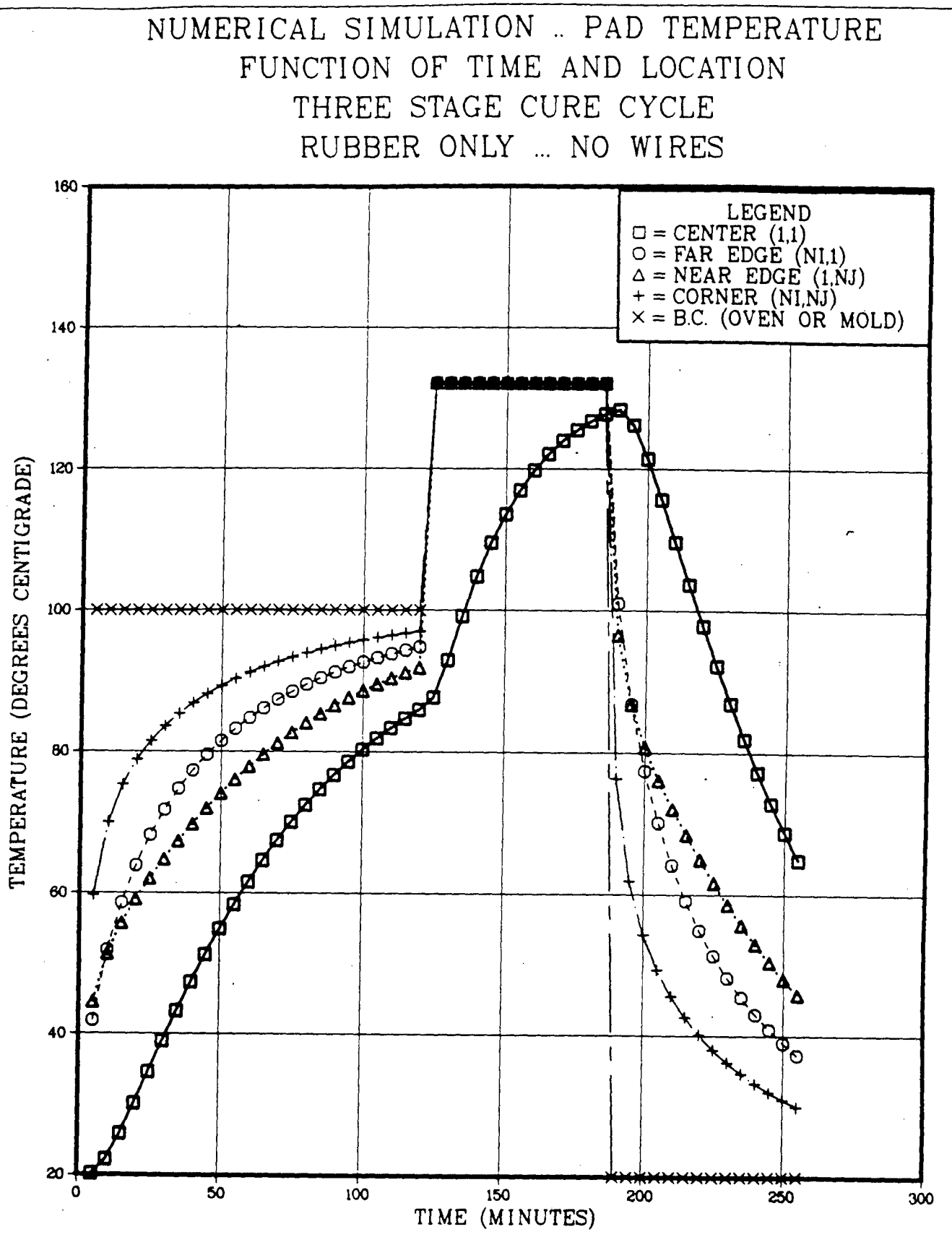

Figure A-13 Three Stage Cure Cycle, Unreinforced Rubber, Temperature vs Time

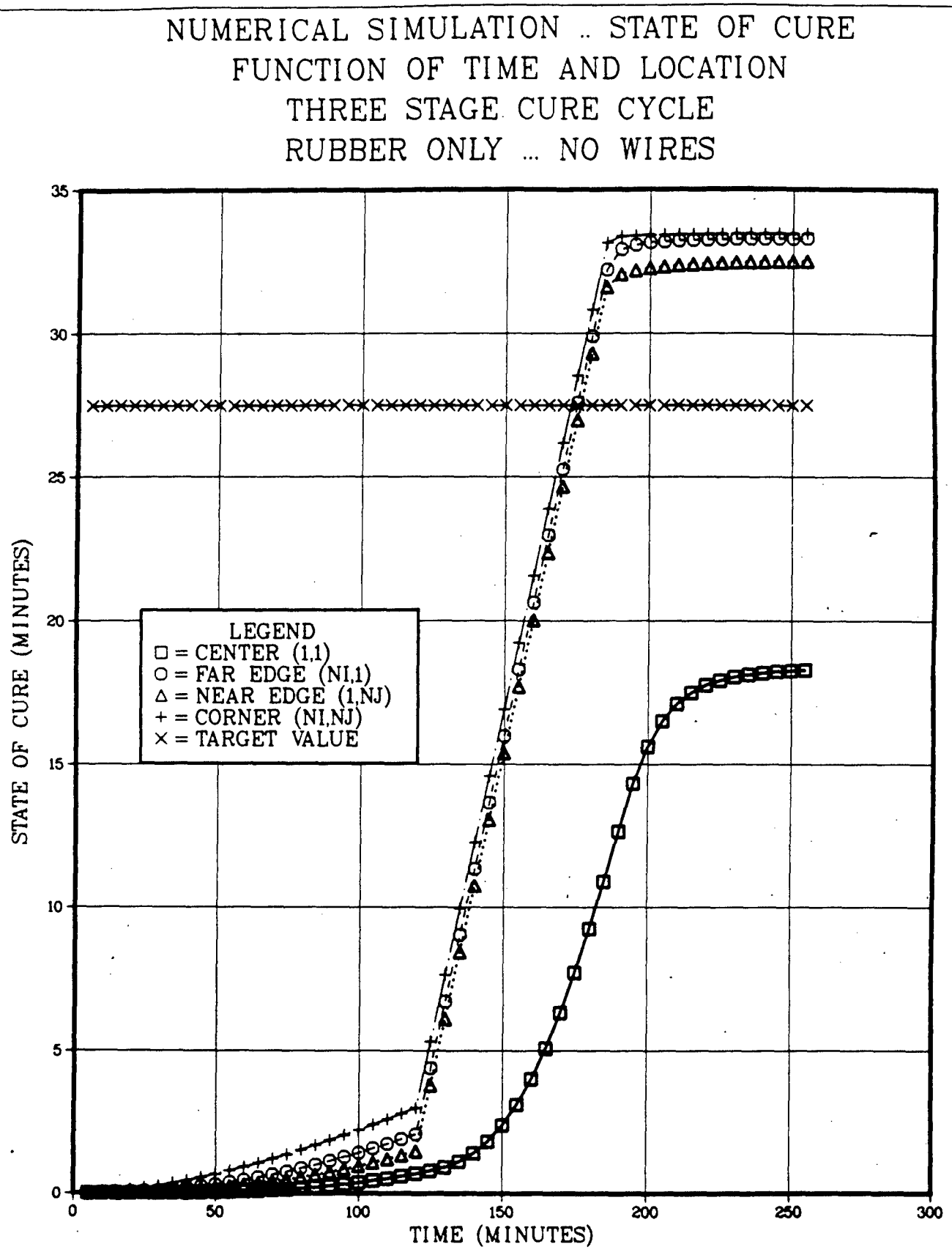

Figure A-14 Three Stage Cure Cycle, Unreinforced Rubber, Cure Stats vs Time

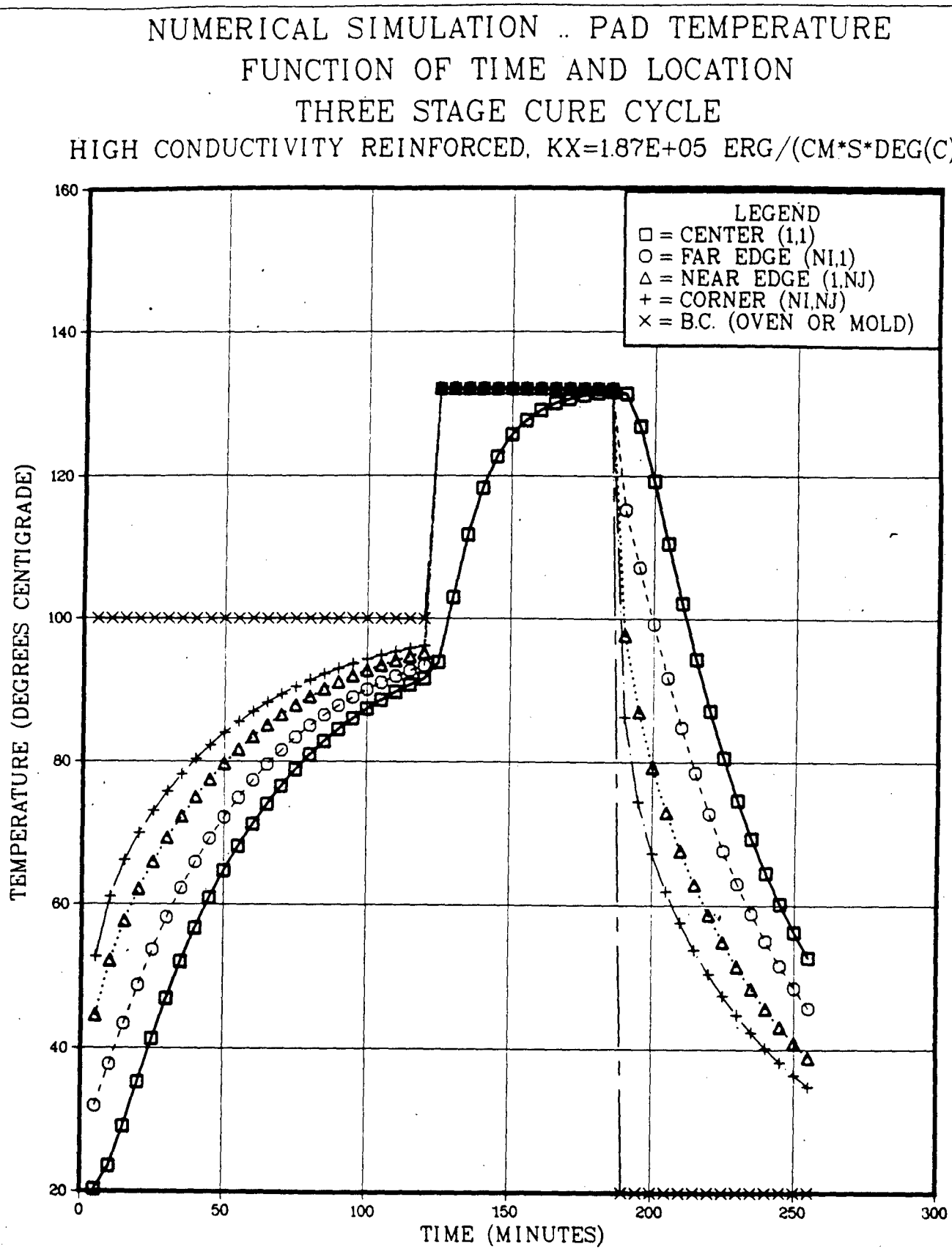

Figure A-15 Three Stage Cure Cycle Temperature vs Time, Highly Reinforced Rubber

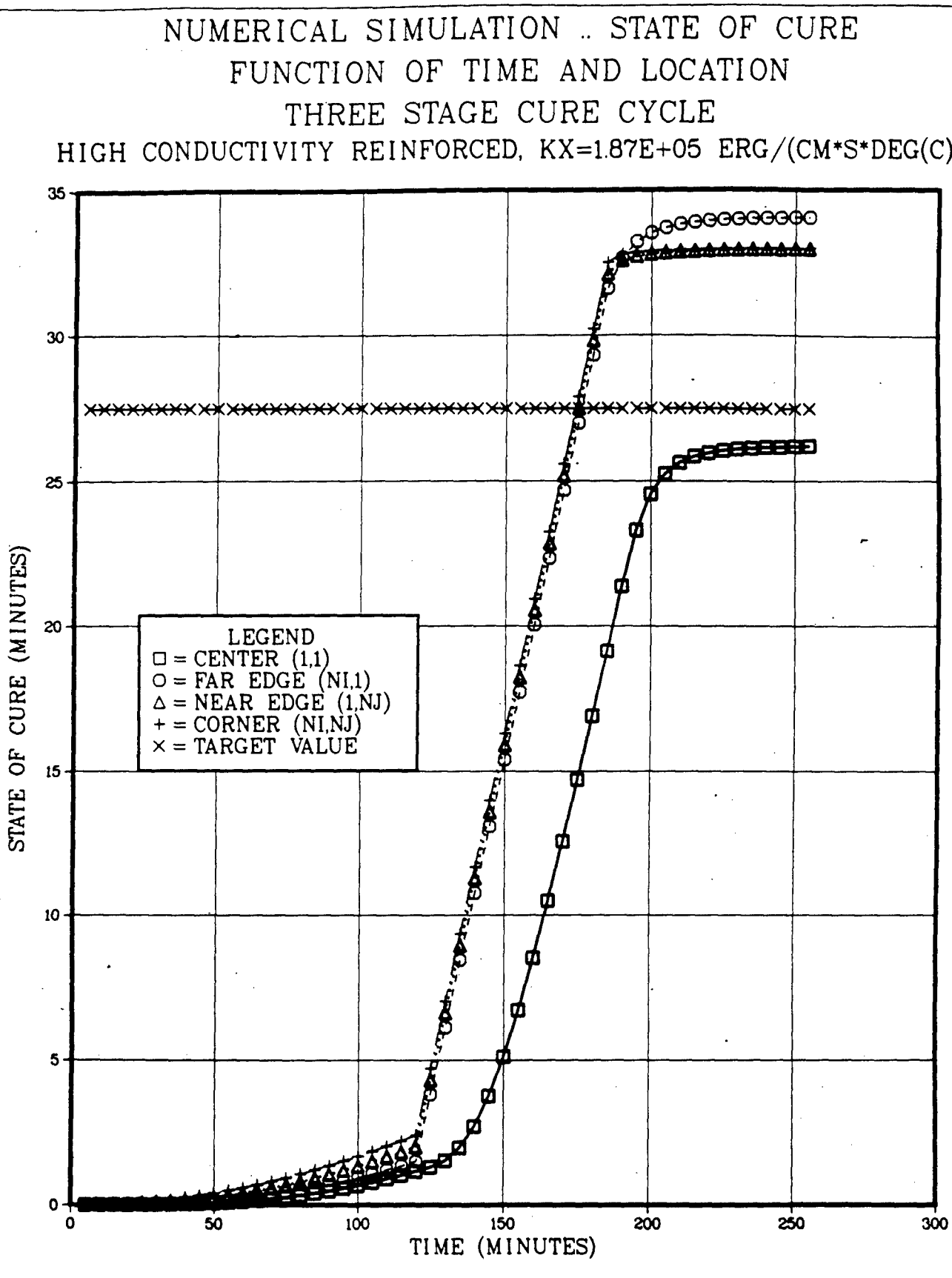

Figure A-16 Three Stage Cure Cycle, Cure State vs Time, Highly Reinforced Rubber

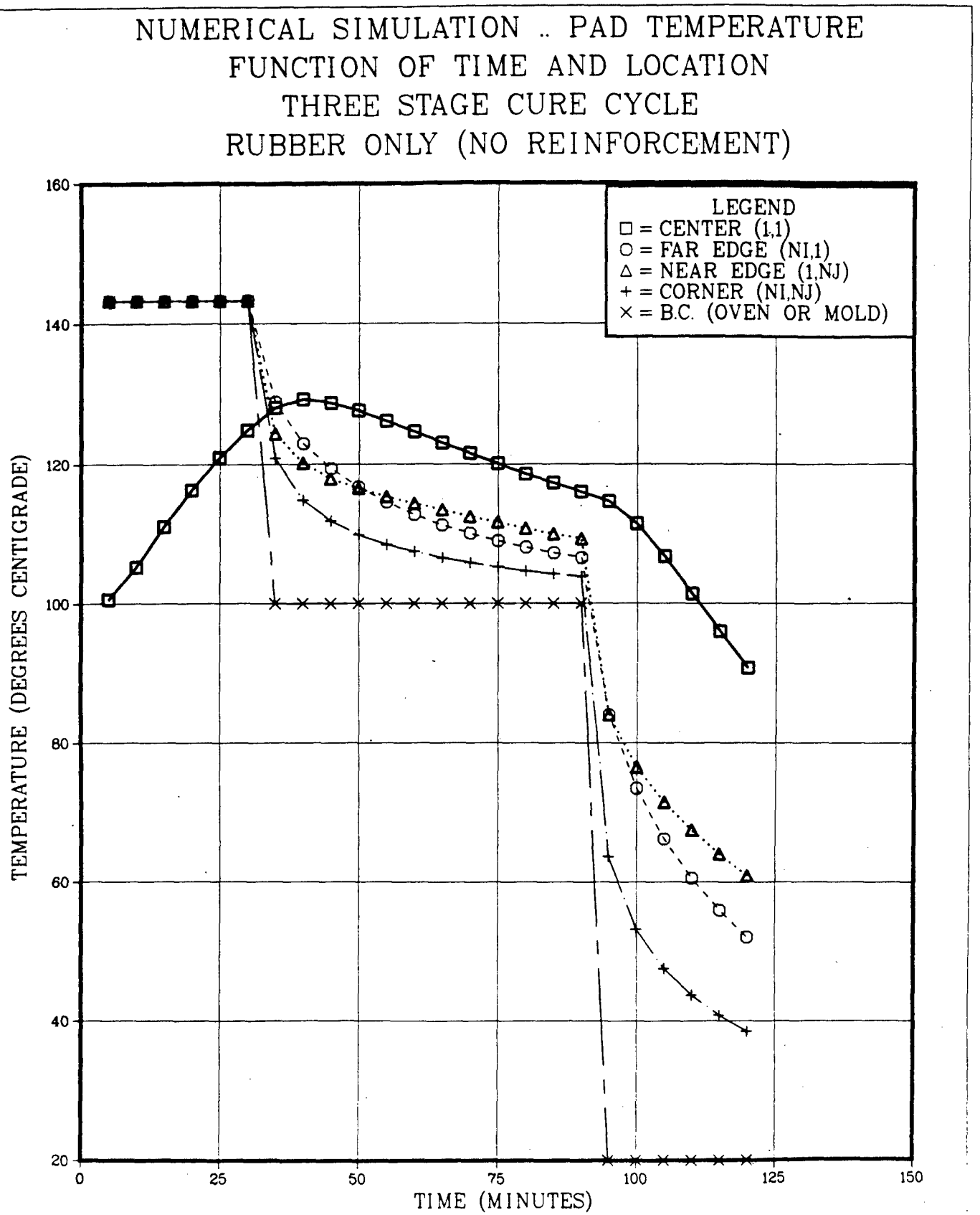

Figure A-17 Injection Mold, Three Stage Cure, Rubber Only, Temperature Vs Time.

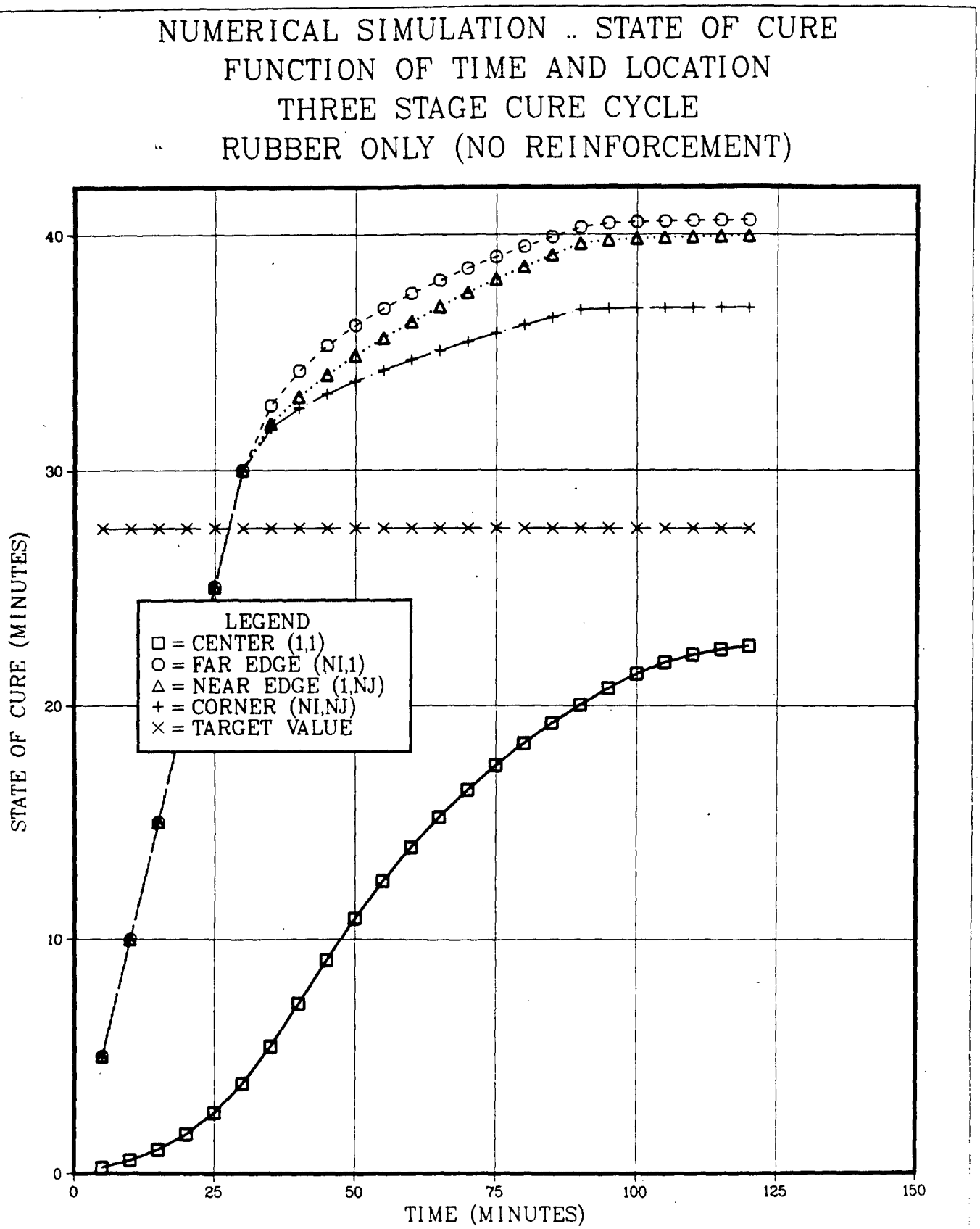

Figure A-18 Injection Mold, Three Stage Cure, Rubber Only, Cure State Vs Time

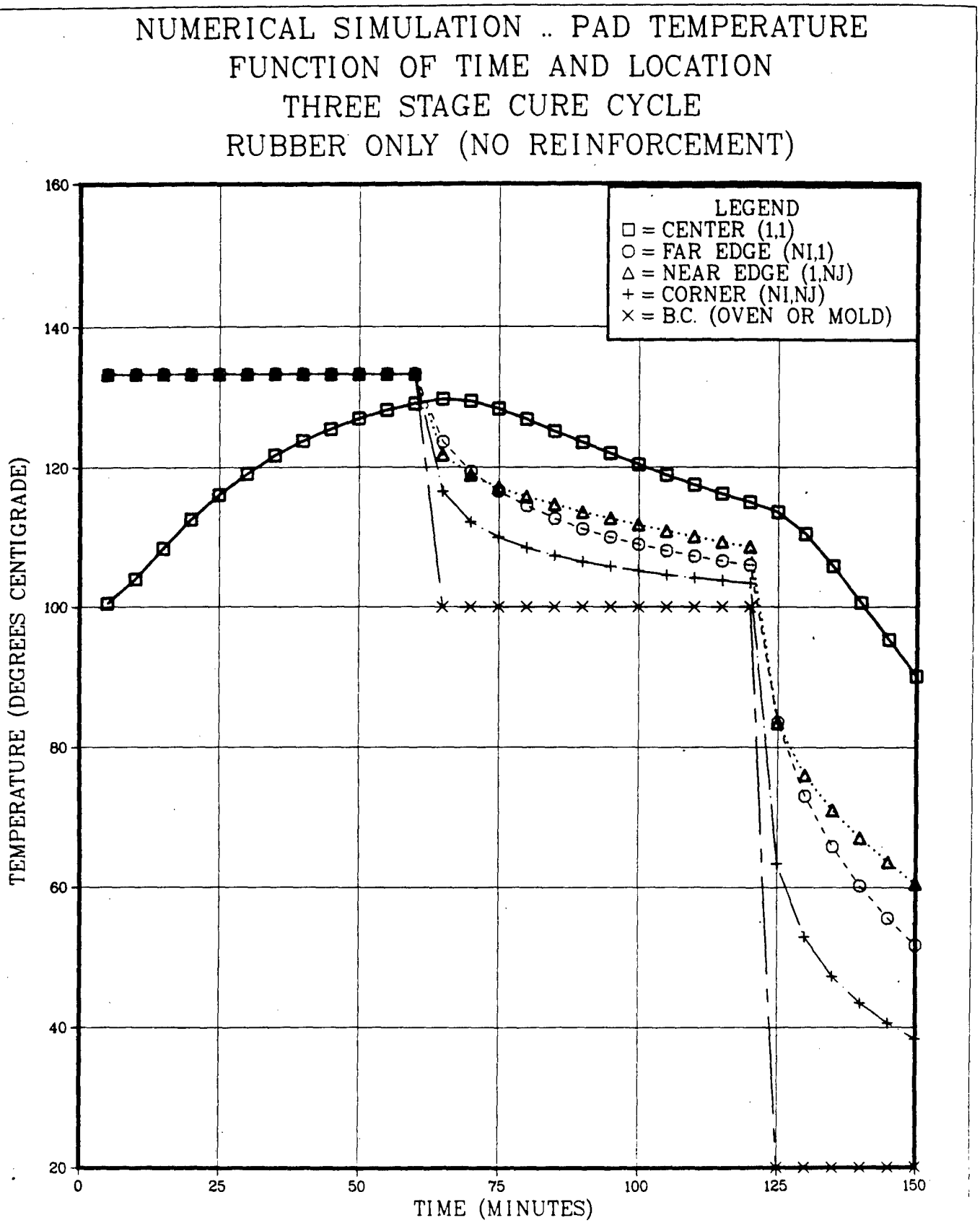

Figure A-19 Injection Mold, Three Stage Cure, Longer Mold Time, Lower Mold Temp.

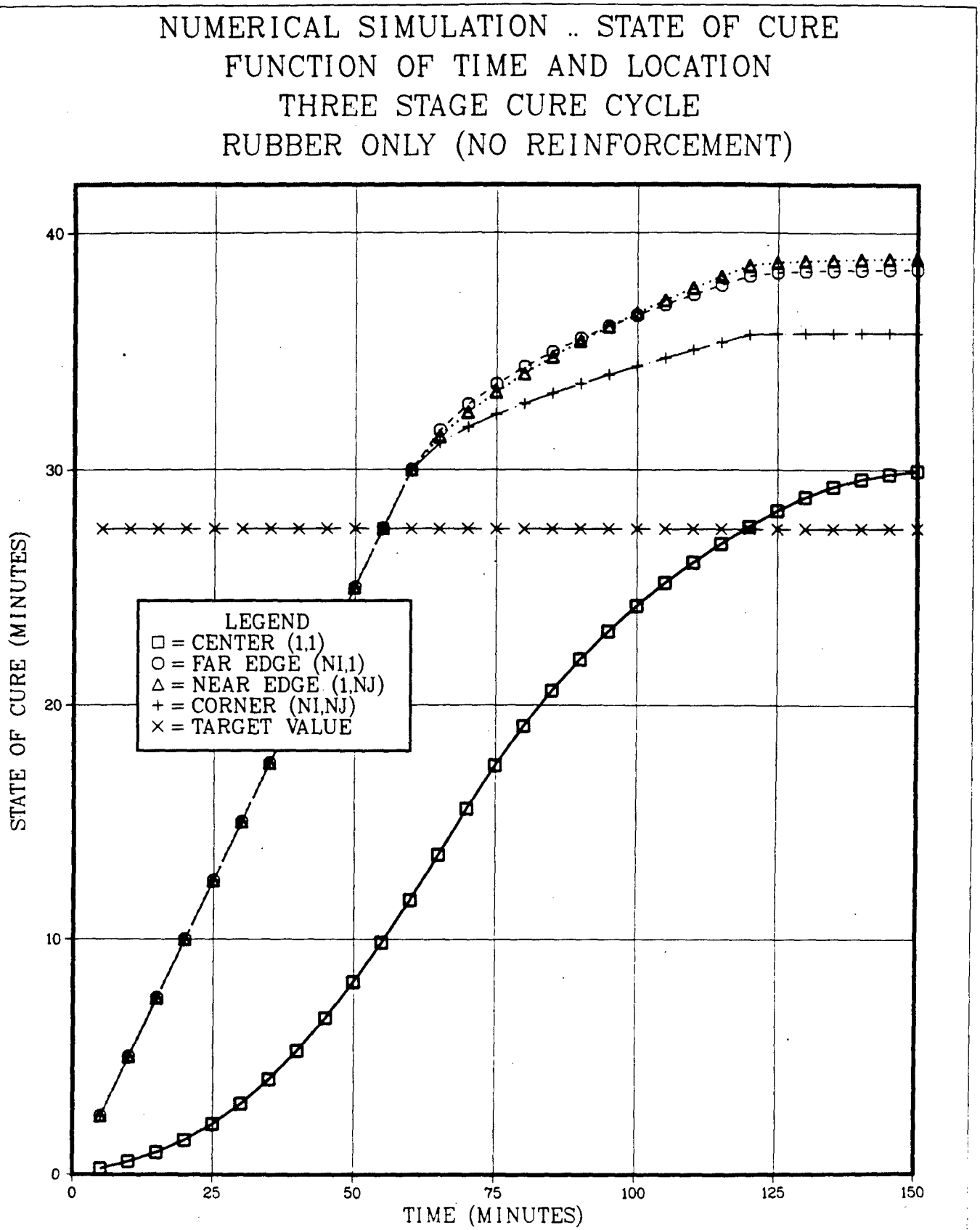

gure A-20 Injection Mold, Three Stage Cure, Longer Mold Time, Lower Mold Temperature

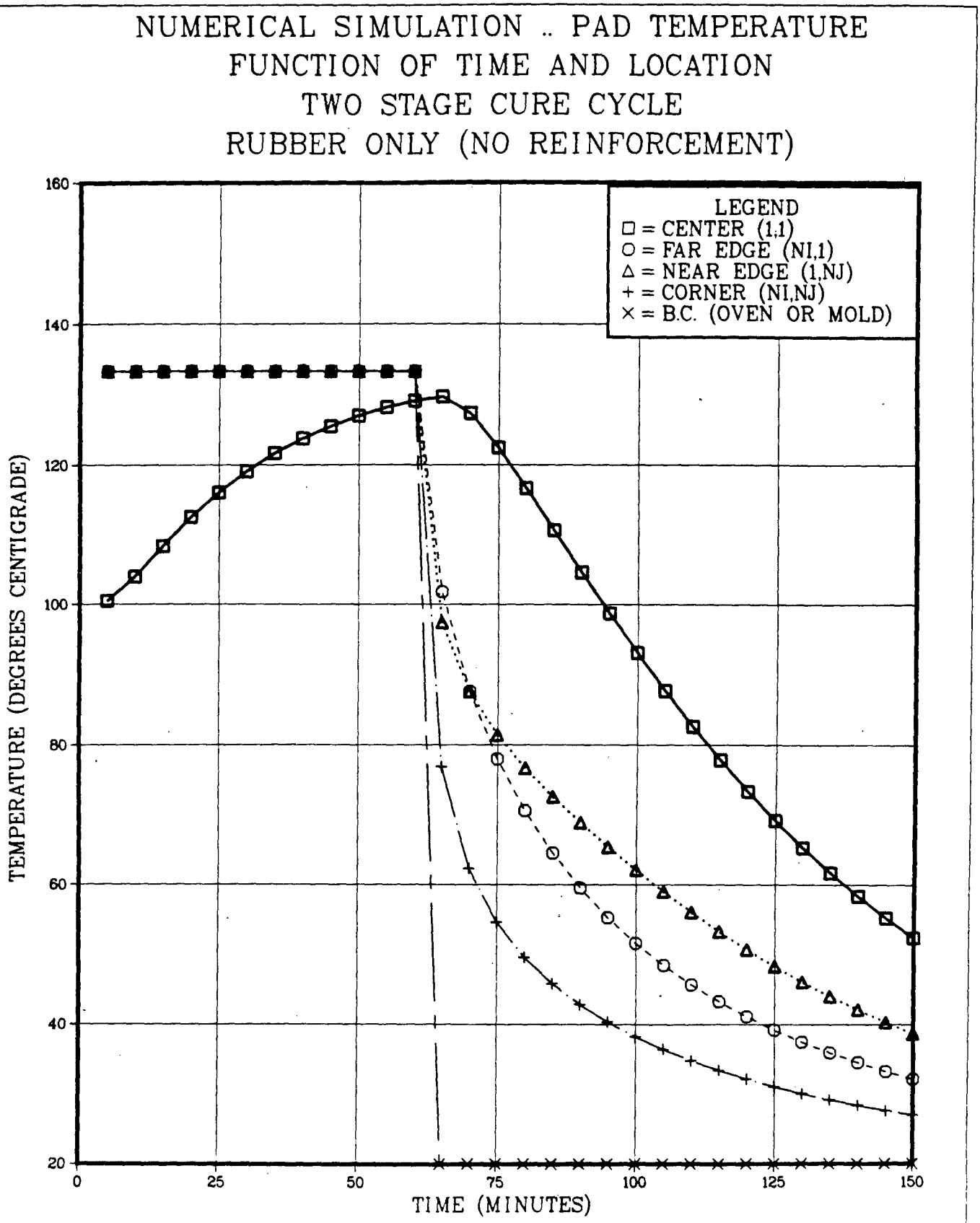

Figure A-21 Injection Mold, Two Stage Cure, Temperature Vs Time

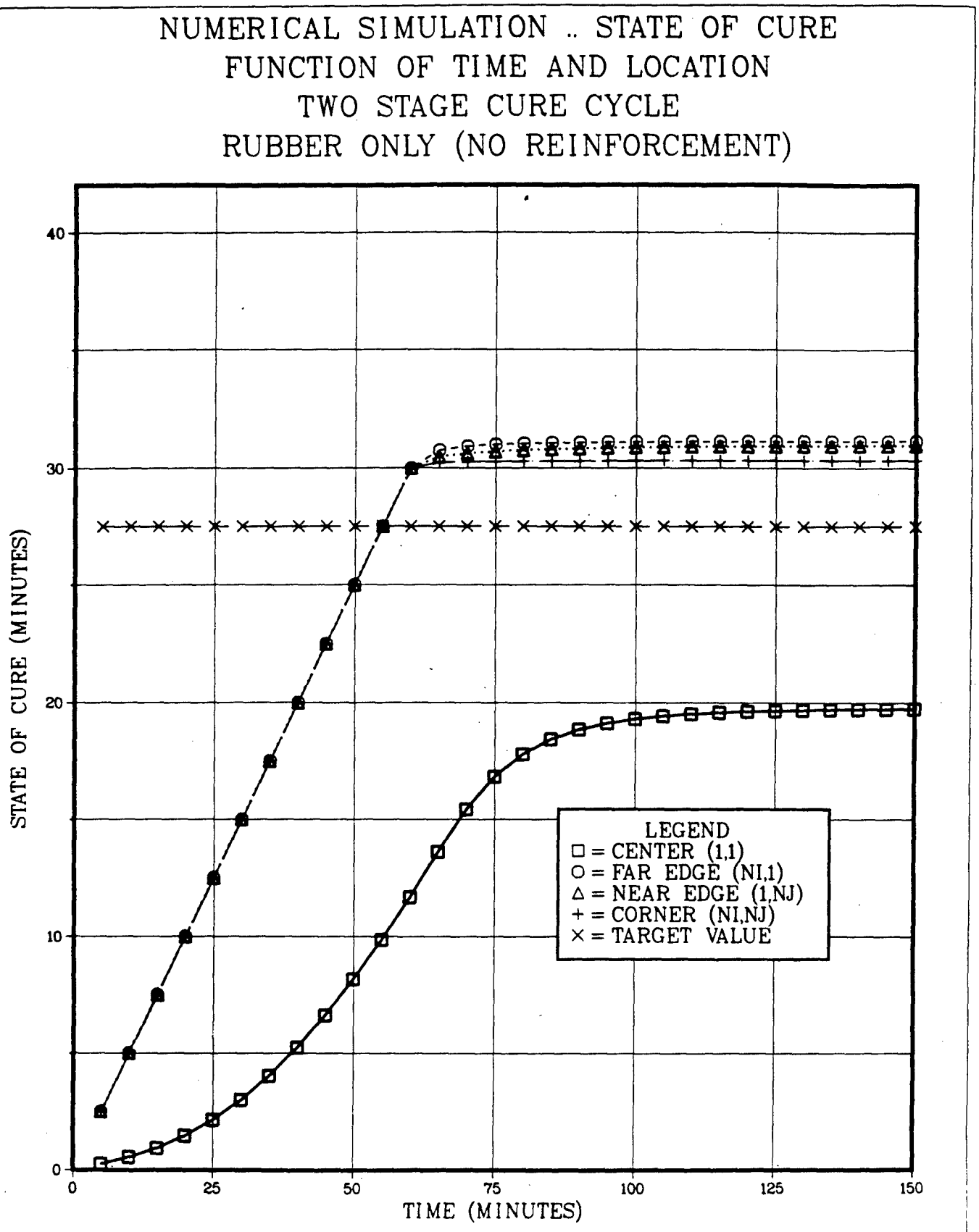

Figure A-22 Injection Mold, Two Stage Cure, Cure State Vs Time

APPENDIX B

COMPUTER PROGRAMS

```
**** TSO FOREGROUND HARDCOPY ****
DSNAME=ALGK610.PAD2D.FORT

      REAL KX,KY,K,KKR                                                  00000010
      DIMENSION CX(7),CY(7),CK(4),CH(2),COR(7),T(7),T0(7)               00000020
      DIMENSION X(7),Y(7)                                               00000030
C 2-D CALC OF TEMP IN TRACK PAD ...                                     00000040
C -A<X<+A, -B<Y<+B                                                      00000050
C ALL UNITS C.G.S.                                                      00000060
C REF. CARSLAW AND JAEGER, CONDUCTION OF HEAT IN SOLIDS,                00000061
C SECTION 5.5, P 170.                                                   00000062
C GIVES STEADY STATE TEMPERATURE IN A 2-D BLOCK WITH INTERNAL HEAT      00000063
C GENERATION AND CONVECTIVE HEAT TRANSFER                               00000064
C KX AND KY ARE THERMAL CONDUCTIVITY IN X AND Y DIRECTIONS              00000065
C HX AND HY ARE COEFFS OF SURFACE HEAT TRANSFER ON X AND Y SURFACES     00000066
C R = (1/HX) = SURFACE THERMAL RESISTANCE                               00000067
C A0 = RATE OF HEATING PER UNIT VOLUME                                  00000068
      CX(1)=0.                                                          00000070
      CY(1)=0.                                                          00000080
      CX(2)=0.5                                                         00000090
      CY(2)=0.                                                          00000100
      CX(3)=1.0                                                         00000110
      CY(3)=0.                                                          00000120
      CX(4)=0.                                                          00000130
      CY(4)=0.5                                                         00000140
      CX(5)=0.                                                          00000150
      CY(5)=1.0                                                         00000160
      CX(6)=0.5                                                         00000170
      CY(6)=1.0                                                         00000180
      CX(7)=1.0                                                         00000190
      CY(7)=1.0                                                         00000200
      PI=3.1415927                                                      00000210
C SIZE OF TEST SPECIMEN CROSS SECTION (A*B)                             00000215
      A=5.715                                                           00000220
      B=2.54                                                            00000230
      EPS=0.10                                                          00000240
      KY=3.2E+04                                                        00000250
      HY=2.35E+04                                                       00000260
      A0=3.50E+05                                                       00000270
C                                                                       00000271
C REDUCE A0 TO ACCOUNT FOR STIFFENING DUE TO REINFORCEMENT              00000272
      A0=2.625E+05                                                      00000273
C                                                                       00000274
      CK(1)=1.0                                                         00000280
      CK(2)=2.9375                                                      00000290
      CK(3)=5.84375                                                     00000300
      CK(4)=18.                                                         00000310
      CH(1)=1.0                                                         00000320
      CH(2)=2.0                                                         00000330
      DO11 ICXY=1,7                                                     00000340
      X(ICXY)=CX(ICXY)*A                                                00000350
      Y(ICXY)=CY(ICXY)*B                                                00000360
   11 CONTINUE                                                          00000370
      DO1 IH=1,2                                                        00000380
      HX=CH(IH)*HY                                                      00000390
      DO2 IK=1,3                                                        00000400
C RESET CORRECTION TERMS                                                00000410
      DO10 J=1,7                                                        00000420
      COR(J)=0.00                                                       00000430
```

```
   10 CONTINUE                                                          00000440
      KX=CK(IK)*KY                                                      00000450
      K=CK(IK)**0.5                                                     00000460
      R=1./HX                                                           00000470
      RP=1./HY                                                          00000480
      KKR=KX*RP/K                                                       00000490
      CAL=1./(R*KX)                                                     00000500
      WRITE(6,120)                                                      00000510
  120 FORMAT(1H1)                                                       00000520
      WRITE(6,101)                                                      00000530
  101 FORMAT(//10X,'2-D THERMAL MODEL OF TRACK PAD'//)                  00000540
      WRITE(6,102) A,B,A0                                               00000550
  102 FORMAT(12X,'A=',E11.4,5X,'B=',E11.4,4X,'A0=',E11.4)               00000560
      WRITE(6,103) IH,HX,HY,R,RP                                        00000570
  103 FORMAT(2X,'IH=',I2,4X,'HX=',E11.4,4X,'HY=',E11.4,                 00000580
     15X,'R=',E11.4,4X,'RP=',E11.4)                                     00000590
      WRITE(6,104) IK,KX,KY,K                                           00000600
  104 FORMAT(2X,'IK=',I2,4X,'KX=',E11.4,4X,'KY=',E11.4,5X,'K=',E11.4)   00000610
      WRITE(6,105) KKR,CAL                                              00000620
  105 FORMAT(10X,'KKR=',E11.4,3X,'CAL=',E11.4)                          00000630
C N IS THE INDEX OF ALPHA                                               00000640
      DO3 N=1,7                                                         00000650
      AN=N                                                              00000660
      AL=((2.*AN-1.)*PI/2.-EPS)/A                                       00000670
      WRITE(6,106)                                                      00000680
  106 FORMAT(//10X,'ITERATIVE SOLUTION FOR AL'//)                       00000690
      DO4 IA=1,8                                                        00000700
      AAL=A*AL                                                          00000710
      Z=AL*TAN(AAL)-CAL                                                 00000720
      ZP=TAN(AAL)+AAL/(COS(AAL)**2)                                     00000730
      DEL=-Z/ZP                                                         00000740
      AL=AL+DEL                                                         00000750
      WRITE(6,107) N,IA,Z,ZP,AL                                         00000760
  107 FORMAT(3X,'N=',I2,2X,'IA=',I2,2X,'Z=',E11.4,2X,'ZP=',E11.4,2X,    00000770
     1'AL=',E13.6)                                                      00000780
    4 CONTINUE                                                          00000790
      AAL=A*AL                                                          00000800
      F1=AL*AL*(2.*AAL+SIN(2.*AAL))                                     00000810
      F2=KKR*AL*SINH(K*B*AL)+COSH(K*B*AL)                               00000820
      F3=SIN(AAL)/(F1*F2)                                               00000830
      WRITE(6,108) AAL,F1,F2,F3                                         00000840
  108 FORMAT(//10X,'AAL=',E11.4,2X,'F1=',E11.4,2X,'F2=',E11.4,2X,       00000850
     1'F3=',E11.4)                                                      00000860
      WRITE(6,109)                                                      00000870
  109 FORMAT(//10X,'SERIES SOL FOR TEMP AS FN OF GEOMETRY'//)           00000880
      DO5 IC=1,7                                                        00000890
      T0(IC)=A0*(A*R+(A*A-X(IC)*X(IC))/(2.*KX))                         00000900
      COR(IC)=COR(IC)+(4.*A0/KX)*F3*COS(X(IC)*AL)*COSH(K*Y(IC)*AL)      00000910
      T(IC)=T0(IC)-COR(IC)                                              00000920
      WRITE(6,110) N,IC,X(IC),Y(IC),T0(IC),COR(IC),T(IC)                00000930
  110 FORMAT(2X,'N=',I2,2X,'IC=',I2,2X,'X=',F8.3,2X,'Y=',F8.3,2X,'T0=', 00000940
     1F8.3,2X,'COR=',F8.3,2X,'T=',F8.3)                                 00000950
    5 CONTINUE                                                          00000960
    3 CONTINUE                                                          00000970
    2 CONTINUE                                                          00000980
    1 CONTINUE                                                          00000990
      STOP                                                              00001000
      END                                                               00001010
```

2-D THERMAL MODEL OF TRACK PAD

A= 0.5715E+01 B= 0.2540E+01 A0= 0.2625E+06
IH= 1 HX= 0.2350E+05 HY= 0.2350E+05 R= 0.4255E-04 RP= 0.4255E-04
IK= 1 KX= 0.3200E+05 KY= 0.3200E+05 K= 0.1000E+01
KKR= 0.1362E+01 CAL= 0.7344E+00

ITERATIVE SOLUTION FOR AL

N= 1 IA= 1 Z= 0.1831E+01 ZP= 0.1575E+03 AL= 0.245737E+00
N= 1 IA= 2 Z= 0.7286E+00 ZP= 0.5714E+02 AL= 0.232984E+00
N= 1 IA= 3 Z= 0.2206E+00 ZP= 0.2780E+02 AL= 0.225049E+00
N= 1 IA= 4 Z= 0.3479E-01 ZP= 0.1973E+02 AL= 0.223285E+00
N= 1 IA= 5 Z= 0.1174E-02 ZP= 0.1842E+02 AL= 0.223221E+00
N= 1 IA= 6 Z= 0.1431E-05 ZP= 0.1837E+02 AL= 0.223221E+00
N= 1 IA= 7 Z= 0.1013E-05 ZP= 0.1837E+02 AL= 0.223221E+00
N= 1 IA= 8 Z=-0.1490E-05 ZP= 0.1837E+02 AL= 0.223221E+00

AAL= 0.1276E+01 F1= 0.1549E+00 F2= 0.1347E+01 F3= 0.4587E+01

SERIES SOL FOR TEMP AS FN OF GEOMETRY

N= 1 IC= 1 X= 0.0 Y= 0.0 T0= 197.800 COR= 150.523 T= 47.277
N= 1 IC= 2 X= 2.858 Y= 0.0 T0= 164.309 COR= 120.926 T= 43.383
N= 1 IC= 3 X= 5.715 Y= 0.0 T0= 63.838 COR= 43.775 T= 20.062
N= 1 IC= 4 X= 0.0 Y= 1.270 T0= 197.800 COR= 156.612 T= 41.188
N= 1 IC= 5 X= 0.0 Y= 2.540 T0= 197.800 COR= 175.372 T= 22.428
N= 1 IC= 6 X= 2.858 Y= 2.540 T0= 164.309 COR= 140.889 T= 23.420
N= 1 IC= 7 X= 5.715 Y= 2.540 T0= 63.838 COR= 51.002 T= 12.836

ITERATIVE SOLUTION FOR AL

N= 2 IA= 1 Z= 0.7309E+01 ZP= 0.4727E+03 AL= 0.791605E+00
N= 2 IA= 2 Z= 0.3418E+01 ZP= 0.1343E+03 AL= 0.766147E+00
N= 2 IA= 3 Z= 0.1475E+01 ZP= 0.4366E+02 AL= 0.732372E+00
N= 2 IA= 4 Z= 0.5246E+00 ZP= 0.1827E+02 AL= 0.703664E+00
N= 2 IA= 5 Z= 0.1166E+00 ZP= 0.1111E+02 AL= 0.693174E+00
N= 2 IA= 6 Z= 0.8358E-02 ZP= 0.9581E+01 AL= 0.692302E+00
N= 2 IA= 7 Z= 0.4691E-04 ZP= 0.9470E+01 AL= 0.692297E+00
N= 2 IA= 8 Z= 0.0 ZP= 0.9469E+01 AL= 0.692297E+00

AAL= 0.3956E+01 F1= 0.4271E+01 F2= 0.5642E+01 F3=-0.3020E-01

SERIES SOL FOR TEMP AS FN OF GEOMETRY

N= 2 IC= 1 X= 0.0 Y= 0.0 T0= 197.800 COR= 149.532 T= 48.268

```
N= 2  IC= 2  X=   2.858  Y=   0.0    TO= 164.309  COR= 121.319  T=  42.990
N= 2  IC= 3  X=   5.715  Y=   0.0    TO=  63.838  COR=  44.455  T=  19.383
N= 2  IC= 4  X=   0.0    Y=   1.270  TO= 197.800  COR= 155.213  T=  42.587
N= 2  IC= 5  X=   0.0    Y=   2.540  TO= 197.800  COR= 172.411  T=  25.388
N= 2  IC= 6  X=   2.858  Y=   2.540  TO= 164.309  COR= 142.062  T=  22.247
N= 2  IC= 7  X=   5.715  Y=   2.540  TO=  63.838  COR=  53.033  T=  10.805

        ITERATIVE SOLUTION FOR AL

 N= 3  IA= 1  Z= 0.1279E+02  ZP= 0.7879E+03  AL= 0.134055E+01
 N= 3  IA= 2  Z= 0.6134E+01  ZP= 0.2139E+03  AL= 0.131187E+01
 N= 3  IA= 3  Z= 0.2786E+01  ZP= 0.6418E+02  AL= 0.126845E+01
 N= 3  IA= 4  Z= 0.1101E+01  ZP= 0.2387E+02  AL= 0.122233E+01
 N= 3  IA= 5  Z= 0.3003E+00  ZP= 0.1284E+02  AL= 0.119894E+01
 N= 3  IA= 6  Z= 0.3201E-01  ZP= 0.1029E+02  AL= 0.119583E+01
 N= 3  IA= 7  Z= 0.4063E-03  ZP= 0.1003E+02  AL= 0.119579E+01
 N= 3  IA= 8  Z=-0.5186E-05  ZP= 0.1003E+02  AL= 0.119579E+01

        AAL= 0.6834E+01  F1= 0.2082E+02  F2= 0.2738E+02  F3= 0.9179E-03

        SERIES SOL FOR TEMP AS FN OF GEOMETRY

N= 3  IC= 1  X=   0.0    Y=   0.0    TO= 197.800  COR= 149.562  T=  48.238
N= 3  IC= 2  X=   2.858  Y=   0.0    TO= 164.309  COR= 121.290  T=  43.019
N= 3  IC= 3  X=   5.715  Y=   0.0    TO=  63.838  COR=  44.481  T=  19.357
N= 3  IC= 4  X=   0.0    Y=   1.270  TO= 197.800  COR= 155.285  T=  42.515
N= 3  IC= 5  X=   0.0    Y=   2.540  TO= 197.800  COR= 172.726  T=  25.074
N= 3  IC= 6  X=   2.858  Y=   2.540  TO= 164.309  COR= 141.760  T=  22.550
N= 3  IC= 7  X=   5.715  Y=   2.540  TO=  63.838  COR=  53.301  T=  10.537

        ITERATIVE SOLUTION FOR AL

 N= 4  IA= 1  Z= 0.1827E+02  ZP= 0.1103E+04  AL= 0.188993E+01
 N= 4  IA= 2  Z= 0.8852E+01  ZP= 0.2938E+03  AL= 0.185979E+01
 N= 4  IA= 3  Z= 0.4106E+01  ZP= 0.8522E+02  AL= 0.181162E+01
 N= 4  IA= 4  Z= 0.1688E+01  ZP= 0.3020E+02  AL= 0.175573E+01
 N= 4  IA= 5  Z= 0.4906E+00  ZP= 0.1562E+02  AL= 0.172431E+01
 N= 4  IA= 6  Z= 0.5568E-01  ZP= 0.1238E+02  AL= 0.171981E+01
 N= 4  IA= 7  Z= 0.7463E-03  ZP= 0.1205E+02  AL= 0.171975E+01
 N= 4  IA= 8  Z= 0.3576E-06  ZP= 0.1205E+02  AL= 0.171975E+01

        AAL= 0.9828E+01  F1= 0.6027E+02  F2= 0.1318E+03  F3=-0.4943E-04

        SERIES SOL FOR TEMP AS FN OF GEOMETRY

N= 4  IC= 1  X=   0.0    Y=   0.0    TO= 197.800  COR= 149.560  T=  48.239
N= 4  IC= 2  X=   2.858  Y=   0.0    TO= 164.309  COR= 121.289  T=  43.020
N= 4  IC= 3  X=   5.715  Y=   0.0    TO=  63.838  COR=  44.482  T=  19.356
N= 4  IC= 4  X=   0.0    Y=   1.270  TO= 197.800  COR= 155.277  T=  42.522
N= 4  IC= 5  X=   0.0    Y=   2.540  TO= 197.800  COR= 172.662  T=  25.138
```

```
N= 4  IC= 6  X=   2.858  Y=   2.540  T0= 164.309  COR= 141.747  T=  22.562
N= 4  IC= 7  X=   5.715  Y=   2.540  T0=  63.838  COR=  53.360  T=  10.478

        ITERATIVE SOLUTION FOR AL

 N= 5  IA= 1  Z= 0.2374E+02  ZP= 0.1418E+04  AL= 0.243945E+01
 N= 5  IA= 2  Z= 0.1157E+02  ZP= 0.3738E+03  AL= 0.240849E+01
 N= 5  IA= 3  Z= 0.5427E+01  ZP= 0.1064E+03  AL= 0.235749E+01
 N= 5  IA= 4  Z= 0.2278E+01  ZP= 0.3674E+02  AL= 0.229550E+01
 N= 5  IA= 5  Z= 0.6807E+00  ZP= 0.1872E+02  AL= 0.225914E+01
 N= 5  IA= 6  Z= 0.7654E-01  ZP= 0.1493E+02  AL= 0.225402E+01
 N= 5  IA= 7  Z= 0.9172E-03  ZP= 0.1458E+02  AL= 0.225395E+01
 N= 5  IA= 8  Z= 0.2980E-06  ZP= 0.1457E+02  AL= 0.225395E+01

        AAL= 0.1288E+02  F1= 0.1339E+03  F2= 0.6235E+03  F3= 0.3711E-05

        SERIES SOL FOR TEMP AS FN OF GEOMETRY

N= 5  IC= 1  X=   0.0    Y=   0.0    T0= 197.800  COR= 149.560  T=  48.239
N= 5  IC= 2  X=   2.858  Y=   0.0    T0= 164.309  COR= 121.289  T=  43.020
N= 5  IC= 3  X=   5.715  Y=   0.0    T0=  63.838  COR=  44.482  T=  19.356
N= 5  IC= 4  X=   0.0    Y=   1.270  T0= 197.800  COR= 155.278  T=  42.521
N= 5  IC= 5  X=   0.0    Y=   2.540  T0= 197.800  COR= 172.681  T=  25.119
N= 5  IC= 6  X=   2.858  Y=   2.540  T0= 164.309  COR= 141.765  T=  22.544
N= 5  IC= 7  X=   5.715  Y=   2.540  T0=  63.838  COR=  53.378  T=  10.460

        ITERATIVE SOLUTION FOR AL

 N= 6  IA= 1  Z= 0.2921E+02  ZP= 0.1732E+04  AL= 0.298904E+01
 N= 6  IA= 2  Z= 0.1429E+02  ZP= 0.4536E+03  AL= 0.295754E+01
 N= 6  IA= 3  Z= 0.6748E+01  ZP= 0.1276E+03  AL= 0.290466E+01
 N= 6  IA= 4  Z= 0.2868E+01  ZP= 0.4337E+02  AL= 0.283854E+01
 N= 6  IA= 5  Z= 0.8693E+00  ZP= 0.2197E+02  AL= 0.279896E+01
 N= 6  IA= 6  Z= 0.9504E-01  ZP= 0.1770E+02  AL= 0.279359E+01
 N= 6  IA= 7  Z= 0.9795E-03  ZP= 0.1733E+02  AL= 0.279353E+01
 N= 6  IA= 8  Z=-0.1258E-04  ZP= 0.1733E+02  AL= 0.279353E+01

        AAL= 0.1597E+02  F1= 0.2530E+03  F2= 0.2898E+04  F3=-0.3467E-06

        SERIES SOL FOR TEMP AS FN OF GEOMETRY

N= 6  IC= 1  X=   0.0    Y=   0.0    T0= 197.800  COR= 149.560  T=  48.239
N= 6  IC= 2  X=   2.858  Y=   0.0    T0= 164.309  COR= 121.289  T=  43.020
N= 6  IC= 3  X=   5.715  Y=   0.0    T0=  63.838  COR=  44.482  T=  19.356
N= 6  IC= 4  X=   0.0    Y=   1.270  T0= 197.800  COR= 155.278  T=  42.522
N= 6  IC= 5  X=   0.0    Y=   2.540  T0= 197.800  COR= 172.674  T=  25.126
N= 6  IC= 6  X=   2.858  Y=   2.540  T0= 164.309  COR= 141.766  T=  22.543
N= 6  IC= 7  X=   5.715  Y=   2.540  T0=  63.838  COR=  53.384  T=  10.454
```

ITERATIVE SOLUTION FOR AL

N= 7	IA= 1	Z= 0.3469E+02	ZP= 0.2048E+04	AL= 0.353867E+01
N= 7	IA= 2	Z= 0.1701E+02	ZP= 0.5338E+03	AL= 0.350680E+01
N= 7	IA= 3	Z= 0.8072E+01	ZP= 0.1489E+03	AL= 0.345261E+01
N= 7	IA= 4	Z= 0.3460E+01	ZP= 0.5006E+02	AL= 0.338350E+01
N= 7	IA= 5	Z= 0.1058E+01	ZP= 0.2529E+02	AL= 0.334167E+01
N= 7	IA= 6	Z= 0.1121E+00	ZP= 0.2058E+02	AL= 0.333622E+01
N= 7	IA= 7	Z= 0.1017E-02	ZP= 0.2021E+02	AL= 0.333617E+01
N= 7	IA= 8	Z=-0.8285E-05	ZP= 0.2021E+02	AL= 0.333617E+01

AAL= 0.1907E+02 F1= 0.4291E+03 F2= 0.1327E+05 F3= 0.3776E-07

SERIES SOL FOR TEMP AS FN OF GEOMETRY

N= 7	IC= 1	X=	0.0	Y=	0.0	T0= 197.800	COR= 149.560	T=	48.239
N= 7	IC= 2	X=	2.858	Y=	0.0	T0= 164.309	COR= 121.289	T=	43.020
N= 7	IC= 3	X=	5.715	Y=	0.0	T0= 63.838	COR= 44.482	T=	19.356
N= 7	IC= 4	X=	0.0	Y=	1.270	T0= 197.800	COR= 155.278	T=	42.521
N= 7	IC= 5	X=	0.0	Y=	2.540	T0= 197.800	COR= 172.677	T=	25.123
N= 7	IC= 6	X=	2.858	Y=	2.540	T0= 164.309	COR= 141.763	T=	22.546
N= 7	IC= 7	X=	5.715	Y=	2.540	T0= 63.838	COR= 53.387	T=	10.451

```
**** TSO FOREGROUND HARDCOPY ****
DSNAME=ALGK610.PADCH2D.FORT

C 2-D MODEL OF A RECTANGULAR RUBBER BLOCK, USING SYMMETRY                    00000100
C MODIFIED FOR GRAPHICS ....                                                 00000110
C CAN MODEL CURING AND HYSTERESIS HEATING                                    00000200
C CAN USE TEMPERATURE AND SURFACE HEAT TRANSFER B.C.                         00000300
C USES FINITE DIFFERENCE METHOD -- REF WORK OF 2/14/85                       00000400
C UNITS ARE GRAM-CENTIMETER-SECOND                                           00000500
C                                                                            00000600
C REFERENCES:                                                                00000610
C HILLS, "HEAT TRANSFER AND VULCANIZATION OF RUBBER"                         00000620
C CARSLAW AND JAEGER, "CONDUCTION OF HEAT IN SOLIDS"                         00000630
C                                                                            00001000
C VARIABLE NAMES:                                                            00001100
C DEGC = DEGREES CENTIGRADE                                                  00001200
C K = THERMAL CONDUCTIVITY, GRAM*CM*(S**(-3))*(DEGC**(-1))                   00001300
C RHO = DENSITY, GRAM*(CM**(-3))                                             00001400
C C = HEAT CAPACITY, (CM**2)*(S**(-2))*(DEGC**(-1)), = ERG/(GRAM*DEGC)       00001500
C I = INDEX IN THE X DIRECTION                                               00001600
C J = INDEX IN THE Y DIRECTION                                               00001700
C DI = THERMAL DIFFUSIVITY IN X(I) DIRECTION, (CM**2)*(S**(-1))              00001800
C DJ = THERMAL DIFFUSIVITY IN Y(J) DIRECTION                                 00001900
C D = K/(RHO*C), GENERAL DEFINITION OF THERMAL DIFFUSIVITY                   00002000
C HX = HEAT TRANSFER COEFFICIENT IN X DIRECTION,                             00002100
C HY = H IN Y DIRECTION, GRAM*(S**(-3))*(DEGC**(-1))                         00002200
C W = HEATING RATE, GRAM*(CM**(-1))*(S(**-3)), = ERG/(S*CM**3)               00002300
C TC = TEMPERATURE COEFFICIENT OF VULCANIZATION                              00002400
C VREF = REFERENCE TEMPERATURE FOR CURING INDEX, DEGC                        00002500
C V0 = INITIAL TEMPERATURE OF THE BLOCK                                      00002610
C NI = NUMBER OF NODES IN X DIRECTION                                        00002700
C NJ = NUMBER OF NODES IN Y DIRECTION                                        00002800
C IBC = BOUNDARY CONDITION INDICATOR ON SURFACE I = NI                       00002900
C JBC = BOUNDARY CONDITION INDICATOR ON SURFACE J = NJ                       00003000
C T = TIME, SECONDS                                                          00003010
C TM = TIME IN A STEP, SEC                                                   00003020
C 1 INDICATES SURFACE TEMPERATURE BC SPECIFIED                               00003100
C 2 INDICATES CONVECTIVE HEAT TRANSFER BC                                    00003200
C VS = SURFACE TEMPERATURE FOR BC TYPE 1                                     00003300
C VS = FREE STREAM TEMPERATURE FOR BC TYPE 2                                 00003400
C VSI = SURFACE TEMPERATURE AT BEGINNING OF STEP (INITIAL TEMP.)             00003500
C VSF = SURFACE TEMPERATURE AT END OF STEP (FINAL TEMP.)                     00003600
C VST = SURFACE TEMPERATURE AT TIME T                                        00003612
C VSX = SURFACE TEMPERATURE ON A "X=CONST" SURFACE                           00003620
C VSY = SURFACE TEMPERATURE ON A "Y=CONST" SURFACE                           00003630
C HERE, FOR NOW, VSX = VSY                                                   00003640
C LX = HALF LENGTH IN X DIRECTION, CM                                        00003700
C LY = HALF LENGTH IN Y DIRECTION, CM                                        00003800
C DX, DY = CELL SIZE                                                         00003900
C DT = TIME STEP                                                             00004000
C A = TIME STEP CALCULATION FACTOR                                           00004010
C V(I,J) = TEMPERATURE AT NODE I,J                                           00004100
C SC(I,J) = CURING INDEX AT NODE I,J                                         00004200
C D2VDX2(I,J) = SECOND DERIVATIVE OF V W.R.T. X                              00004300
C SAME IDEA FOR Y                                                            00004400
C NPPL = NUMBER OF POINTS PLOTTED                                            00004410
C SCTV = TARGET VALUE OF SC (CURE NUMBER) (UNITS ARE TIME (MINUTES))
      REAL KX,KY,LX,LY                                                       00004500
      COMMON/A/ KX,KY,RHO,C,DI,DJ,HX,HY,W,DT,DX,DY,DXS,DYS,TC                00004600
```

```
                                                                        00004610
     2,VREF,T                                                           00004620
      COMMON/B/ NI,NJ,NPR,NPRM,NPPL                                     00004630
      COMMON/C/ V(11,11),SC(11,11)                                      00004640
      COMMON/D/ TP(100),V11(100),VNI1(100),V1NJ(100),VNINJ(100)         00004650
      COMMON/E/ SC11(100),SCNI1(100),SC1NJ(100),SCNINJ(100),VBC(100)    00004845
      DIMENSION TM(10),VSI(10),VSF(10),IBC(10),JBC(10)
      DIMENSION XDATA(1000),YDATA(1000),ZDATA(1000)
      SCTV=27.5                                                         00004846
      NPPL=0                                                            00004848
      KY=3.2E+04                                                        00004849
C                                                                       00004948
C     KX=6.4E+04                                                        00004949
C                                                                       00004950
C SPECIAL CASE .. NO WIRES ...                                          00004951
      KX=KY                                                             00004955
C                                                                       00004956
C FROM CWW2D CALCULATION, STEEL WIRE ...                                00004957
C     KX=1.2E+05                                                        00004958
C                                                                       00004959
C CORRECTION .. SIMPLE VOLUME AVERAGE, STEEL WIRE ...                   00004960
C     KX=9.4E+04                                                        00004970
C                                                                       00004980
C SPECIAL CASE .. 30% CONDUCTIVITY COPPERPLY ...                        00004990
C     KX=1.87E+05                                                       00004991
C                                                                       00005000
      RHO=1.15                                                          00005100
      C=1.8E+07                                                         00005200
      DI=KX/(RHO*C)                                                     00005300
      DJ=KY/(RHO*C)                                                     00005402
C                                                                       00005403
C MOVING AIR .. CHANGE HX AND HY                                        00005404
C     HX=2.35E+04                                                       00005405
C     HY=2.35E+04                                                       00005406
C                                                                       00005407
C STILL AIR .. CHANGE HX AND HY                                         00005408
      HX=1.70E+04                                                       00005409
      HY=1.70E+04                                                       00005410
C                                                                       00005411
C FOR FINNED SURFACE ...                                                00005412
C     HX=4.70E+04                                                       00005420
C                                                                       00005430
C     W=3.5E+05                                                         00005440
C REDUCE W TO ACCOUNT FOR STIFFENING EFFECT OF WIRES ...                00005450
C     W=2.625E+05                                                       00005460
C                                                                       00005470
C FOR CURING CYCLE ...                                                  00005612
      W=0.00                                                            00005617
C                                                                       00005700
      TC=2.0                                                            00005800
      VREF=143.3                                                        00005810
      V0=20.                                                            00006000
      NI=6                                                              00006100
      NJ=6                                                              00006600
      T=0.                                                              00007000
      LX=5.715                                                          00007100
      LY=2.54                                                           00007200
      AI=NI-1                                                           00007300
      AJ=NJ-1                                                           00007400
      DX=LX/AI                                                          00007500
      DY=LY/AJ
```

```
      DXS=DX**2                                                          00007600
      DYS=DY**2                                                          00007700
      DO1 I=1,NI                                                         00008000
      DO2 J=1,NJ                                                         00008100
      V(I,J)=V0                                                          00008200
      SC(I,J)=0.0                                                        00008300
    2 CONTINUE                                                           00008400
    1 CONTINUE                                                           00008500
      A=0.2                                                              00008501
      DT=A/((DI/DXS)+(DJ/DYS))                                           00008502
C ANOTHER WAY ...                                                        00008503
      DTX=A*DXS/DI                                                       00008504
      DTY=A*DYS/DJ                                                       00008505
      DT=AMIN1(DTX,DTY)                                                  00008506
      WRITE(6,11) DTX,DTY,DT                                             00008507
   11 FORMAT('1'///20X,'CALCULATED DTX,DTY,DT =',3(E11.4,2X)//)          00008508
C                                                                        00008509
      DT=25.                                                             00008510
C                                                                        00008511
      WRITE(6,12) DT                                                     00008512
   12 FORMAT(20X,'MODIFIED DT =',E11.4//)                                00008513
      WRITE(6,14) DX,DY
   14 FORMAT(20X,'CELL SIZE: DX =',E11.4,3X,'DY =',E11.4//)
      WRITE(6,13) DI,DJ                                                  00008514
   13 FORMAT(20X,'DIFFUSIVITIES: DI =',E11.4,3X,'DJ =',E11.4//)          00008515
      NPR=0                                                              00008516
      NPRM=12                                                            00008517
      MT=3                                                               00008532
      TM(1)=7200.                                                        00008534
      VSI(1)=100.                                                        00008535
      VSF(1)=100.                                                        00008536
      IBC(1)=2                                                           00008537
      JBC(1)=2                                                           00008538
      TM(2)=3900.                                                        00008539
      VSI(2)=132.22                                                      00008540
      VSF(2)=132.22                                                      00008541
      IBC(2)=1                                                           00008542
      JBC(2)=1                                                           00008543
      TM(3)=4200.                                                        00008544
      VSI(3)=20.                                                         00008545
      VSF(3)=20.                                                         00008546
      IBC(3)=2                                                           00008547
      JBC(3)=2                                                           00008548
      TM(4)=1800.                                                        00008549
      VSI(4)=20.0                                                        00008550
      VSF(4)=20.0                                                        00008551
      IBC(4)=2                                                           00008552
      JBC(4)=2                                                           00008553
      TM(5)=3600.                                                        00008554
      VSI(5)=143.3                                                       00008555
      VSF(5)=20.0                                                        00008556
      IBC(5)=2                                                           00008557
      JBC(5)=2                                                           00008558
C     MT=2
C     TM(1)=4500.
C     VSI(1)=148.89
C     VSF(1)=148.89
C     IBC(1)=1
C     JBC(1)=1
C     TM(2)=7200.
```

```
C     VSI(2)=20.
C     VSF(2)=20.
C     IBC(2)=2
C     JBC(2)=2
C     MT=1
C     TM(1)=7200.
C     VSI(1)=20.
C     VSF(1)=20.
C     IBC(1)=2
C     JBC(1)=2
      WRITE(6,101)                                                    00008562
  101 FORMAT('1'//10X,'***** 2 - D  BLOCK CYCLE *****'//)             00008563
      WRITE(6,105) LX,LY
  105 FORMAT(10X,'LX, LY =',2(E11.4,2X)/)
      WRITE(6,102) DX,DY,DT                                           00008564
  102 FORMAT(10X,'DX, DY, DT =',3(E11.4,2X)//)                        00008570
      WRITE(6,106) KX,KY
  106 FORMAT(10X,'KX, KY =',2(E11.4,2X)/)
      WRITE(6,104) DI,DJ
  104 FORMAT(10X,'DI, DJ =',2(E11.4,2X)/)
      WRITE(6,103) HX,HY                                              00008571
  103 FORMAT(10X,'HX, HY =',4(E11.4,2X)//)                            00008572
      WRITE(6,111)                                                    00008580
  111 FORMAT(//10X,'TIME-TEMPERATURE-B.C.-HEATING HISTORY'//)         00008590
      DO22 NT=1,MT                                                    00008591
      WRITE(6,112) NT,TM(NT),VSI(NT),VSF(NT),IBC(NT),JBC(NT),W        00008592
  112 FORMAT(5X,'NT=',I2,2X,'TM(NT)=',F7.1,2X,'VSI(NT)=',F7.1,2X      00008593
     1,'VSF(NT)=',F7.1,2X,'IBC(NT)=',I1,2X,'JBC(NT)=',I1,2X,'W='      00008594
     2,E11.4/)                                                        00008595
   22 CONTINUE                                                        00008596
      DO3 NT=1,MT                                                     00008597
      CALL STEP(TM(NT),VSI(NT),VSF(NT),IBC(NT),JBC(NT))               00008598
    3 CONTINUE                                                        00008599
      WRITE(6,71) NPPL                                                00008600
   71 FORMAT('1'//10X,'*** PLOTTING OUTPUT, NPPL =',I3//)             00008610
      WRITE(6,72)                                                     00008620
   72 FORMAT(16X,'NP',3X,'T(MINUTES)',6X,'V(B.C.)',8X,'V11/',8X,'VNI1/' 00008630
     2,8X,'V1NJ/',7X,'VNINJ/')                                        00008631
      WRITE(6,73)                                                     00008640
   73 FORMAT(51X,'SC11',8X,'SCNI1',8X,'SC1NJ',7X,'SCNINJ'//)          00008650
      DO74 NP=1,NPPL                                                  00008660
      WRITE(6,75) NP,TP(NP),VBC(NP),V11(NP),VNI1(NP),V1NJ(NP),VNINJ(NP) 00008670
   75 FORMAT(15X,I3,6(2X,E11.4))                                      00008680
      WRITE(6,76) SC11(NP),SCNI1(NP),SC1NJ(NP),SCNINJ(NP)             00008690
   76 FORMAT(44X,4(2X,E11.4)/)                                        00008691
   74 CONTINUE                                                        00008692
      NEX=0
      DO201 NL=1,5
      DO202 NP=1,NPPL
      NEX=NEX+1
      XDATA(NEX)=TP(NP)
      IF(NL.EQ.1) YDATA(NEX)=V11(NP)
      IF(NL.EQ.2) YDATA(NEX)=VNI1(NP)
      IF(NL.EQ.3) YDATA(NEX)=V1NJ(NP)
      IF(NL.EQ.4) YDATA(NEX)=VNINJ(NP)
      IF(NL.EQ.5) YDATA(NEX)=VBC(NP)
      IF(NL.EQ.1) ZDATA(NEX)=SC11(NP)
      IF(NL.EQ.2) ZDATA(NEX)=SCNI1(NP)
      IF(NL.EQ.3) ZDATA(NEX)=SC1NJ(NP)
      IF(NL.EQ.4) ZDATA(NEX)=SCNINJ(NP)
```

```
      IF(NL.EQ.5) ZDATA(NEX)=SCTV
  202 CONTINUE
  201 CONTINUE
      WRITE(6,203)
  203 FORMAT('1'//10X,'***** EZGRAF INPUT *****'//)
      DO204 NE=1,NEX
      WRITE(6,205) NE,XDATA(NE),YDATA(NE),ZDATA(NE)
  205 FORMAT(10X,'NE=',I4,3X,'XDATA=',E11.4,3X,'YDATA=',E11.4,3X
     2'ZDATA=',E11.4)
  204 CONTINUE
      WRITE(6,210)
  210 FORMAT('1'//10X,'FORMATTED PARTIAL EZGRAF INPUT'//)
      WRITE(6,206)
  206 FORMAT('  XDATA')
      WRITE(6,207) (XDATA(N),N=1,NEX)
  207 FORMAT(8X,E11.4,2X,E11.4,2X,E11.4,2X,E11.4,2X,E11.4)
      WRITE(6,208)
  208 FORMAT('  YDATA')
      WRITE(6,207) (YDATA(N),N=1,NEX)
      WRITE(6,209)
  209 FORMAT('  ZDATA')
      WRITE(6,207) (ZDATA(N),N=1,NEX)
      STOP                                                          00008700
      END                                                           00008800
      SUBROUTINE STEP(TM,VSI,VSF,IBC,JBC)                           00008900
      REAL KX,KY                                                    00009000
      COMMON/A/ KX,KY,RHO,C,DI,DJ,HX,HY,W,DT,DX,DY,DXS,DYS,TC       00009010
     2,VREF,T                                                       00009020
      COMMON/B/ NI,NJ,NPR,NPRM,NPPL                                 00009310
      COMMON/C/ V(11,11),SC(11,11)                                  00009320
      COMMON/D/ TP(100),V11(100),VNI1(100),V1NJ(100),VNINJ(100)     00009330
      COMMON/E/ SC11(100),SCNI1(100),SC1NJ(100),SCNINJ(100),VBC(100) 00009340
      DIMENSION D2VDX2(11,11),D2VDY2(11,11),DSCDT(11,11)            00009400
      NTSUB=TM/DT                                                   00009500
      TSUB=0.0                                                      00009600
      DELVS=VSF-VSI                                                 00009700
      DO1 NT=1,NTSUB                                                00009800
      VS=VSI+DELVS*(TSUB+0.5*DT)/TM                                 00009900
      VSX=VS                                                        00010000
      VSY=VS                                                        00010100
      DO11 I=1,NI                                                   00010191
      DO12 J=1,NJ                                                   00010192
      IF(I.EQ.1) D2VDX2(I,J)=2.*(V(2,J)-V(1,J))/DXS                 00010193
      IF((I.NE.1).AND.(I.NE.NI)) D2VDX2(I,J)=(V((I+1),J)-2.*V(I     00010194
     2,J)+V((I-1),J))/DXS                                           00010195
      IF((I.EQ.NI).AND.(IBC.EQ.2)) VOUT=V((NI-1),J)-2.*DX*HX*(V     00010196
     2(NI,J)-VS)/KX                                                 00010197
      IF((I.EQ.NI).AND.(IBC.EQ.2)) D2VDX2(NI,J)=(VOUT-2.*V(NI,J     00010198
     2)+V((NI-1),J))/DXS                                            00010199
      IF((I.EQ.NI).AND.(IBC.EQ.1)) D2VDX2(NI,J)=9999.               00010200
      IF(J.EQ.1) D2VDY2(I,1)=2.*(V(I,2)-V(I,1))/DYS                 00010201
      IF((J.NE.1).AND.(J.NE.NJ)) D2VDY2(I,J)=(V(I,(J+1))-2.*V(I     00010202
     2,J)+V(I,(J-1)))/DYS                                           00010203
      IF((J.EQ.NJ).AND.(JBC.EQ.2)) VOUT=V(I,(NJ-1))-2.*DY*HY*(V     00010204
     2(I,NJ)-VS)/KY                                                 00010205
      IF((J.EQ.NJ).AND.(JBC.EQ.2)) D2VDY2(I,NJ)=(VOUT-2.*V(I,NJ     00010206
     2)+V(I,(NJ-1)))/DYS                                            00010207
      IF((J.EQ.NJ).AND.(JBC.EQ.1)) D2VDY2(I,NJ)=9999.               00010208
   12 CONTINUE                                                      00010209
   11 CONTINUE                                                      00010210
```

```
                                                                      00010220
      DO21 I=1,NI                                                     00010221
      DO22 J=1,NJ                                                     00010222
      DV=(DI*D2VDX2(I,J)+DJ*D2VDY2(I,J)+(W/(RHO*C)))*DT               00010223
      V(I,J)=V(I,J)+DV                                                00010226
   22 CONTINUE                                                        00010227
   21 CONTINUE                                                        00010228
      IF(IBC.NE.1) GO TO 24                                           00010229
      DO23 J=1,NJ                                                     00010230
      V(NI,J)=VSX                                                     00010231
   23 CONTINUE                                                        00010232
   24 IF(JBC.NE.1) GO TO 26                                           00010233
      DO25 I=1,NI                                                     00010234
      V(I,NJ)=VSY                                                     00010235
   25 CONTINUE                                                        00010236
   26 CONTINUE                                                        00010237
      DO51 I=1,NI                                                     00010238
      DO52 J=1,NJ                                                     00010239
      DSCDT(I,J)=(TC**(0.1*(V(I,J)-VREF)))
C
C NOTE .. DT/60. SO SC(I,J) HAS UNITS OF MINUTES ...                  00010240
      SC(I,J)=SC(I,J)+DSCDT(I,J)*DT/60.
C                                                                     00010241
   52 CONTINUE                                                        00010242
   51 CONTINUE                                                        00010243
      TSUB=TSUB+DT                                                    00010244
      VST=VSI+DELVS*TSUB/TM                                           00010245
      T=T+DT                                                          00010246
      NPR=NPR+1                                                       00010250
      IF(NPR.NE.NPRM) GO TO 41                                        00010310
      WRITE(6,31) T                                                   00010320
   31 FORMAT('1'//50X,'TIME(SEC)=',F8.2//)                            00010331
      WRITE(6,36) VST                                                 00010332
   36 FORMAT(50X,'VS AT TIME T (DEG. C)=',F7.2//)                     00010333
      WRITE(6,32)                                                     00010340
   32 FORMAT(50X,'BLOCK TEMPERATURE (DEGREES C)'//)                   00010350
      WRITE(6,33)                                                     00010360
   33 FORMAT(12X,'I=1',7X,'I=2',7X,'I=3',7X,'I=4',7X,'I=5',7X,        00010370
     2'I=6',7X,'I=7',7X,'I=8',7X,'I=9',6X,'I=10',6X,'I=11'/)          00010380
      DO27 J=1,NJ                                                     00010390
      WRITE(6,34) J,(V(I,J),I=1,NI)                                   00010391
   34 FORMAT(3X,'J=',I2,2X,11(F8.2,2X))                               00010392
   27 CONTINUE                                                        00010393
      WRITE(6,61)                                                     00010394
   61 FORMAT(//50X,'RATE OF CURE'//)                                  00010395
      WRITE(6,33)                                                     00010396
      DO62 J=1,NJ                                                     00010397
      WRITE(6,63) J,(DSCDT(I,J),I=1,NI)                               00010398
   63 FORMAT(3X,'J=',I2,3X,11(F7.5,3X)/)                              00010400
   62 CONTINUE                                                        00010401
      WRITE(6,35)                                                     00010402
   35 FORMAT(///50X,'CURE STATE (MINUTES)'//)                         00010403
      WRITE(6,33)                                                     00010404
      DO28 J=1,NJ                                                     00010405
      WRITE(6,37) J,(SC(I,J),I=1,NI)
   37 FORMAT(3X,'J=',I2,3X,11(F8.3,2X))                               00010406
   28 CONTINUE                                                        00010407
      NPPL=NPPL+1                                                     00010408
      TP(NPPL)=T/60.
      VBC(NPPL)=VS                                                    00010409
      V11(NPPL)=V(1,1)
```

```
      VNI1(NPPL)=V(NI,1)                                              00010410
      VINJ(NPPL)=V(1,NJ)                                              00010411
      VNINJ(NPPL)=V(NI,NJ)                                            00010412
      SC11(NPPL)=SC(1,1)                                              00010413
      SCNI1(NPPL)=SC(NI,1)                                            00010414
      SC1NJ(NPPL)=SC(1,NJ)                                            00010415
      SCNINJ(NPPL)=SC(NI,NJ)                                          00010416
   41 CONTINUE                                                        00010417
      IF(NPR.EQ.NPRM) NPR=0                                           00010418
    1 CONTINUE                                                        00010420
      RETURN                                                          00010500
      END                                                             00010600
```

CALCULATED DTX,DTY,DT = 0.1690E+03 0.3339E+02 0.3339E+02

MODIFIED DT = 0.2500E+02

CELL SIZE: DX = 0.1143E+01 DY = 0.5080E+00

DIFFUSIVITIES: DI = 0.1546E-02 DJ = 0.1546E-02

***** 2 - D BLOCK CYCLE *****

LX, LY = 0.5715E+01 0.2540E+01

DX, DY, DT = 0.1143E+01 0.5080E+00 0.2500E+02

KX, KY = 0.3200E+05 0.3200E+05

DI, DJ = 0.1546E-02 0.1546E-02

HX, HY = 0.1700E+05 0.1700E+05

TIME-TEMPERATURE-B.C.-HEATING HISTORY

NT= 1 TM(NT)= 7200.0 VSI(NT)= 100.0 VSF(NT)= 100.0 IBC(NT)=2 JBC(NT)=2 W= 0.0

NT= 2 TM(NT)= 3900.0 VSI(NT)= 132.2 VSF(NT)= 132.2 IBC(NT)=1 JBC(NT)=1 W= 0.0

NT= 3 TM(NT)= 4200.0 VSI(NT)=   20.0 VSF(NT)=   20.0 IBC(NT)=2 JBC(NT)=2 W= 0.0

TIME(SEC)= 300.00

VS AT TIME T (DEG. C)= 100.00

BLOCK TEMPERATURE (DEGREES C)

	I=1	I=2	I=3	I=4	I=5	I=6	I=7	I=8	I=9	I=10	I=11
1	20.17	20.17	20.19	20.51	23.61	41.88					
2	20.42	20.42	20.44	20.76	23.85	42.07					
3	21.57	21.57	21.59	21.91	24.96	42.94					
4	24.82	24.82	24.84	25.15	28.10	45.35					
5	31.99	31.99	32.01	32.29	34.97	50.61					
6	44.48	44.48	44.49	44.73	46.92	59.70					

RATE OF CURE

	I=1	I=2	I=3	I=4	I=5	I=6	I=7	I=8	I=9	I=10	I=11
1	0.00020	0.00020	0.00020	0.00020	0.00025	0.00088					
2	0.00020	0.00020	0.00020	0.00020	0.00025	0.00090					
3	0.00022	0.00022	0.00022	0.00022	0.00027	0.00095					
4	0.00027	0.00027	0.00027	0.00028	0.00034	0.00113					
5	0.00045	0.00045	0.00045	0.00046	0.00055	0.00162					
6	0.00106	0.00106	0.00106	0.00108	0.00126	0.00304					

CURE STATE (MINUTES)

	I=1	I=2	I=3	I=4	I=5	I=6	I=7	I=8	I=9	I=10	I=11
1	0.001	0.001	0.001	0.001	0.001	0.003					
2	0.001	0.001	0.001	0.001	0.001	0.003					
3	0.001	0.001	0.001	0.001	0.001	0.003					
4	0.001	0.001	0.001	0.001	0.001	0.003					
5	0.002	0.002	0.002	0.002	0.002	0.004					
6	0.004	0.004	0.004	0.004	0.004	0.008					

TIME(SEC)= 600.00

VS AT TIME T (DEG. C)= 100.00

BLOCK TEMPERATURE (DEGREES C)

	I=1	I=2	I=3	I=4	I=5	I=6	I=7	I=8	I=9	I=10	I=11
J= 1	22.18	22.20	22.45	23.96	30.84	51.87					
J= 2	23.04	23.07	23.31	24.81	31.61	52.41					
J= 3	25.85	25.88	26.11	27.56	34.12	54.16					
J= 4	31.17	31.20	31.42	32.76	38.87	57.47					
J= 5	39.59	39.62	39.81	40.99	46.36	62.69					
J= 6	51.31	51.33	51.48	52.44	56.77	69.93					

RATE OF CURE

	I=1	I=2	I=3	I=4	I=5	I=6	I=7	I=8	I=9	I=10	I=11
J= 1	0.00023	0.00023	0.00023	0.00026	0.00041	0.00177					
J= 2	0.00024	0.00024	0.00024	0.00027	0.00043	0.00184					
J= 3	0.00029	0.00029	0.00030	0.00033	0.00052	0.00207					
J= 4	0.00042	0.00042	0.00043	0.00047	0.00072	0.00261					
J= 5	0.00076	0.00076	0.00077	0.00083	0.00121	0.00374					
J= 6	0.00170	0.00170	0.00172	0.00184	0.00248	0.00619					

CURE STATE (MINUTES)

	I=1	I=2	I=3	I=4	I=5	I=6	I=7	I=8	I=9	I=10	I=11
J= 1	0.002	0.002	0.002	0.002	0.003	0.009					
J= 2	0.002	0.002	0.002	0.002	0.003	0.010					
J= 3	0.002	0.002	0.002	0.002	0.003	0.011					
J= 4	0.003	0.003	0.003	0.003	0.004	0.013					
J= 5	0.005	0.005	0.005	0.005	0.006	0.018					
J= 6	0.011	0.011	0.011	0.011	0.013	0.032					

TIME(SEC)= 7200.00

VS AT TIME T (DEG. C)= 100.00

BLOCK TEMPERATURE (DEGREES C)

	I=1	I=2	I=3	I=4	I=5	I=6	I=7	I=8	I=9	I=10	I
J= 1	86.02	86.40	87.56	89.42	91.90	94.86					
J= 2	86.27	86.65	87.78	89.61	92.05	94.96					
J= 3	87.03	87.39	88.46	90.18	92.48	95.23					
J= 4	88.26	88.58	89.55	91.11	93.20	95.69					
J= 5	89.92	90.20	91.03	92.37	94.16	96.30					
J= 6	91.94	92.17	92.83	93.90	95.33	97.04					

RATE OF CURE

	I=1	I=2	I=3	I=4	I=5	I=6	I=7	I=8	I=9	I=10
J= 1	0.01886	0.01938	0.02099	0.02388	0.02835	0.03482				
J= 2	0.01920	0.01971	0.02132	0.02420	0.02865	0.03505				
J= 3	0.02023	0.02074	0.02234	0.02518	0.02953	0.03573				
J= 4	0.02203	0.02254	0.02410	0.02686	0.03103	0.03687				
J= 5	0.02472	0.02520	0.02669	0.02930	0.03316	0.03846				
J= 6	0.02845	0.02889	0.03025	0.03258	0.03598	0.04050				

CURE STATE (MINUTES)

	I=1	I=2	I=3	I=4	I=5	I=6	I=7	I=8	I=9	I=10
J= 1	0.688	0.716	0.808	0.994	1.350	2.071				
J= 2	0.709	0.737	0.830	1.019	1.378	2.101				
J= 3	0.776	0.805	0.902	1.096	1.464	2.196				
J= 4	0.902	0.933	1.035	1.239	1.620	2.364				
J= 5	1.114	1.147	1.256	1.473	1.869	2.622				
J= 6	1.467	1.503	1.618	1.844	2.251	3.002				

TIME(SEC)=11100.00

VS AT TIME T (DEG. C)= 132.22

BLOCK TEMPERATURE (DEGREES C)

	I=1	I=2	I=3	I=4	I=5	I=6	I=7	I=8	I=9	I=10	I=1
J= 1	127.81	128.01	128.61	129.57	130.81	132.22					
J= 2	128.03	128.22	128.79	129.70	130.88	132.22					
J= 3	128.65	128.82	129.30	130.08	131.08	132.22					
J= 4	129.63	129.75	130.10	130.66	131.39	132.22					
J= 5	130.86	130.92	131.10	131.40	131.79	132.22					
J= 6	132.22	132.22	132.22	132.22	132.22	132.22					

RATE OF CURE

	I=1	I=2	I=3	I=4	I=5	I=6	I=7	I=8	I=9	I=10	I=1
J= 1	0.34180	0.34661	0.36126	0.38609	0.42088	0.46394					
J= 2	0.34695	0.35160	0.36571	0.38958	0.42290	0.46394					
J= 3	0.36234	0.36646	0.37894	0.39988	0.42879	0.46394					
J= 4	0.38768	0.39088	0.40050	0.41646	0.43813	0.46394					
J= 5	0.42214	0.42397	0.42943	0.43834	0.45018	0.46394					
J= 6	0.46394	0.46394	0.46394	0.46394	0.46394	0.46394					

CURE STATE (MINUTES)

	I=1	I=2	I=3	I=4	I=5	I=6	I=7	I=8	I=9	I=10	I=
J= 1	10.899	11.194	12.200	14.358	18.922	32.226					
J= 2	11.326	11.621	12.622	14.767	19.280	32.257					
J= 3	12.722	13.011	13.990	16.077	20.404	32.351					
J= 4	15.498	15.766	16.672	18.588	22.476	32.519					
J= 5	20.693	20.899	21.595	23.055	25.947	32.777					
J= 6	31.623	31.658	31.773	31.999	32.406	33.157					

TIME(SEC)=15300.00

VS AT TIME T (DEG. C)= 20.00

BLOCK TEMPERATURE (DEGREES C)

	I=1	I=2	I=3	I=4	I=5	I=6	I=7	I=8	I=9	I=10	I=1
J= 1	64.81	63.76	60.52	54.98	47.14	37.30					
J= 2	64.00	62.96	59.78	54.34	46.64	36.98					
J= 3	61.57	60.59	57.59	52.45	45.17	36.05					
J= 4	57.63	56.74	54.02	49.37	42.79	34.52					
J= 5	52.31	51.55	49.21	45.22	39.57	32.47					
J= 6	45.82	45.21	43.34	40.15	35.63	29.97					

RATE OF CURE

	I=1	I=2	I=3	I=4	I=5	I=6	I=7	I=8	I=9	I=10	I=1
J= 1	0.00434	0.00403	0.00322	0.00219	0.00127	0.00064					
J= 2	0.00410	0.00381	0.00306	0.00210	0.00123	0.00063					
J= 3	0.00347	0.00324	0.00263	0.00184	0.00111	0.00059					
J= 4	0.00264	0.00248	0.00205	0.00149	0.00094	0.00053					
J= 5	0.00182	0.00173	0.00147	0.00112	0.00075	0.00046					
J= 6	0.00116	0.00111	0.00098	0.00079	0.00057	0.00039					

CURE STATE (MINUTES)

	I=1	I=2	I=3	I=4	I=5	I=6	I=7	I=8	I=9	I=10	I=1
J= 1	18.294	18.540	19.278	20.541	22.980	33.298					
J= 2	18.274	18.526	19.294	20.638	23.196	33.312					
J= 3	18.468	18.730	19.552	21.070	23.893	33.352					
J= 4	19.614	19.868	20.691	22.290	25.245	33.410					
J= 5	23.091	23.290	23.948	25.266	27.723	33.462					
J= 6	32.512	32.543	32.640	32.815	33.081	33.469					

*** PLOTTING OUTPUT, NPPL = 51

NP	T(MINUTES)	V(B.C.)	V11/ SC11	VNI1/ SCNI1	V1NJ/ SC1NJ	VNINJ/ SCNINJ
1	0.5000E+01	0.1000E+03	0.2017E+02	0.4188E+02	0.4448E+02	0.5970E+02
			0.9733E-03	0.2717E-02	0.3570E-02	0.8199E-02
2	0.1000E+02	0.1000E+03	0.2218E+02	0.5187E+02	0.5131E+02	0.6993E+02
			0.2020E-02	0.9470E-02	0.1063E-01	0.3204E-01
3	0.1500E+02	0.1000E+03	0.2583E+02	0.5862E+02	0.5570E+02	0.7530E+02
			0.3311E-02	0.2110E-01	0.2078E-01	0.7067E-01
4	0.2000E+02	0.1000E+03	0.3012E+02	0.6386E+02	0.5910E+02	0.7886E+02
			0.5024E-02	0.3850E-01	0.3397E-01	0.1224E+00
5	0.2500E+02	0.1000E+03	0.3457E+02	0.6814E+02	0.6205E+02	0.8152E+02
			0.7348E-02	0.6254E-01	0.5033E-01	0.1862E+00
6	0.3000E+02	0.1000E+03	0.3898E+02	0.7170E+02	0.6474E+02	0.8365E+02
			0.1051E-01	0.9394E-01	0.7019E-01	0.2612E+00
7	0.3500E+02	0.1000E+03	0.4325E+02	0.7472E+02	0.6726E+02	0.8542E+02
			0.1478E-01	0.1333E+00	0.9397E-01	0.3470E+00
8	0.4000E+02	0.1000E+03	0.4734E+02	0.7732E+02	0.6965E+02	0.8693E+02
			0.2048E-01	0.1810E+00	0.1221E+00	0.4429E+00
9	0.4500E+02	0.1000E+03	0.5123E+02	0.7957E+02	0.7190E+02	0.8823E+02
			0.2799E-01	0.2373E+00	0.1552E+00	0.5485E+00
10	0.5000E+02	0.1000E+03	0.5491E+02	0.8155E+02	0.7402E+02	0.8937E+02
			0.3774E-01	0.3024E+00	0.1936E+00	0.6634E+00
11	0.5500E+02	0.1000E+03	0.5836E+02	0.8329E+02	0.7601E+02	0.9037E+02
			0.5021E-01	0.3764E+00	0.2380E+00	0.7871E+00
12	0.6000E+02	0.1000E+03	0.6159E+02	0.8483E+02	0.7787E+02	0.9126E+02
			0.6592E-01	0.4593E+00	0.2886E+00	0.9191E+00
13	0.6500E+02	0.1000E+03	0.6460E+02	0.8621E+02	0.7961E+02	0.9205E+02
			0.8540E-01	0.5509E+00	0.3459E+00	0.1059E+01
14	0.7000E+02	0.1000E+03	0.6740E+02	0.8744E+02	0.8122E+02	0.9277E+02
			0.1092E+00	0.6511E+00	0.4102E+00	0.1206E+01
15	0.7500E+02	0.1000E+03	0.7000E+02	0.8855E+02	0.8272E+02	0.9340E+02
			0.1379E+00	0.7597E+00	0.4818E+00	0.1360E+01
16	0.8000E+02	0.1000E+03	0.7241E+02	0.8955E+02	0.8410E+02	0.9398E+02
			0.1720E+00	0.8765E+00	0.5610E+00	0.1521E+01
17	0.8500E+02	0.1000E+03	0.7463E+02	0.9046E+02	0.8538E+02	0.9450E+02
			0.2120E+00	0.1001E+01	0.6477E+00	0.1688E+01

18	0.9000E+02	0.1000E+03	0.7668E+02 0.2583E+00	0.9128E+02 0.1134E+01	0.8657E+02 0.7421E+00	0.9497E+02 0.1861E+01
19	0.9500E+02	0.1000E+03	0.7858E+02 0.3114E+00	0.9202E+02 0.1273E+01	0.8766E+02 0.8443E+00	0.9540E+02 0.2040E+01
20	0.1000E+03	0.1000E+03	0.8032E+02 0.3716E+00	0.9270E+02 0.1420E+01	0.8866E+02 0.9541E+00	0.9579E+02 0.2223E+01
21	0.1050E+03	0.1000E+03	0.8193E+02 0.4392E+00	0.9332E+02 0.1574E+01	0.8959E+02 0.1071E+01	0.9615E+02 0.2411E+01
22	0.1100E+03	0.1000E+03	0.8341E+02 0.5144E+00	0.9388E+02 0.1733E+01	0.9044E+02 0.1196E+01	0.9647E+02 0.2604E+01
23	0.1150E+03	0.1000E+03	0.8477E+02 0.5973E+00	0.9439E+02 0.1899E+01	0.9122E+02 0.1328E+01	0.9677E+02 0.2801E+01
24	0.1200E+03	0.1000E+03	0.8602E+02 0.6880E+00	0.9486E+02 0.2071E+01	0.9194E+02 0.1467E+01	0.9704E+02 0.3002E+01
25	0.1250E+03	0.1322E+03	0.8776E+02 0.7875E+00	0.1322E+03 0.4390E+01	0.1322E+03 0.3787E+01	0.1322E+03 0.5322E+01
26	0.1300E+03	0.1322E+03	0.9300E+02 0.9159E+00	0.1322E+03 0.6710E+01	0.1322E+03 0.6107E+01	0.1322E+03 0.7641E+01
27	0.1350E+03	0.1322E+03	0.9916E+02 0.1110E+01	0.1322E+03 0.9030E+01	0.1322E+03 0.8426E+01	0.1322E+03 0.9961E+01
28	0.1400E+03	0.1322E+03	0.1048E+03 0.1403E+01	0.1322E+03 0.1135E+02	0.1322E+03 0.1075E+02	0.1322E+03 0.1228E+02
29	0.1450E+03	0.1322E+03	0.1096E+03 0.1820E+01	0.1322E+03 0.1367E+02	0.1322E+03 0.1307E+02	0.1322E+03 0.1460E+02
30	0.1500E+03	0.1322E+03	0.1136E+03 0.2385E+01	0.1322E+03 0.1599E+02	0.1322E+03 0.1539E+02	0.1322E+03 0.1692E+02
31	0.1550E+03	0.1322E+03	0.1170E+03 0.3114E+01	0.1322E+03 0.1831E+02	0.1322E+03 0.1771E+02	0.1322E+03 0.1924E+02
32	0.1600E+03	0.1322E+03	0.1198E+03 0.4013E+01	0.1322E+03 0.2063E+02	0.1322E+03 0.2002E+02	0.1322E+03 0.2156E+02
33	0.1650E+03	0.1322E+03	0.1221E+03 0.5084E+01	0.1322E+03 0.2295E+02	0.1322E+03 0.2234E+02	0.1322E+03 0.2388E+02
34	0.1700E+03	0.1322E+03	0.1240E+03 0.6320E+01	0.1322E+03 0.2527E+02	0.1322E+03 0.2466E+02	0.1322E+03 0.2620E+02
35	0.1750E+03	0.1322E+03	0.1255E+03 0.7711E+01	0.1322E+03 0.2759E+02	0.1322E+03 0.2698E+02	0.1322E+03 0.2852E+02
36	0.1800E+03	0.1322E+03	0.1268E+03 0.9243E+01	0.1322E+03 0.2991E+02	0.1322E+03 0.2930E+02	0.1322E+03 0.3084E+02
37	0.1850E+03	0.1322E+03	0.1278E+03 0.1090E+02	0.1322E+03 0.3223E+02	0.1322E+03 0.3162E+02	0.1322E+03 0.3316E+02

38	0.1900E+03	0.2000E+02	0.1284E+03	0.1010E+03	0.9655E+02	0.7635E+02
			0.1266E+02	0.3294E+02	0.3207E+02	0.3339E+02
39	0.1950E+03	0.2000E+02	0.1262E+03	0.8690E+02	0.8685E+02	0.6189E+02
			0.1433E+02	0.3309E+02	0.3220E+02	0.3341E+02
40	0.2000E+03	0.2000E+02	0.1214E+03	0.7742E+02	0.8074E+02	0.5431E+02
			0.1562E+02	0.3317E+02	0.3228E+02	0.3343E+02
41	0.2050E+03	0.2000E+02	0.1157E+03	0.7008E+02	0.7606E+02	0.4932E+02
			0.1651E+02	0.3320E+02	0.3234E+02	0.3344E+02
42	0.2100E+03	0.2000E+02	0.1097E+03	0.6411E+02	0.7204E+02	0.4559E+02
			0.1711E+02	0.3323E+02	0.3238E+02	0.3344E+02
43	0.2150E+03	0.2000E+02	0.1037E+03	0.5914E+02	0.6837E+02	0.4262E+02
			0.1750E+02	0.3325E+02	0.3241E+02	0.3345E+02
44	0.2200E+03	0.2000E+02	0.9787E+02	0.5493E+02	0.6492E+02	0.4015E+02
			0.1776E+02	0.3326E+02	0.3243E+02	0.3345E+02
45	0.2250E+03	0.2000E+02	0.9228E+02	0.5132E+02	0.6167E+02	0.3805E+02
			0.1793E+02	0.3327E+02	0.3245E+02	0.3345E+02
46	0.2300E+03	0.2000E+02	0.8697E+02	0.4819E+02	0.5859E+02	0.3624E+02
			0.1805E+02	0.3328E+02	0.3247E+02	0.3346E+02
47	0.2350E+03	0.2000E+02	0.8194E+02	0.4545E+02	0.5569E+02	0.3467E+02
			0.1813E+02	0.3328E+02	0.3248E+02	0.3346E+02
48	0.2400E+03	0.2000E+02	0.7722E+02	0.4304E+02	0.5296E+02	0.3328E+02
			0.1819E+02	0.3329E+02	0.3249E+02	0.3346E+02
49	0.2450E+03	0.2000E+02	0.7279E+02	0.4091E+02	0.5041E+02	0.3204E+02
			0.1824E+02	0.3329E+02	0.3250E+02	0.3347E+02
50	0.2500E+03	0.2000E+02	0.6866E+02	0.3900E+02	0.4803E+02	0.3095E+02
			0.1827E+02	0.3330E+02	0.3251E+02	0.3347E+02
51	0.2550E+03	0.2000E+02	0.6481E+02	0.3730E+02	0.4582E+02	0.2997E+02
			0.1829E+02	0.3330E+02	0.3251E+02	0.3347E+02

APPENDIX C
LITERATURE SEARCH

APPENDIX C .. LITERATURE SEARCH - BONDING OF RUBBER TO NONMETALLIC FIBERS

The attached bibliography is a result of a literature search on adhesion of nonmetallic fiber materials to rubber. The reports covered aramid, nylon, carbon, cellulose, and glass fibers. In some cases, adhesive was applied directly to the fibers, in other cases, bonding agents were added to the rubber, and in other cases, no adhesives or bonding agents were used. The fiber diameters were on the order of 10um, which is much smaller than the steel wire diameter of 0.032 inches (0.8 mm) which would be used in our baseline materials.

In reference C3 (from the bibliography), it is shown that bond strength depends on the viscoelastic properties of the rubber. Rate and temperature effects are important. Adhesion energy as measured by peel tests for a range of rates and temperatures showed a reasonable fit to a "universal" form of the WLF rate-temperature equivalence principle:

$$\log_{10}[a(T)] = \frac{-17.4(T-T_g)}{51.6+T-T_g}, \quad T_g = -90°C$$

This form is compared to a previous form (Equation 1) in Figures C1 and C2. The difference is very slight.

A direct comparison of the effect on rubber of chopped fibers of aramid, nylon, carbon, cellulose, and glass, with and without bonding agents, appears in reference C6. The materials were milled to get good uniaxial fiber alignment, and tensile strength and modulus in the fiber and transverse directions were measured. Samples with the bonding agent HRH showed the largest increases in modulus and strength, indicating a superior bond over that given by the other bonding agents tested. When this bonding agent was used, the strongest materials were those with the aramid and nylon fibers. Carbon and cellulose formed a lower class, with glass fiber reinforcement the least effective.

According to Reference C1, the problem with the glass fibers may be that they are too brittle, and break up in processing. Their studies showed that chopped fibers are most effective when their L/D is above 100, and that their glass fibers after processing had L/D of 25 to 50.

The effect of Monsanto Santoweb^R treated cellulose fiber on cut growth, cutting, and chipping was examined in reference C7. Fiber loadings of 2 phr showed significant reduction in cut growth rate and improvements in cut and chip resistance. The reference does not discuss fiber alignment. Processing was done using a Banbury mixer, with no milling, so fiber orientation may have been random.

A direct comparison of fiber pullout force in rubber, between Kevlar aramid cords treated with an epoxy/RFL adhesive and brass coated steel tire cords of similar diameter, was presented in reference C10. It is not known if the adhesive treatment restricts the fiber-rubber interface to the outer surface of the Kevlar cord, or if the larger total surface area of all of the Kevlar filaments plays a role. In any case, the fiber pullout forces for the Kevlar and the steel cords were roughly comparable, staying closer than a factor of 2 for varying rubber formulations and heat aging programs.

WLF FORMULATION

RELATIVE TEAR GROWTH RATE IN SBR AS FUNCTION OF TEMPERATURE

LOG10(A(T)) = −8.86*(T−TS)/(101.6+T−TS), TS=TG+20C, TG=−63C

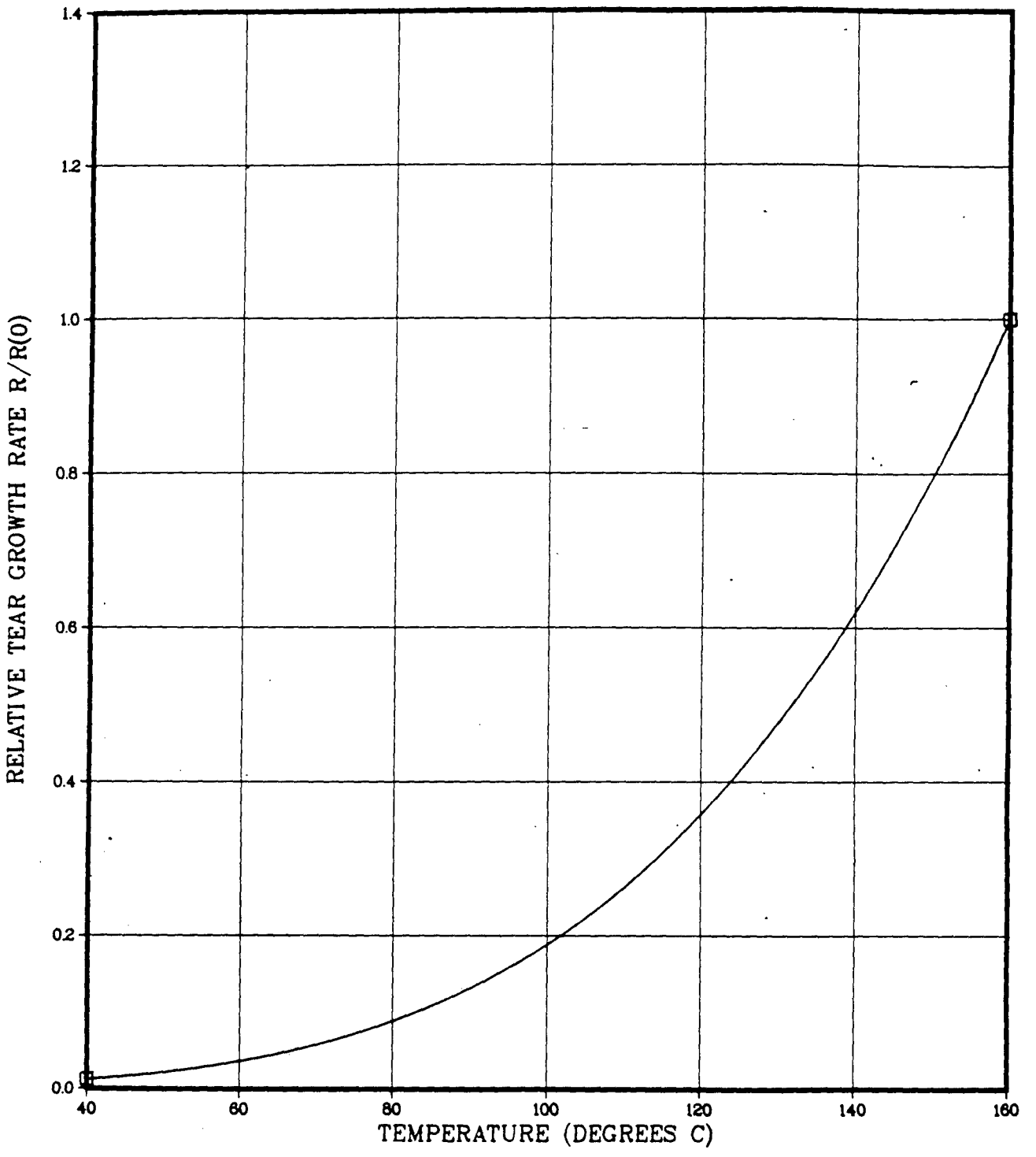

Figure C1 - WLF Formulation

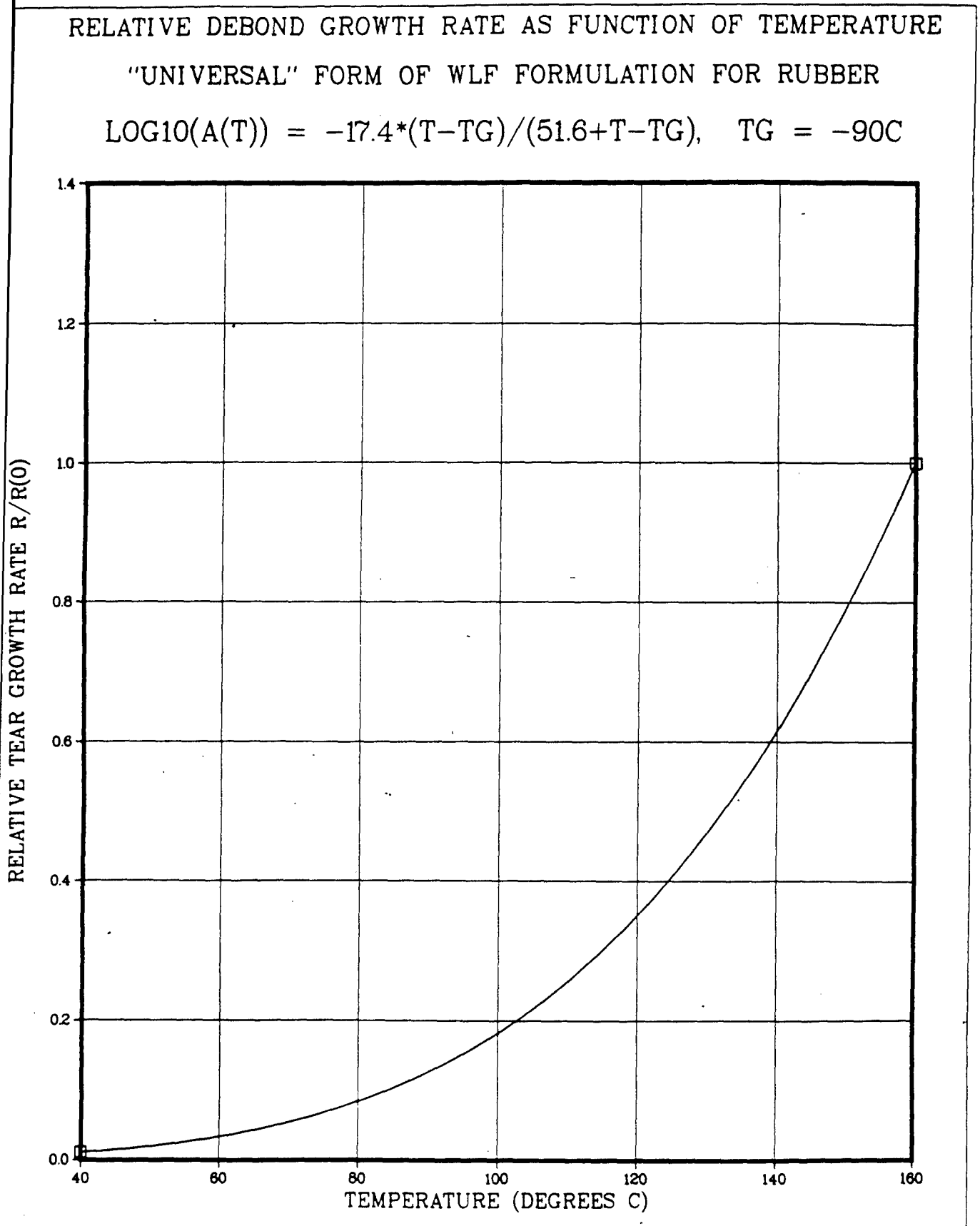

Figure C2 - "Universal"Form of WLF Formulation for Rubber

APPENDIX C REFERENCES

C 1 K. Boustany and P. Hamed, "Short Cellulosic Fibers - New Reinforcers for Rubber," Rubber World, Nov. 1974, pp. 39-40.

C 2 S. R. Moghe, "Short Fiber Reinforcement of Elastomers" Rubber Chemistry and Technology, V. 47, 1974, pp. 1074-1081.

C 3 A. Ahagon and A. N. Gent, "Effect of Interfacial Bonding on the Strength of Adhesion," Journal of Polymer Science, V. 13, 1975, pp. 1285-1300.

C 4 S. R. Moghe, "Mechanical Properties of Short Fiber Elastomer Composites," Rubber Chemistry and Technology, V. 49, 1976, pp. 1160-1166.

C 5 A. Y. Coran, P. Hamed, and L. A. Goettler, "The Mechanical Behavior of Short-Fiber Elastomer Composites," Rubber Chemistry and Technology, V. 49, 1976, pp. 1167-1181.

C 6 J. E. O'Connor, "Short-Fiber-Reinforced Elastomer Composites," Rubber Chemistry and Technology, V. 50, 1977, pp. 945-958.

C 7 J. R. Beatty and R. Hamed, "Effect of Treated Cellulose Fibers on Cut Growth, Cutting and Chipping Characteristics of Rubber Compounds," Elastomerics, August 1978, pp. 27-34.

C 8 D. D. Dunnom, "A Study of the Nylon Dry-Bonding Adhesion Mechanism," Journal of Elastomers and Plastics, V. 10, January 1978, pp. 44-58.

C 9 A. N. Gent and G. R. Hamed, "Adhesion of Elastomers, with Special Reference to Triblock Copolymers," Rubber Chemistry and Technology, V. 51, 1978, pp. 354-364.

C 10 Y. Iyengar, "Adhesion of Kevlar Aramid Cords to Rubber," Journal of Applied Polymer Science, V. 22, 1978, pp. 801-812.

DISTRIBUTION LIST

	Copies
Commander U.S. Army Tank-Automotive Command ATTN: AMSTA-RCKT - Mr. J. Patt Warren, MI 48397-5000	14